ON THE DETERMINATION OF PYROXENES BY X-RAY POWDER DIAGRAMS

BY

P. C. ZWAAN

CONTENTS

PREFACE

The investigation which is described here was made in the Mineralogical-Petrological Department of the Geological Institute of Leyden University (Netherlands).

First of all I want to acknowledge the help of Professor Dr. E. NIGGLI, who showed his interest in all the problems which arose during the investigation. His comprehensive knowledge of mineralogy and petrography has contributed especially to define clearly the ideas which are stated in this paper.

Pyroxene specimens were placed at my disposal by Professor Dr. B. G. ESCHER of Leiden; Professor Dr. H. H. HESS of Princeton, New Jersey, U.S.A.; Professor Dr. A. STRECKEISEN of Bern, Switzerland; Dr. H. KUNO of Tokyo, Japan; Dr. H. M. E. SCHÜRMANN of The Hague; Mr. H. KONING of Leiden; Mr. P. N. J. BODES, F. G. A. and Mr. A. G. BODE of The Hague. The pyroxene collection of the Museum has been greatly enlarged through these gifts.

I am indebted to Mrs. J. GREVE—HARRIS, Dr. R. VAN VLOTEN and Mr. T. VOLKER, who assisted me in correcting the English manuscript.

Mr. A. VERHOORN prepared with great conscientiousness the X-ray powder diagrams; the chemical analyses were done by Miss B. HAGEMAN in the Petrochemical Laboratory of Leiden. Mr. M. DEYN made the many oriented thin sections. The illustrations were made by Mr. B. F. M. COLLET. A crystal model of enstatite was constructed by Mr. E. H. HEMMEN. I am grateful to all for their helpfulness in this work.

I want to express my gratitude also to Miss J. M. FASEL and Miss J. A. A. VAN WERKHOVEN, who typed the manuscript.

Last, but not least, I want to acknowledge the great debt I owe to my adopted parents, who enabled me to obtain my university education.

INTRODUCTION

The common methods for the identification of minerals are the optical and the chemical analysis. The optical method in many cases gives an exact determination, but every mineralogist or petrographer knows the limitations of the optical investigation and knows therefore that certain difficulties may occur with some groups of minerals, as, for instance, with ore minerals, carbonates and isotropic isomorphous series. It is not always possible to determine the exact identity in these groups, particularly to determine the chemical composition of a member of an isomorphous series. The röntgenographic analysis is very suitable to give a valuable amplification of the methods of analysis and in many cases even a definitive determination can be made in the very cases where the usual methods of examination fail, e. g. with very fine grained rocks.

In the Mineralogical-Petrological Laboratory of the University of Leiden successful use is being made of the X-ray powder analysis of DEBYE-SCHERRER. This method is very useful because only a little quantity of material is needed and this does not have to consist of idiomorphic crystals, moreover. Since the X-ray powder diagrams can be easily compared and give no great difficulties as regards reproduction for publication, this powder method is suitable in every respect for our purpose.

The X-ray powder diagram has a different reflection pattern for each mineral and therefore is characteristic. The positions of these reflections conform to the law of BRAGG:

$$n\lambda = 2d\sin\theta$$

in which

n is some integer;
λ is the wave-length of the X-ray;
d is the distance between the parallel reflecting planes (lattice spacing);
θ is the angle between the path of the X-ray and the reflecting plane (glancing angle).

Besides the positions of the reflections, their intensity is of importance; this intensity depends on the crystal structure and therefore is also characteristic for the mineral.

To determine the mineral with the aid of the powder diagram one may calculate the lattice spacings of the reflections using the formula:

$$90^\circ - \theta = e.\,k$$

in which

e is the distance in millimeters between corresponding reflections;
k is a constant factor for a certain camera.

When θ has been calculated then d can be read off from a table compiled for this purpose. With the aid of the values for d and the accessory intensity values it is possible to determine the mineral on the basis of a collection of data. These data have been gathered, among others, by HANAWALT, RINN and FREVEL (1938) and were published in the form of tables. In this system the minerals are arranged according to the lattice spacings of the three strongest reflections, in such a way that the line with the strongest intensity is mentioned first. In the same way the card-index system of the American Society for Testing Materials [1]) was designed while HARCOURT has published a similar system for the ore minerals in 1942. In this way it is often possible to identify a mineral without knowing anything about crystal form, habit, colour, etcetera.

Another method of determination is based on comparison of the powder diagram with diagrams of already known minerals, provided that these diagrams have been produced under exactly the same conditions. It is very useful therefore, to set up a collection of photographs for comparison, as is being done in the Mineralogical-Petrological Laboratory of Leiden. One can often identify a mineral very rapidly by simply comparing the powder diagram with already identified photographs, so that this method of determination may be really considered as a routine method and is used as such in Leiden. When composing the collection, the desirability arose to submit to a further examination the important rock-forming mineral group of the pyroxenes.

The purpose of this thesis is to investigate the possibility of distinguishing the different pyroxenes from each other by röntgenographic methods and to determine the different chemical compositions without chemical analyses. For that purpose X-ray powder diagrams were made of pyroxenes, which vary in chemical composition and paragenesis. It was tried to obtain to pyroxenes of greatly different origins. In addition the connection between the optical and the röntgenographic results was traced.

The röntgenographic method for determining minerals was already successfully applied to different minerals or groups of minerals.

CLAISSE (1950) managed to determine the anorthite content of plagioclase feldspars with the aid of the variation in the relative distance between characteristic reflections of the X-ray powder diagram and found a connection between this variation and the chemical composition.

OSTEN succeeded in 1951 to divide the alkali feldspars in groups on the ground of differences in the positions and the intensities of certain reflections in the X-ray powder diagram and indicated that the determination of the alkali feldspars was much simplified by these results when combined with an optical and chemical investigation.

A good example is given in a publication of CLARINGBULL and HEY (1952). They describe a new mineral, sinhalite, which was formerly thought to be an iron-rich olivine. Besides by differences in optical properties they were able to distinguish sinhalite from olivine by X-ray powder diagrams (CuKα radiation) although both reflection patterns are very similar.

NIGGLI and TOBI (1953) were able to distinguish clearly three groups of amphiboles on the ground of differences in the relative distance between

[1]) Cited under the references as: Alphabetical and Grouped Numerical Index .....

a few strong reflections in the X-ray powder diagram; a cummingtonite-grunerite group, a grammatite-actinolite group and a group of common hornblendes. For this purpose they made use of $FeK\alpha_1$ radiation and a camera with a diameter of 9 centimeters.

Likewise with the aid of powder diagrams E. NIGGLI could indicate in 1953 that varlamoffite is slightly different from cassiterite in the position of the reflections in the diagram.

In 1953 NIGGLI, OVERWEEL and VAN DER VLERK described a method for determining the age of fossil bones. By means of X-ray crystallography they determined the fluorine contents of the apatite substance in such fossil bones. This determination was carried out by close observation of the variation in the relative distance between two suitable lines; it turned out that there was a connection between this variation and the fluorine content. Use was made of a camera with a diameter of 19 centimeters and $CuK\alpha$ radiation.

More recently (1954) GOODYEAR and DUFFIN have applied the X-ray powder method on plagioclase feldspars. With the aid of small differences in the reflection pattern of the different specimens they could determine the chemical composition of these feldspars without chemical analyses. Unlike CLAISSE (1950) they also distinguished between high- and low-temperature modifications.

From the above-mentioned examples it is seen that the röntgenographic method for determining minerals is of great importance and therefore it must be considered a deplorable fact that this method is used so little by petrographers in our country.

In the investigation which will be described here, it was tried to distinguish the pyroxenes by the variation in the relative distance between generally strong, characteristic diffraction lines. This method was, as far as we know, first introduced by CLAISSE (1950), although simultaneously it was being applied already by Dr. J. F. OSTEN in Leiden.

Data about pyroxenes in the literature are numerous; many papers deal with the optical and chemical investigation and we will treat this subject when describing the results of the optical and chemical investigations.

The X-ray method for determining pyroxenes has already been applied in many instances. Some of the publications may be mentioned here.

GOSSNER and MUSZGNUG indicated in 1929 the relation between enstatite, diopside and actinolite. Further they also distinguished between these minerals on the basis of the dimensions of the unit cell, which they determined for each case.

Important papers have been published by HESS (1952) and KUNO (1954) on the pyroxenes. They describe the possibility of determining the Mg per centage of orthopyroxenes together with the Al- and Ca content; this is done by tracing the changes of the unit cell dimensions and by correlating these changes with the chemical composition. In the discussion of the röntgenographic investigation on the orthopyroxenes we will compare this method with the relative distance method (see p. 201) and on the basis of an example estimate its value. KUNO and HESS made use of the above-mentioned method in 1953 and 1955 for the investigation of clinopyroxenes; we will treat this subject on p. 241.

The X-ray method has also been used for determining the structure of pyroxenes.

WARREN and BRAGG (1929) described the structure of diopside which

they determined by means of rotation photographs; in addition they gave the indices of numerous reflections.

In 1930 WARREN and MODELL described the structure of enstatite; this also was determined with rotation photographs, it was seen that enstatite and diopside have closely related structures. Both pyroxenes have single Si-O chains which are not directly connected with each other in contrast with the amphiboles where they are connected.

Regarding the determination of pyroxenes by the X-ray method it is seen from these publications that the X-ray powder diagrams of the various pyroxenes are very similar. It is desirable therefore to spread the characteristic diffraction lines as much as possible. To obtain this spread a medium sized camera with a diameter of 9 centimeters is used; coupled with an iron tube with Mn filter. Cameras with this diameter are not commonly used in the Netherlands and for that reason the true distance between corresponding reflections is indicated in millimeters on the reproductions of the powder diagrams. The drawback of the procedure is that with a small glancing angle a dark area is produced on the powder diagrams; this dark area has been eliminated as much as possible on the reproductions, so that the relative intensity of these reflections lies somewhat higher than that which can be observed on the X-ray powder photographs. The different powders are fixed with gum arabic on a rod of Sibor glass with an average diameter of 0.25 millimeters.

Finally it may be noted that first the orthopyroxenes will be described and afterwards the clinopyroxenes. The results of the röntgenographic investigation will be preceded by the optical and chemical analyses. To facilitate reference the optical description of the pyroxenes will be arranged according to the chemical composition.

The results of the X-ray investigation on the orthopyroxenes will be discussed with a crystal model of enstatite ($MgSiO_3$).

The clinopyroxenes will be divided in groups on the basis of the röntgenographic results; the differences between the groups will lie in the variation in the position and intensity of certain reflections in the reflection pattern of the X-ray powder diagram.

Here it may already be mentioned that the general formula of the pyroxenes may be written, in accordance with P. and E. NIGGLI (1948), as:

$$[(Si, Al)_{16}\, O_{48} / B^{VI}_{8-16}]\, A_{0-8}$$

where

$$B^{VI} = Mg^{+2}, Fe^{+2}, Mn^{+2}, Ni^{+2}, Al^{+3}, Fe^{+3}, Cr^{+3}, Ti^{+4};$$
$$A = Ca^{+2}, Na^{+1}, K^{+} .$$

This formula is based on 48 0 atoms.

The B^{VI} elements have a coordination number of six, while the A elements generally have a coordination number larger than six, but with orthopyroxenes it is equal to six. The B^{VI} elements may substitute each other while they also may be replaced by the A elements although in a lesser degree. It is seen from this formula that the chemical composition of the pyroxenes is rather complicated and we will return to this subject in detail at the description of the chemical investigation of the orthopyroxenes.

THE ORTHOPYROXENES

Introduction

The pyroxenes are important rock-forming minerals and for this reason many publications have appeared as a result of the research on this group of minerals. First we will deal with the orthorhombic pyroxenes, afterwards we will submit the monoclinic pyroxenes to a closer examination.

The orthopyroxenes form an isomorphous series of minerals, with the end members $MgSiO_3$ and $FeSiO_3$. The pure end member $FeSiO_3$ is not found in nature however. In addition small admixtures of other elements may occur in the orthopyroxenes mainly such as Al and Ca. Since the nomenclature of the orthopyroxenes is rather varied in different publications and even the mineralogical standard works (e. g.: WINCHELL 1948, FORD 1949, RAMDOHR 1954) never observe the same rules, we will in this publication, employ the nomenclature as used by POLDERVAART (1950) and KUNO (1954).

The classification, based on chemical composition, is as follows (in molecular percents):

En_{100}—En_{90}	Enstatite
En_{90} —En_{70}	Bronzite
En_{70} —En_{50}	Hypersthene
En_{50} —En_{30}	Ferrohypersthene
En_{30} —En_{10}	Eulite
En_{10} —En_{0}	Orthoferrosilite

The variation of the optical properties of the orthopyroxenes is connected with their chemical composition. Therefore it is of great importance to determine these properties as accurately as possible.

Thus first we will consider the optical results, next the chemical analyses will be discussed and lastly we will describe the X-ray investigation that will form the principal feature of this thesis.

Optical Investigation

Introduction

The question whether lamellar structures are present or not is of great importance in the optical research of orthopyroxenes. There are different opinions about the nature of these lamellae.

HESS and PHILIPS (1938) describe orthopyroxenes of the Bushveld Complex. They occur in slowly cooled plutonics and in metamorphic rocks and have an R_2O_3 percentage of 2.75 % (R consists mainly of Al). The Ca percentage is about 2.25 %, this is also the case for a number of investigated volcanic orthopyroxenes. This Ca content is equivalent to a little less than 9 percent of the diopsidic molecule. With slow cooling this diopsidic material

exsolves after HESS and PHILIPS and forms lamellae oriented parallel to the optic plane of the orthopyroxene. The visibility of these lamellae is the result of a difference in birefringence and extinction position of the orthopyroxene and the diopside.

HENRY (1942), however, reports that the lamellae consist of the same orthorhombic material as the main crystal. The visibility of the structure is due after him to differences in extinction position between the sets of lamellae. The structure appears to be due to deformation and is evidently formed during crystallization.

The plutonic character can be inferred from the presence of a lamellar structure. This is of great importance to us, as will be shown later on.

In the volcanic orthopyroxenes neither HESS and PHILIPS, nor HENRY have been able to find lamellae. KUNO (1954) says that all volcanic orthopyroxenes show a zonal structure; he has never found pyroxenes of volcanic origin which do not have this property. This zoning is so strong, that KUNO is forced to give mean values for the optical properties and correlates these results with the corresponding chemical compositions.

The variation of the optical properties has been given by POLDERVAART (1950), HESS (1952) and KUNO (1954), among others.

Of the refractive indices, N_z appears to change regularly with the chemical composition. The refractive indices of orthopyroxenes of high Al content (as described by KUNO) appear to be nearly always higher than that of orthopyroxenes of low Al content, if both contain the same percentage of enstatite in molecular %. It was found, that the birefringence increases with a decrease in the percentage of enstatite in molecular %, while practically no difference can be observed between plutonic and volcanic orthopyroxenes.

The optic axial angle 2 V between En_{80} and En_{15} appears to be smaller for volcanic orthopyroxenes than for orthopyroxenes of the Bushveld type.

Since pyroxenes of high Ti percentage have been found to have strong pleochroism, it appears that this pleochroism is proportional to the Ti percentage.

In some plutonic pyroxenes a so-called "Schiller structure" is found. According to KUNO (1954) this structure is formed by ilmenite lamellae that cause the characteristic metallic lustre of bronzite and hypersthene.

Methods of Determination

The occurrence of the orthopyroxenes has been studied macroscopically in the samples whenever possible and in thin sections by microscope.

The determination of the refractive indices has been done with the aid of immersion liquids. As most of the cleavage sections are oriented parallel to (110), it is rather easy to determine N_z accurately; the accuracy of the measurements is correct to $\pm$ .004. The measurement of N_x meets with difficulties because the real N_x value cannot be determined from cleavage sections.

The optic axial angle 2 V was measured by means of a LEITZ Universal Rotating Stage. Average error amounts to $\pm$ 1°; this constant was corrected with the aid of the nomogram according to TRÖGER (1952, op. cit., p. 124). The optic plane is parallel to (100).

The order of the description of the minerals is based on the nomenclature; first will be described the enstatite samples, next the bronzite

samples and finally the hypersthene samples. It will be noted, that the sample numbers of the orthopyroxenes are current numbers, which are true upon the whole thesis.

Finally I wish to express my gratitude to Dr. H. KUNO of Tokyo, Japan, who was so kind to make available for research the analyzed samples Nos. 4, 7, 10, 11 and 12; and to Dr. H. M. E. SCHÜRMANN of the Hague, Holland, who afforded me the samples Nos. 2, 3 and 5.

Macroscopic and Optical Description of the Röntgenographically Investigated Samples.

No. 1 *Enstatite from Great Dyke, Southern Rhodesia.* (St 28685) [2] — Macroscopically the material resembles a monomineral rock, composed of dark green to yellow-green crystals, which show distinct planes of cleavage and fine striation. In thin section colourless to pale green, large hypidiomorphic crystals were observed; this enstatite shows a distinct lamellar structure. The light colour of the mineral in thin section made it rather difficult to observe the weak pleochroism: X = pale yellow; Y = brownish yellow; Z = pale greenish.

The optical properties were measured and gave the following results: $N_z = 1.674$; $N_x = 1.665$ and $2V = +83.5°$. The composition according to chemical analysis done in our Laboratory is $En_{91}\,Hy_8$.

In the rock were also found little quantities of quartz, plagioclase feldspar ($\pm$ 24 mol % anorthite) and magnetite; the latter mineral was observed as inclusion in the enstatite, occurring in slightly curved planes.

Moreover liquid inclusions, oriented lengthwise, more or less parallel with N_z were observed. The rock has a plutonic character.

No. 2 *Enstatite in basalt from Finkenberg, Bonn, Germany.* (Fbg 229, Collection No. Dr. H. M. E. SCHÜRMANN). — The rock consists of a basalt, surrounding an olivine nodule. Dark brownish green enstatite crystals are observed in both the basalt and the nodulelike inclusion of olivine.

The microscopic investigation indicates that the enstatite in the olivine nodule shows a lamellar structure, while the phenocrysts in the basalt have a zonal structure and distinct extinction dispersion. In fig. 1 this zonal structure is shown. Although the orthopyroxenes occurring in the olivine nodule betray a plutonic character, those in the basalt are evidently of volcanic origin; the following optical properties were measured for the pyroxene in the basalt: $N_z = 1.678$; $N_x = 1.668$ and $2V = +83.5°$. The chemical composition according to the N_z curve for orthopyroxenes of high Al content in KUNO's paper (1954) is: $En_{90.6}\,Hy_{9.4}$.

The enstatite occurring in the olivine nodule shows an undulatory extinction, which may be due to deformation. In addition were observed in the olivine nodule a magnesium-rich olivine (with $2V = -85°$) with the secondary minerals serpentine and calcite; a reddish brown, optically isotropic mineral (probably picotite, as is mentioned by ZIRKEL in 1903). Biotite and a black opaque mineral, probably magnetite are found as accessory minerals.

In the basalt occur besides enstatite phenocrysts of a magnesium-rich

[2]) Registration number of the Rijksmuseum van Geologie en Mineralogie, Leiden, Holland.

olivine (with $2V = -86°$), while in the matrix were observed plagioclase feldspar with ± 53 mol % anorthite, olivine and enstatite. The rock has a holocrystalline, hypidiomorphic, porphyritic, massive structure, the groundmass is intersertal.

Fig. 1. Enstatite No. 2 with zonal structure in basalt. Finkenberg, Bonn, Germany. Crossed nicols × 60.

No. 3 *Enstatite in olivine nodule in basalt from Finkenberg, Bonn, Germany.* (Fbg 5, Collection No. Dr. H. M. E. SCHÜRMANN). — Macroscopically the rock is similar to sample No. 2. One can distinguish phenocrysts of olivine in the basalt, while in the olivine nodule occur, besides olivine, dark brownish green crystals of orthopyroxenes.

The following results are derived from microscopic inspection. Large hypidiomorphic olivine crystals (magnesium-rich with $2V = -85°$) occur as phenocrysts in the basalt, just like enstatite, while the matrix besides these minerals consists of plagioclase feldspar with ± 56 mol % anorthite. In the olivine nodule are found enstatite and olivine, together with the same reddish brown isotropic mineral (probably picotite) as is already described in sample No. 2. The optical properties of the enstatite are as follows: $N_z = 1.676$;

$N_x = 1.666$ and $2V = +84.5°$; the chemical composition according to the N_z curve for orthopyroxenes of moderate Al content in KUNO's paper (1954) is: $En_{90}Hy_{10}$. The enstatite shows an undulatory extinction, probably due to deformation, together with a lamellar structure.

In the magnesium-rich olivine (with $2V = -86.5°$) pseudo-twinning was observed also due to deformation. This mineral has altered to serpentine and calcite. Magnetite is present as accessory mineral. The olivine nodule has a holocrystalline, hypidiomorphic, massive structure. The basalt is porphyritic with an intersertal matrix.

No. 4 *Bronzite in peridotite.* (Sample No. 3a in HESS' paper 1952). — The sample contains dark green crystals, sometimes with a bronze lustre; these crystals possess a variable size up to 8 millimeters. They show distinct cleavage planes. Greenish yellow grains are also present, showing conchoidal fracture; they probably belong to olivine. Finally a yellowish powder can be observed.

Microscopic inspection shows bronzite, weakly pleochroic; X = pale orange; Y = pale yellow and Z = pale green. The optical properties are as follows: $N_z = 1.678$; $N_x = 1.668$; $2V = +82.5°$. The chemical composition of the same specimen is according to HESS (1952); $En_{89.5}Hy_{10.5}$. The mineral shows a distinct lamellar structure.

In addition pale greenish crystals occur of magnesium-rich olivine ($2V = +88.5°$), together with grass-green diopside grains, which show weak pleochroism: X = pale green and Z = pale orange-green; the angle $Z \wedge c = 38.5°$. Finally quartz and an opaque mineral were observed in thin section.

According to HESS (1952) this orthopyroxene is a plutonic one of the Bushveld type.

No. 5 *Bronzite from Kraubat, Austria.* (535 Collection No. Dr. H. M. E. SCHÜRMANN) — In the hand specimen one can recognize a bronze-coloured mineral aggregate at intervals covered with a white powdery material. Macroscopically large crystals can be observed, with a variable size up to 6 centimeters. The crystal faces and cleavage planes of these crystals are finely striated.

In thin section bronzite crystals can be seen in which a well-developed lamellar structure is visible. The pleochroism (X = pale yellow to colourless; Y = pale green-yellow to colourless and Z = pale brownish-yellow) is very weak. Moreover the observation of this property is difficult, because the bronzite is somewhat altered to bastite, partly in veins, partly through the whole crystals.

The optical properties are as follows: $N_z = 1.676$; $N_x = 1.664$ and $2V = +87.5°$. The composition according to chemical analysis done in our Laboratory is $En_{88}Hy_{12}$.

Furthermore little quantities of serpentine, quartz, carbonate, feldspar and an ore-mineral occur. The rock has a plutonic character.

No. 6 *Bronzite from Kupferberg, Bayreuth, Germany* (St 24582). — The hand specimen is characterized by large (up to 2 centimeters) greenish bronze-coloured to dark brown crystals with a silky lustre, at intervals covered with yellowish green material.

In thin section bronzite crystals occur, containing a nice lamellar struc-

ture (see fig. 2); sometimes the crystals are slightly curved, which is due to deformation, while small quantities of so-called Schiller inclusions can be observed. The bronzite is partly altered to bastite and serpentine. The optical properties, as determined, are: $N_z = 1.679$; $N_x = 1.669$; $2V = +85.5°$. According to WALLS (1935) is $2V = +82°$ and $N_y = 1.668$ for a bronzite of the same locality. The chemical composition according to the

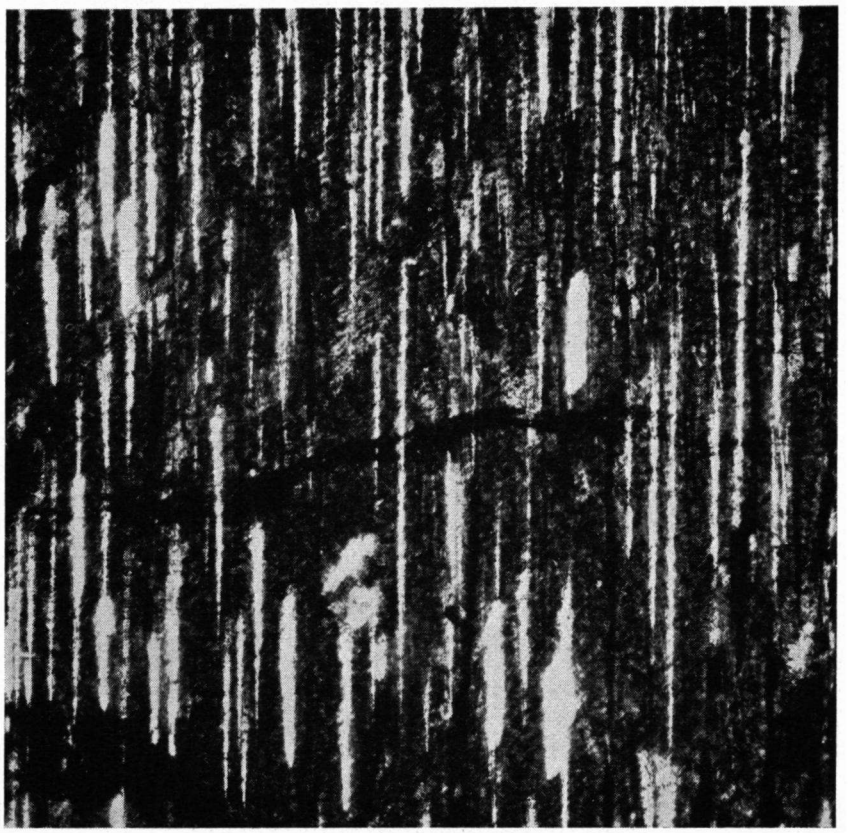

Fig. 2. Lamellar structure in bronzite No. 6. Kupferberg, Germany (st. 24582). Crossed nicols × 140.

N_z curve for orthopyroxenes of moderate alumina content in KUNO's paper (1954) is $En_{86.7}Hy_{13.3}$.

The pleochroism is too weak to describe exactly. Further serpentine and quartz occur in the rock, together with some ores as accessory minerals. The rock has a plutonic character.

No. 7 *Bronzite in andesite from Bonin Islands, Japan.* (Sample No. 2 in KUNO's paper 1954) — The sample contains dark to yellow-green grains with distinct cleavage planes, together with rounded white grains.

In thin section bronzite and plagioclase feldspar occur. The bronzite shows weak pleochroism: X = orange-yellow, Y = nearly colourless and

Z = pale green. The optical properties are as follows: $N_z = 1.682$; $N_x = 1.672$ and $2V = -85°$. The chemical composition of the same specimen is according to HESS (1952) and KUNO (1954): $En_{85}Hy_{15}$. The mineral contains ore inclusions.

The plagioclase feldspar appears to be oligoclase with ± 28 mol % anorthite; this mineral is partly altered to carbonate. One ore mineral was observed.

According to KUNO (1954) this bronzite occurs in andesite as a phenocryst, which agrees with our results. This orthopyroxene has a volcanic origin.

No. 8 *Bronzite in quartz-gabbro-diorite from Radauthal, Harz, Germany.* (St 51466). — In the hand specimen yellow-brown to dark-brown crystals occur, which vary in size from 1.5 to 2 centimeters and have a bronzy metallic lustre and finely striated cleavage planes. These crystals lie irregularly in a gray-white to white material, which here and there shows polysynthetic twinning and cleavage planes. Some quartz can be recognized by its typical greasy lustre.

Microscopically predominant plagioclase feldspar can be seen; this is labradorite with 56 mol % anorthite; showing complex twinning after the Manebach-Acline law ⊥ [100] in (001), and in places altered to sericite, kaolin and epidote. The bronzite shows lamellae. Sometimes the mineral is almost entirely altered to bastite. Serpentine and chlorite occur as secondary minerals.

The pleochroism of the bronzite is very weak: (X = brownish pale yellow; Y = brownish yellow-gray and Z = greyish pale yellow to colourless.)

The following optical properties were measured: $N_z = 1.688$; $N_x = 1.676$ and $2V = -75.5°$. The chemical composition according to the N_z curve for orthopyroxenes of moderate Al content in KUNO's paper (1954) is $En_{80.6}Hy_{19.4}$.

In addition have been observed quartz, showing undulatory extinction; biotite in small quantities and a few pieces of Na-K-feldspar. Apatite and an ore-mineral occur as accessory minerals. Plagioclase feldspar and bronzite especially showed a slightly curved character due to deformation. The structure of the rock is holocrystalline, hypidiomorphic and massive; it has a plutonic character.

No. 9 *Bronzite from Labrador.* (St 24587). — The colour of the sample is black-brown; the cleavage planes which occur show a metallic lustre as of bronze and are finely striated. Since we have no material of the mother-rock at our disposal no further detail can be given about this.

According to HESS and PHILIPS (1940) the mineral occurs in a gabbro and can be classified as a plutonic orthopyroxene.

The optical properties were measured and are as follows: $N_z = 1.693$; $N_x = 1.682$ and $2V = -71°$. The chemical composition of a bronzite of the same locality is $E_{76}Hy_{24}$. (HESS and PHILIPS 1940). Because of the modification of the nomenclature, the name of this mineral, which was originally hypersthene, is changed into bronzite; the characteristic bronze lustre can be seen clearly in this sample.

The mineral shows a fine lamellar structure (see fig. 3) and contains so-called Schiller inclusions, which are mentioned by WINCHELL (1948), together with ore inclusions. In addition a distinct pleochroism can be seen:

X = pale orange-pink and Z = grayish white to colourless. The lamellar structure indicates almost definitely the plutonic character of this mineral.

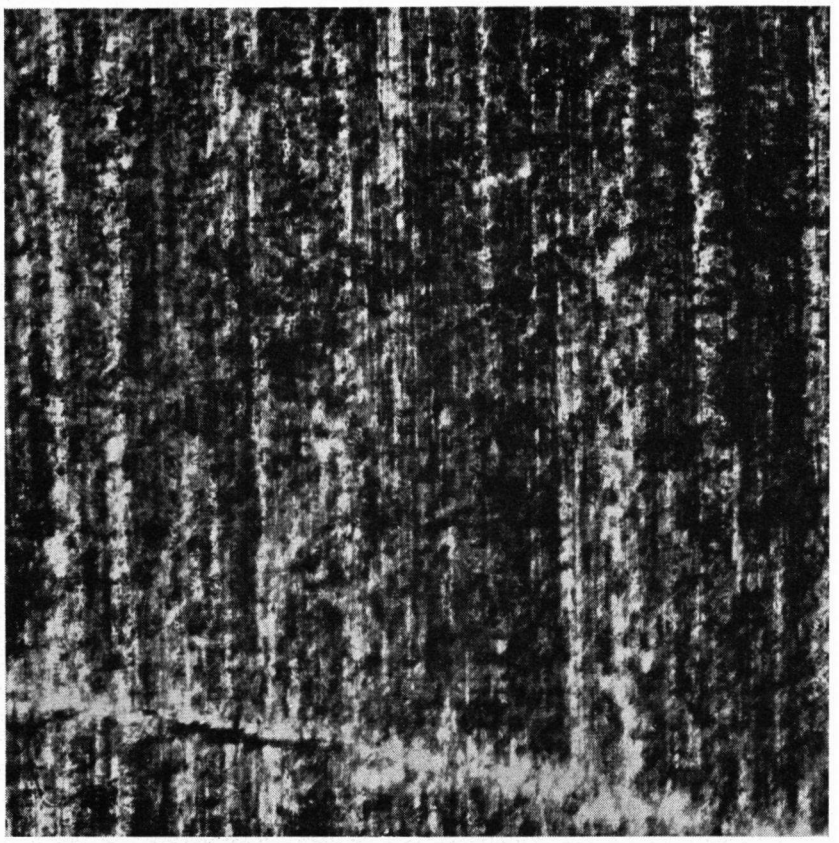

Fig. 3. Lamellar structure in bronzite No. 9. Labrador (st. 24587). Crossed nicols × 140.

No. 10 *Hypersthene in dacite pumice from Odawara, eastern foot of Hakone volcano, Kanagawa Prefecture, Japan.* (Sample No. 8 in KUNO's paper 1954) — The sample contains loose hypersthene crystals, which are black in reflected light; in transmitted light a deep brownish red colour can be seen and with the aid of a simple pocket lens (8×) black inclusions can be easily recognized in the crystals.

Often crystal faces can be seen (orthorhombic prism faces) and a few idiomorphic crystals occur. The maximum size is 8 millimeters. According to KUNO (1954) these hypersthene crystals occur as phenocrysts in hypersthene-augite dacite (pumice).

The augite will be described on page 229. Besides the minerals mentioned, also pink and white grains occur, with finely striated cleavage planes. In thin section the hypersthene shows a distinct pleochroism (X = brownish red; Y = brownish yellow and Z = pale grass-green).

The optical properties are: $N_z = 1.706$; $N_x = 1.692$ and $2V = -61°$.

The chemical composition of the same specimen is according to KUNO (1938 and 1954) $En_{67}Hy_{33}$. The mineral also shows zoning and contains apatite and ore inclusions; according to KUNO this is ilmenite (see fig. 4).

On account of the deep brown-red colour, the absorption spectrum of the hypersthene crystals was examined with the aid of a HARTRIDGE Reversion Spectroscope. A distinct but weak absorption band could be observed at 5053 Å.

The white grains were powdered and appeared to be mainly plagioclase feldspar (andesine with ± 37 mol % anorthite) and a small quantity of quartz. Because of this mineral association we can join the name of the rock (dacite). This hypersthene has a volcanic origin.

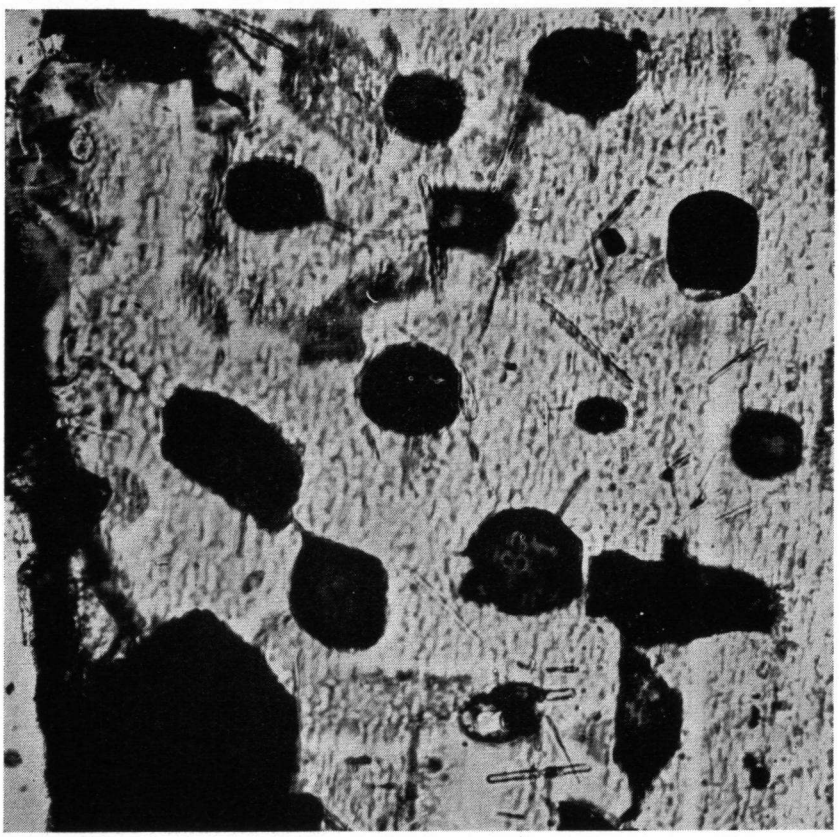

Fig. 4. Apatite and ore inclusions in hypersthene No. 10. Odawara, Kanagawa Prefecture, Japan. × 170.

No. 11 *Hypersthene in andesite (tuff) from Sitisei-zan, near Tai-pei, North Formosa.* (Sample No. 11 of KUNO 1954) — Not much information can be gained on macroscopic inspection about this sample; on the whole it is a fine-grained rock; in addition to various large crystals (a few millimeters in size) with distinct cleavage planes, there is a fine-grained material with a gray brownish yellow colour.

In thin section practically no other mineral besides hypersthene can be seen. This mineral is hypidiomorphic and shows a very distinct pleochroism (X = weak brown-red; Y = brownish yellow; and Z = pale bluish green).

The following data were obtained: $N_z = 1.707$; $N_x = 1.694$; and $2V = -60°$. The chemical composition of the same specimen is according to KUNO (1954): $En_{65}Hy_{35}$. There are various inclusions of ore minerals. Very small quantities of plagioclase feldspar consist of oligoclase with ± 22 mol % anorthite.

In addition a rather large quantity of ore grains occurs while small quantities of oxyhornblende and augite can be recognized. The oxyhornblende is strongly pleochroic (X = yellow-brown; Y = dark red-brown and Z = dark red-brown, while $Z \wedge c = 5°$ to 6°). In the augite a weak pleochroism can be observed: (X = pale grass-green and Z = grass-green, while $Z \wedge c = 44°$).

KUNO (1954) called this sample an augite-hypersthene-hornblende andesite (tuff); hypersthene phenocrysts occur in the rock. Essentially we are in complete agreement with this determination. On account of the quantitative mineral composition however, it is better to speak about an augite-hornblende-hypersthene andesite. This hypersthene is a volcanic orthopyroxene.

No. 12 *Hypersthene from Kaziya, Southeastern foot of Hakone volcano, Kanagawa Prefecture.* (Sample No. 15 of KUNO 1954) — The sample consists of a very fine-grained material in which occur small crystals with distinct cleavage planes. The specimen as a whole has a yellow to brown-gray colour.

In thin section practically all the grains appear to be hypersthene; this orthopyroxene shows a rather distinct pleochroism (X = pale orange-red; Y = pale reddish yellow and Z = pale bluish green); it contains inclusions of ore.

The optical properties are $N_z = 1.729$; $N_x = 1.717$ and $2V = -52°$. The chemical composition of the same specimen is according to KUNO (1954) $En_{51}Hy_{49}$.

In addition there occur small quantities of a green-coloured weakly pleochroic augite (X = pale blue-green and Z = pale yellow-green, $Z \wedge c = 41°$). Various ore grains can be observed.

According to KUNO this sample belongs to an augite-bearing hypersthene dacite (obsidian), in which occur phenocrysts of hypersthene. This hypersthene has a volcanic character.

Discussion of the Results.

The optical properties of the orthopyroxenes that were examined are plotted against the chemical composition in fig. 5, while in Table 1 these properties are stated.

In fig. 5 are also given the curves for optical properties, which are published by KUNO (1954). If we consider the change of the optical data of our samples, it would appear first that the samples with high Al content that were examined do not suggest obvious higher N_z values than the samples of low Al content with the same molecular percentage of enstatite. Generally the N_z values of our samples lie between the two N_z curves; only sample number 5 has a low N_z value. It should be remarked, that according to KUNO

(1954) the plutonic orthopyroxenes of the "Bushveld type" lie on a N_z curve, which is situated between the two curves in our diagram. This can be ex-

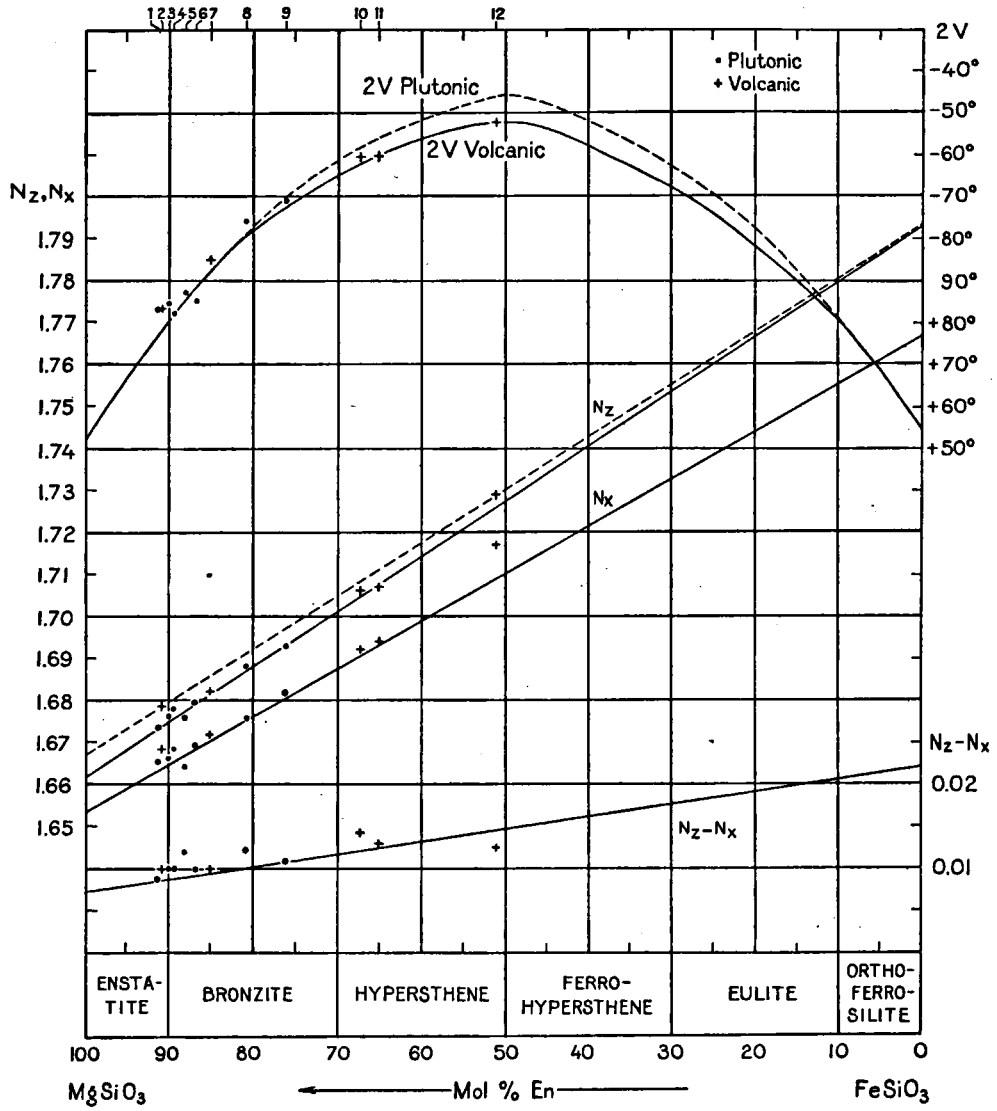

Fig. 5. Variation of optical properties of orthopyroxenes. The numbers in the upper part of the diagram refer to those in Table 1. The full and the dashed curve for N_z apply to orthopyroxenes with a low and a high Al content, respectively. Diagram after KUNO (1954).

plained by the fact, that these latter orthopyroxenes have a moderate Al content, while the full and the dotted curve in the diagram apply to orthopyroxenes with a low and a high Al content, respectively. It seems better

TABLE 1.

Optical properties of orthopyroxenes.

Sample number	N_z*	N_z according to KUNO (1954) (same specimen)	N_x*	N_x according to KUNO (1954) (same specimen)	N_z—N_x*	N_z—N_x according to KUNO (1954) (same specimen)	2 V*	mol % Enstatite			
								2 V according to KUNO (1954) (same specimen)	From chemical analysis	From N_z curve KUNO (1954)	Occurrence
1. Enstatite, S. Rhodesia	1.674		1.665		.009		+ 83.5°		91 (see Table 2)		plutonic
2. Enstatite, Finkenberg	1.678		1.668		.010		+ 83.5°			90.6	volcanic
3. Enstatite, Bonn	1.676		1.666		.010		+ 84.5°			90	plutonic
4. Bronzite in peridotite	1.678		1.668		.010		+ 82.5°		89.5 (HESS 1952)		plutonic
5. Bronzite, Austria	1.676		1.664		.012		+ 87.5°		88 (see Table 2)		plutonic
6. Bronzite, Kupferberg	1.679		1.669		.010		+ 85.5°			86.7	plutonic
7. Bronzite, Bonin Islands	1.682	1.681	1.672	1.672	.010	.009	— 85°	n. d.	85 (KUNO 1954)		volcanic
8. Bronzite, Harz	1.688		1.676		.012		— 75.5°			80.6	plutonic
9. Bronzite, Labrador	1.693		1.682		.011		— 71°		76 (HESS 1940)		plutonic
10. Hypersthene, Odawara	1.706	1.705	1.692	1.691	.014	.014	— 61°	— 60.5°	67 (KUNO 1954)		volcanic
11. Hypersthene, Sitisei-zan	1.707	1.7075	1.694	1.6945	.013	.013	— 60°	— 60°	65 (KUNO 1954)		volcanic
12. Hypersthene, Kaziya	1.729	1.726	1.717	n. d.	.012	n. d.	— 52°	— 52°	51 (KUNO 1954)		volcanic

* As measured by the author.

to us to neglect the influence of Al on N_z because this influence is very slight. In that case, one curve for N_z is sufficient.

The variation of N_x is in accordance with that of N_z. Sample number 5 has a lower N_x value than would be the case according to the curve of KUNO; further the hypersthene of Kaziya (No. 12) has an abnormally high N_x value; obviously the real N_x value has not been measured by us; this can be a result of the fact, that this real N_x value cannot be determined directly from cleavage sections as already was mentioned on p. 175. It may be noted, that KUNO does not give the N_x value of this particular sample.

The variation in birefringence (N_z—N_x) is as irregular as may be seen in KUNO's diagram (1954). Most of the samples' values lie above the (N_z—N_x) curve, only one of them (No. 12) is situated below this curve.

In the introduction it has already been mentioned that the N_z and N_x measurements are correct to $\pm$ 0.004; the average N_z and N_x values of different measurements are always given but it is evident now, that the ordinary immersion method for refractive index determination however convenient it may be as an approximate method, cannot be recommended for accurate measurements of the optical constants, therefore another method is necessary as for instance a Double Variation method.

The different optic axial angle values (2 V) lie close to the curve of KUNO. As can be seen in the diagram, the volcanic orthopyroxenes between En_{80} and En_{15} have a smaller optic axial angle than the plutonic orthopyroxenes in this range (according to KUNO 1954). This might be explained by the possibility that the volcanics have more Ca in their crystal structure than the plutonics, where it is exsolved. This Ca ion has a great influence on the shape of the cell and consequently on the optic axial angle (2 V).

From our results it turns out that the three volcanic samples, which lie between these limits, indeed have 2 V lower than those for plutonics with the same magnesium percentages. The other 2 V values lie on or close to the 2 V curve and only the samples Nos. 1, 2 and 3 have a rather high 2 V value. One may safely say, that it is striking that almost by every investigator of pyroxenes the 2 V curve has been given in a different way; the 2 V curve mentioned by TRÖGER (1952) almost coincides with these three samples.

Most of the samples had a weak pleochroism; only the samples Nos. 9, 10, 11 and 12 showed a distinct to very distinct pleochroism. These orthopyroxenes except number 11 have a much higher Ti content than the remainder of the samples. Therefore we agree with KUNO's opinion that the Ti content exerts an influence on the pleochroism.

Finally it may be said, that our optical results, except for some samples, practically agree with those of Dr. KUNO.

A lamellar structure has been observed in the plutonic orthopyroxenes, while the volcanic orthopyroxenes did not show this. The latter mostly have a zonal structure.

With the aid of the optical examination it might be possible to determine Mg percentage of orthopyroxenes, and since N_z depends only slightly on the Al content, almost accurate Mg percentage determinations are possible. It is of great importance now to find a method, besides chemical analysis, with which a more accurate result can be reached for determining the Al and Ca contents and which would not present great difficulties for the investigator. We will discuss a proposed method after having treated with the results of the chemical analyses.

Chemical Analyses

Introduction

If the chemical composition of the orthopyroxenes could be expressed by the formula (Mg, Fe) SiO_3, it would be very simple to find a method for the determination of the exact composition. This is not the case, however; complications arise because there are present in the structure, besides the above elements a rather large number of other elements.

HESS (1949) gives the general formula for pyroxenes as follows:

$$(W)_{1-p}\ (X, Y)_{1+p}\ Z_2O_6$$

in which:

$$W = Ca^{+2},\ Na^{+1},\ K^{+1}$$
$$X = Mg^{+2},\ Fe^{+2},\ Mn^{+2},\ Ni^{+2}$$
$$Y = Al^{+3},\ Fe^{+3},\ Cr^{+3},\ Ti^{+4}$$
$$Z = Si^{+4},\ Al^{+3}.$$

For orthopyroxenes eight of these units will be necessary for the unit cell, while p will be nearly equal to 1. Furthermore HESS states, that undoubtedly even more elements may be present in the structure, which will depend upon the circumstances of crystallization.

For comparison we give here the general formula for pyroxenes mentioned by P. and E. NIGGLI (1948):

$$[(Si, Al)_{16}\ O_{48}/B^{VI}{}_{8-16}]\ A_{0-8}$$

This formula is based upon 48 O atoms.

It is seen that the W positions of HESS correspond with the A elements of P. and E. NIGGLI; the X- and Y ions with the B^{VI} elements and the Z positions with the B^{IV} elements. It may be remarked, that the W positions of HESS have a coordination number larger than six.

Although it was thought formerly, that the orthopyroxenes would have a simple chemical composition, it now appears that this composition is a rather complicated one. Besides Mg^{+2} and Fe^{+2} also Al^{+3} and Ca^{+2} especially may occur in small percentages.

In 1938 HESS and PHILIPS have described the orthopyroxenes of the Bushveld Complex; these are plutonic pyroxenes, of which the writers studied the chemical composition. It appeared, that all specimens, that they examined contained about 2.15 weight % CaO; in addition a rather large Fe_2O_3 percentage was present and some Na_2O and K_2O. Some Cr_2O_3, present in a few samples, was attributed to chromite, found as an impurity. The TiO_2 content seemed to be low in most samples and was somewhat higher in a few samples containing more FeO. A number of investigated volcanic orthopyroxenes contained 2.28 % CaO; this clearly suggested that orthopyroxenes from both sources contained about the same percent of CaO, which is equivalent to a little less than 9 percent of the diopsidic molecule. It is suggested by the writers that this represents the solubility of the diopsidic molecule in Mg-rich orthopyroxenes at high temperatures. With slow cooling this diopsidic material exsolves and forms lamellae.

HESS and PHILIPS studied various magnesium-rich orthopyroxenes in 1940;

they give a number of chemical analyses. They suggest that TiO_2 and MnO increase as FeO increases and CaO seems to increase in relation to FeO, up to En_{50} for with members richer in Fe the Ca content decreases. The Al content tends to increase according to the FeO content (also up to En_{50}) although it varies irregularly.

In a more recent publication of HESS (1952) about orthopyroxenes of the Bushveld type he maintains his previous opinion that with slow cooling Ca has been almost completely removed by exsolution of diopside-hedenbergite lamellae, Na and K are virtually absent and the R_2O_3 content is about 2.75 weight % in most specimens in which R is mainly Al. Very small quantities of Ti and Ni are present, while Mn, except in the Fe-rich samples, is represented in small percentages. It is striking that the Ca content of the analyzed orthopyroxenes is rather low but usually not less than 1.00 %, pyroxenes of the Bushveld Complex contain about 2.15 % Ca according to HESS and PHILIPS (1938).

KUNO (1954) states, that the volcanic orthopyroxenes have a very variable Ca content; this Ca content can be correlated with the temperature of crystallization of the orthopyroxenes. Orthopyroxenes crystallized at high temperatures contain from 0.104 to 0.057 Ca in atomic proportion, whereas those crystallized at low temperatures contain less than 0.033 Ca. The Al content of the volcanic orthopyroxenes varies with the proportion of Ca, although there are some exceptions. Thus the Al content is high if the Ca content is high. KUNO agrees with the opinion of HESS that the amount of Ca depends on the temperature of crystallization. One might conclude from KUNO's data on the chemical composition of the orthopyroxenes that those of the Bushveld type in general have a moderate Al content, (Al is about 0.015 in the B^{VI} position); some of them have a lower proportion of Al and a few show a high Al content.

Generally it is seen however, that the volcanic orthopyroxenes contain larger amounts of Al, while the proportion of Ca is nearly always high. These Al and Ca percentages are more often than not higher than the corresponding values of the plutonic orthopyroxenes of the Bushveld type.

Chemical Results

Of the examined orthopyroxenes there are two analyses given in Table 2. The rest was not analyzed again as their analyses were taken from publications on the same specimens. We will consider the behaviour of the samples in respect to the Al and Ca content. For that purpose the atomic proportions of those pyroxenes, of which we had a complete analysis at our disposal, are calculated on the basis of six oxygen atoms. It is assumed, that Z positions should be always filled up completely. After calculation it is clear that both the Z ions and the sum of the W-, X- and Y ions become approximately 2.000 which is in keeping with the theoretical formula of orthopyroxenes. These results are stated in Table 3. It may be mentioned that the atomic proportions of specimen number 6 were calculated from an old analysis of HINTZE (1897) for a bronzite of the same locality.

First we will confine to the *plutonic orthopyroxenes*:

Enstatite No. 1 has a low Ca content while the atomic proportion of Al may be considered as moderate.

Of *Enstatite No. 3* we had no complete chemical analysis at our disposal;

TABLE 2.

New chemical analyses of two orthopyroxenes, made in the Petrochemical Laboratory of Leiden.

Sample No. 1. Enstatite, Great Dyke, Southern Rhodesia.			Sample No. 5. Bronzite, Kraubat, Austria.
	a	*b**	
SiO_2	56.15	56.39	56.29
TiO_2	0.13	0.15	0.11
Al_2O_3	1.38	1.45	0.75
P_2O_5	0.38	0.42	tr
Fe_2O_3	1.24	0.42	3.87
FeO	6.06	5.51	3.82
MgO	33.21	33.49	31.81
MnO	± 0.08	0.11	0.12
CaO	0.46	0.51	1.68
Na_2O	0.34	0.38	0.33
K_2O	0.20	0.23	0.21
H_2O+	0.17	0.19	1.02
H_2O-	0.08	0.09	0.10
Total:	99.88	99.34	100.11
NIGGLI-values.			
si		99.4	100
al		1.48	0.80
fm		96.7	95.3
c		0.95	3.09
alk		0.90	0.78
k		0.29	0.27
mg		0.91	0.88

* Analysis No. 1b is corrected for 0.7 % magnetite and recalculated to 100 %.
Analyzed by Miss B. HAGEMAN (under supervision of Mrs. Dr. C. M. DE SITTER-KOOMANS).

ZIRKEL (1903) mentions a low Ca content and HINTZE (1897) reports a varying proportion of Al for an enstatite of the same locality.

Bronzite No. 4 has a R_2O_3 content of 4 % as is mentioned by HESS (1952); so this orthopyroxene has an abnormally high Al content. Nothing can be said about the proportion of Ca, unfortunately, because no complete analysis is available.

Bronzite No. 5 is showing a low Al content but the proportion of Ca is exceptionally high for a plutonic orthopyroxene of the Bushveld type. It is quite possible, however, that a part of this Ca content is present in exsolved diopside lamellae according to the hypothesis of HESS.

TABLE 3.

Atomic proportions of orthopyroxenes calculated on the basis of 6 oxygen atoms.

Sample Number	1		5		6		7	
Si	1.970	2.000	1.971	2.000	1.962	2.000	1.962	2.000
Al	0.030		0.029		0.038		0.038	
Al	0.030		0.002		0.005		0.001	
Ti	0.004		0.003		0.000		0.000	
Fe^{+3}	0.011		0.103		0.000		0.017	
Fe^{+2}	0.161		0.112		0.209		0.274	
Mn	0.003	2.007	0.004	1.981	0.000	2.016	0.004	2.016
Mg	1.743		1.659		1.746		1.638	
Ca	0.019		0.063		0.056		0.068	
Na	0.026		0.024		0.000		0.014	
K	0.010		0.011		0.000		0.000	
Sample Number	9		10		11		12	
Si	1.889	1.982	1.961	2.000	1.980	1.997	1.928	2.000
Al	0.093		0.039		0.017		0.072	
Al	0.000		0.021		0.000		0.069	
Ti	0.020		0.007		0.002		0.005	
Fe^{+3}	0.124		0.029		0.042		0.019	
Fe^{+2}	0.425		0.576		0.606		0.851	
Mn	0.004	2.011	0.027	1.990	0.033	1.992	0.025	2.000
Mg	1.334		1.281		1.275		0.935	
Ca	0.076		0.049		0.034		0.072	
Na	0.027		0.000		0.000		0.018	
K	0.001		0.000		0.000		0.006	

For weight percentages of samples Nos 1 and 5, see Table 2.
For weight percentage of sample No. 6, see HINTZE (1897).
For weight percentages of samples Nos 7, 10, 11 and 12, see KUNO (1954).
For weight percentage of sample No. 9, see HESS and PHILIPS (1940).

Bronzite No. 6 has a low proportion of Al, while the Ca content is high. Since these proportions were calculated from an old analysis of a bronzite of the same locality (HINTZE 1897) this high proportion of Ca may be explained by the fact that old analyses often indicate a very high Ca content, even exceeding the newest analyses of volcanic orthopyroxenes. On the ground of the presence of a lamellar structure, however, it is possible that a part of this Ca content is present in exsolved diopside lamellae.

Bronzite No. 8 has high proportions for Ca and Al according to an old

analysis of HINTZE for a bronzite of the same locality; for the above mentioned reasons however, it is better not to draw conclusions from these obsolete data. For the Ca content see bronzite No. 5.

Bronzite No. 9 shows a rather high proportion of Ca being an orthopyroxene of the Bushveld type and an abnormally low Al content; the atomic proportions are calculated from an analysis mentioned by HESS in 1940 for a bronzite of the same locality; possibly there were impurities present in the analysed material, such as plagioclase feldspar for instance, because this bronzite occurs in a gabbro. It may be mentioned however, that POLDERVAART (1947) gave approximately the same analysis for an orthopyroxene of this locality. For the Ca content see bronzite No. 5.

The volcanic orthopyroxenes give the following results:

No details can be given about *Enstatite No. 2,* because we have no complete analysis at our disposal. HINTZE is giving both high Ca- and Al percentages, but it remains to be seen, if these percentages concern the enstatite from the basalt or that from the olivine nodules.

Bronzite No. 7 has a high Ca content and a low proportion of Al.

Hypersthene No. 10 shows a rather high Ca content and a moderate Al content.

Hypersthene No. 11 has a moderate proportion of Ca but an abnormally low Al content.

Hypersthene No. 12 shows a high Ca and Al proportion.

Discussion of the Results

It turns out that the orthopyroxenes of the Bushveld type generally have a wide range of Ca content and a low to moderate Al content. The atomic proportions of Al of these plutonic orthopyroxenes varies from 0.000 to 0.030 (in the B^{VI} position) and Ca varies from 0.019 to 0.076.

The volcanic orthopyroxenes show about the same variation in Al and Ca atomic proportions. In our samples Ca varies from 0.034 to 0.072 while Al ranges from 0.000 to 0.069 in the B^{VI} position.

It is seen that the variation of the Al content is somewhat greater with volcanics than with plutonics. It is quite possible that a part of the Ca content of the plutonic orthopyroxenes is present in exsolved diopside lamellae according to the hypothesis of HESS and PHILIPS (1938).

At any rate it will be interesting to determine the Al- and Ca contents of orthopyroxenes somehow without making use of chemical analyses. This we will try to do with the aid of a röntgenographic examination.

X-ray Investigation

Introduction:

The X-ray method for determining minerals was first applied in 1929 by GOSZNER and MUSZGNUG on pyroxenes; they made use of this method to examine the connection between enstatite, other pyroxenes and amphiboles. With the aid of rotation photographs they could at that time already distinguish three subgroups as follows: a. orthopyroxenes, b. clinopyroxenes and c. clinoamphiboles.

Ten years later a number of data were given by MEHMEL (1939) about mineral determination with the aid of X-rays. He gave for each mineral the unit cell dimensions, the lattice spacings with the intensity of the strongest reflections, the space group and the structure type, the axial ratios together with log sin θ for CuKα_1-, FeKα_1- and CrKα_1-radiation. Regarding the pyroxenes, he only gave data for a diopside and he stated (op. cit., p. 108) that the distinction of different pyroxenes is very difficult because the differences in the unit cell dimensions are very small and lie close to the limit of error in a powder diagram. In a mineral mixture it will therefore hardly be possible to analyze the pyroxenes further with the aid of the powder method. So he already tried to indicate in this paper the differences within one mineral group by means of the X-ray method.

Further study of this problem was made by HESS (1952) and KUNO (1954) who specialized in orthopyroxenes.

HESS describes different orthopyroxenes of the Bushveld type, which, as is already mentioned on p. 174, occur in slowly cooled plutonic rocks and in metamorphic rocks. His object was to coordinate the chemical composition of orthopyroxenes with the unit cell dimensions. When, as he says, these dimensions are measured, they give together with the optical properties, the chemical composition with reasonably good accuracy without chemical analysis. HESS states, that indeed ordinary orthopyroxenes of the Bushveld type (these are orthopyroxenes with about 2.75 % R_2O_3, in which R is mainly Al) show a linear function between the unit cell dimensions and the chemical composition. He plots these results on a diagram, which also shows that a high Al content influences particularly the b dimension, while the a and c dimensions depend in a lesser degree on a high Al content. This is why some volcanic orthopyroxenes, with a higher Al content as well as plutonic orthopyroxenes with an abnormally high proportion of Al (also examined by HESS), do not lie on the curves of the orthopyroxenes with a moderate Al content.

The behaviour of these volcanic orthopyroxenes was studied by KUNO (1954). He gives in one diagram the variation of unit cell dimensions of both the orthopyroxenes of the Bushveld type and the volcanic orthopyroxenes. Generally his results show a variable Ca content in the first place and secondly a rather variable Al content for the volcanic orthopyroxenes. The a dimension is shown to be higher for orthopyroxenes with high Ca content than for orthopyroxenes of low Ca content with the same molecular percentage of enstatite; this goes for the c dimension as well, though in a lesser degree. The b dimension, on the contrary, has lower values which depends on the proportion of Al present. The higher values for the a and c dimensions are due, says KUNO, to the substitution of Ca for Mg. The lower values of the b dimension he explains by substitution of Al for Mg. That his point of view is right, will be considered on p. 219 where the structure of enstatite will be discussed. Finally KUNO says that the Mg percentage of orthopyroxenes can be determined by measuring N_z; to obtain the Ca and Al contents one must measure the a and b dimensions respectively. We can agree with this determination of the Mg percentage because N_z will almost not be influenced by the Al content; one can derive with a fair accuracy the Mg percentage from the value of N_z. Finally it may be noted that to measure the unit cell dimensions both HESS and KUNO have made use of spectrometer powder diagrams, obtained with a North American Philips X-ray spectrometer equiped with FeKα_1-radiation.

Besides for the determination of minerals the X-ray method has also

been applied for determining crystal structures and to examine the structure of pyroxenes which is important for our thesis.

In 1929 WARREN and BRAGG described the structure of diopside CaMg $(SiO_3)_2$, determined with the aid of rotation photographs. In 1930 WARREN and MODELL described the structure of enstatite $MgSiO_3$, by means of rotation photographs. The principal conclusions arrived at in these papers are, that both diopside and enstatite appear to be built up of tetrahedral groups, consisting of Si and 4 O, linked together by shared oxygen atoms, forming endless chains parallel to the c axis of the crystal; they lie side by side and are held together by the Mg plus Ca or Mg atoms respectively. We will return to this subject on p. 217.

In this thesis only the X-ray method for determining pyroxenes will be considered as it is our intention to determine the chemical composition of different orthopyroxenes with the aid of X-ray powder diagrams. However, no use will be made of the unit cell dimensions but the relative distances between characteristic reflections will be used as a means of determination. Before going into detail about this, first we will give some general data about instruments, photographic techniques, etc.

General Data About Photographic Techniques

For taking powder photographs use was made of a medium sized UNICAM camera (BRADLEY type) with a diameter of 9 cm; to it was fitted an iron tube with Mn filter. By means of this construction the following results were obtained:

a. the characteristic reflections of the complicated pattern of the pyroxenes were spread out to make easier reading;
b. the intensity of these reflections was very little reduced, because $FeK\alpha_1$-radiation ($\lambda = 1.93597$ Å) is particularly suitable for work on Mg-Fe-silicates.

The average exposure was two hours with a collimator aperture of 0.3 mm at 18 mA and 40 kV. The different powders were fixed with the aid of gum arabic on a rod of Sibor glass; the average diameter of these rods with powder is 0.25 millimeters.

In those cases, in which the pyroxenes occurred in fine grained rocks, they were bored out of the rock after examining the thin section and in the case of mixtures of pyroxene crystals, for instance from a volcanic crater, they were separated under a binocular microscope.

The accuracy of the measurement of the powder photographs amounted to about 0.2 millimeters, corresponding with $\theta = 0.06°$; the relative distance of characteristic reflections has been measured correctly to within 0.01 millimeters with the aid of a CAMBRIDGE Universal Measuring Machine.

The intensities of the reflections were estimated visually and indicated as VS, S, SM, M, MW, W and VW, from strong to weak.

The drawback of the procedure is, that at a small glancing angle a dark area is produced on the powder diagrams; this dark area has been eliminated as much as possible on the reproductions, so that the relative intensity of these reflections lies something higher than that which can be observed on the X-ray powder photographs.

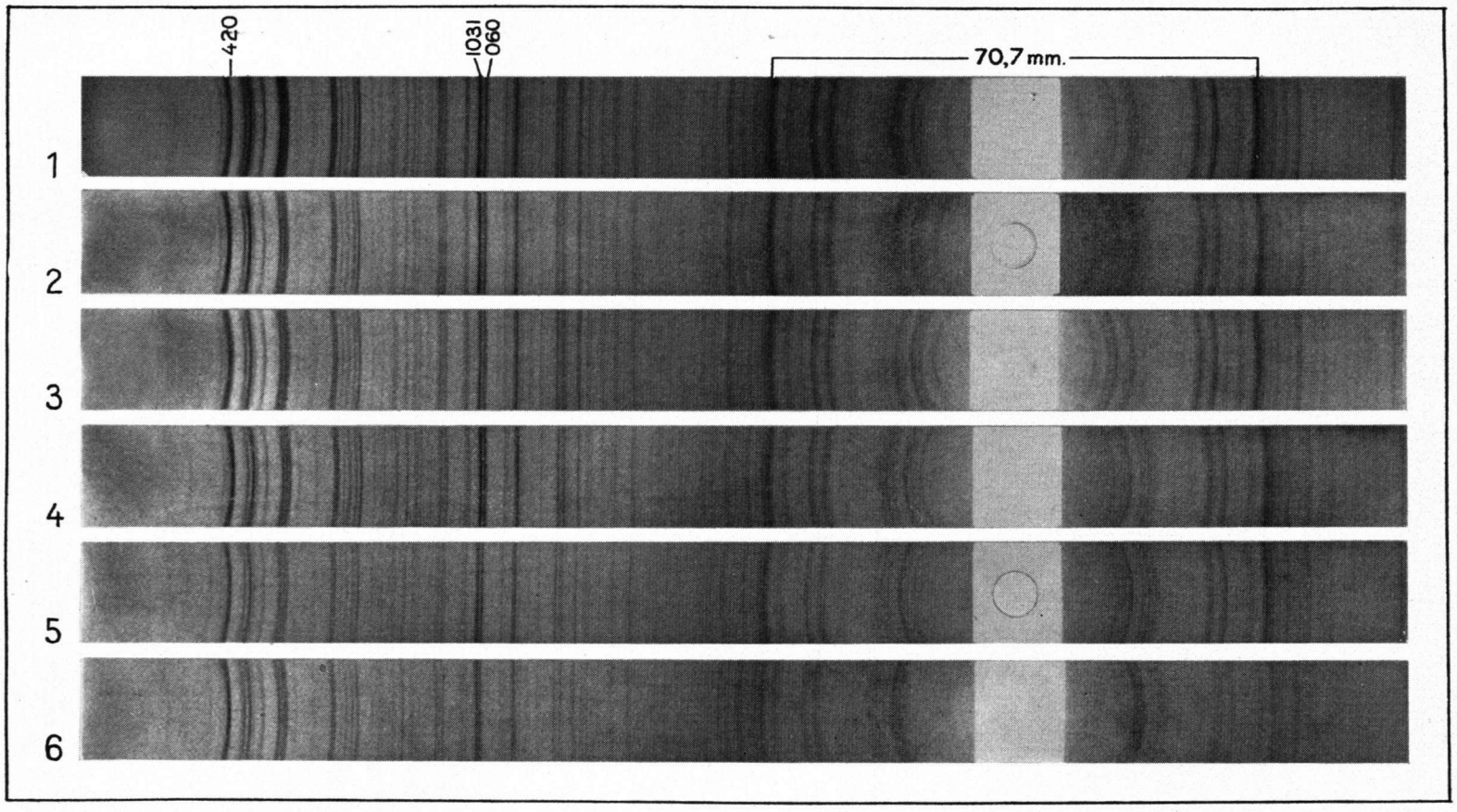

Fig. 6. X-ray powder photographs of six orthopyroxenes. ($FeK\alpha_1$ radiation, Camera diameter 9 cm)

No. 1	Bronzite No. 4, from peridotite	m* 1319	No. 4	Bronzite No. 9, Labrador, st. 24587	m 806
No. 2	Enstatite No. 1, Southern Rhodesia, st. 28685	m 859	No. 5	Hypersthene No. 11, Sitisei-zan, Japan	m 1187
No. 3	Bronzite No. 5, Kraubat, Austria	m 901	No. 6	Hypersthene No. 12, Kaziya, Japan	m 1188

* Number X-ray photograph.

Results of the X-ray Investigation

The X-ray powder diagrams of orthopyroxenes turned out to bear a good resemblance with each other; in fig. 6 a number of these photographs has been reproduced and by a superficial examination practically no differences can be seen. From this one may conclude, that in the crystal structure of different orthopyroxenes only small differences will be present. Yet the X-ray photographs must show differences because the size and shape of the unit cell are different with orthopyroxenes of different chemical composition; after all this can be concluded from the results of HESS (1952) and KUNO (1954), these results show that also the axial ratios (that is to say also the shape of the unit cell) are different with orthopyroxenes of different chemical composition. This can be seen in the following table:

mol % enstatite	a/b
100	2.068
75	2.059
50	2.051
25	2.041
0	2.033

By these changes in the size and shape of the cell certain reflections, which are very sensitive, will move. One can observe, that the distance between the strong reflections 10 3 1 and 0 6 0 is greater with enstatite than with hypersthene. The diagrams have been arranged in such a way that this distance from bronzite No. 4 to hypersthene No. 12 gradually becomes smaller.

The investigation showed, that there is a connection between this relative distance and the chemical composition. When this distance is measured on the diagram, one may read off immediately how much is the value of $\frac{Mg}{Mg}$ percent. Since these reflections have a high intensity (even in X-ray powder photographs of a mixture of different minerals) and lie close to each other, one may neglect the usual corrections for shrinking of the film, the absorption for the thickness of the used rod, etc.

Although the matter seems rather simple now, it will turn out that some complications will occur yet because besides Mg and Fe, Al and Ca are also present in the orthopyroxene structure.

When a difference in the relative distance between 10 3 1 and 0 6 0 can be observed then this must have its origin in their lattice spacings for the orthopyroxenes of different chemical composition. For that purpose in Table 4 for some powder diagrams are given the estimated intensities, the lattice spacings with θ_{Fe} together with the reflection indices. Studying the lattice spacings of 10 3 1 and 0 6 0 for the orthopyroxenes indicated in Table 4 the following can be seen:

Enstatite No. 1[3])

d (10 3 1) = 1.486 Å
d (0 6 0) = 1.472 Å
> difference: 0.014 Å.

Bronzite No. 5

d (10 3 1) = 1.487 Å
d (0 6 0) = 1.474 Å
> difference: 0.013 Å.

[3]) $\lambda FeK\alpha_1 = 1.93597$ Å.

TABLE 4

X-ray powder patterns of some orthopyroxenes (group A).

λ FeKα_1 = 1.93597 Å

Enstatite, Great Dyke S. Rhodesia (No. 1) 2 V = +83.5°; 91 mol% En				Bronzite, Kraubat Austria (No. 5) 2 V = +87.5°; 88 mol% En			Hypersthene, Kaziya Shizuoka, Japan (No. 12) 2 V = — 52°; 51 mol% En		
D^{15}_{2h} hkl	θ_{Fe}	d(Å)	Relative Intensity	θ_{Fe}	d(Å)	Relative Intensity	θ_{Fe}	d(Å)	Relative Intensity
400	12.27	4.56	VW	12.27	4.56	VW	12.21	4.58	VW
220	14.43	3.88	VW	14.27	3.93	VW	14.18	3.95	VW
311?	15.99	3.51	VW	15.96	3.52	VW	15.96	3.52	VW
021	16.88	3.33	W	17.01	3.31	W	16.88	3.33	VW
420 / 221	17.77	3.17	VS	17.81	3.17	VS	17.65	3.19	VS
600	18.60	3.04	VW	18.60	3.04	VW	18.41	3.07	VW
321?	19.18	2.946	MW	19.24	2.938	MW	19.02	2.970	MW
610	19.65	2.879	VS	19.62	2.883	VS	19.53	2.896	VS
230	19.97	2.834	W	20.07	2.821	W	19.88	2.847	W
421?	20.93	2.709	MW	20.89	2.715	MW	20.74	2.733	MW
002	21.63	2.626	VW	21.50	2.641	VW	21.37	2.657	VW
102	21.98	2.586	VW	21.98	2.586	VW	21.69	2.619	VW
620	22.45	2.535	M	22.42	2.538	M	22.17	2.565	MW
202	22.80	2.498	MW	22.80	2.498	MW	22.55	2.524	MW
430	23.03	2.474	MW	23.09	2.468	MW	22.90	2.488	MW
302	23.95	2.385	VW	23.92	2.387	VW	23.73	2.405	VW
022	25.51	2.248	VW	25.51	2.248	VW	25.35	2.261	VW
040	26.05	2.204	VW	26.12	2.199	VW	26.18	2.194	VW
502	27.10	2.125	M	27.16	2.120	M	26.94	2.137	MW
630	27.32	2.109	MW	27.48	2.098	MW	27.26	2.113	MW
531	27.48	2.098	MW	28.02	2.060	MW	27.80	2.075	W
721?	28.03	2.059	MW	28.53	2.027	W	28.31	2.041	MW
820	28.53	2.027	W	29.07	1.992	MW	28.85	2.006	W
440	29.87	1.940	MW	29.55	1.963	MW	29.33	1.976	MW
441?	30.86	1.887	W	30.83	1.889	W	30.64	1.899	VW
702	31.62	1.846	VW	31.37	1.860	VW	31.40	1.858	VW
1010	32.70	1.791	W	32.77	1.788	W	32.61	1.796	W
250	33.88	1.736	MW	33.88	1.736	W	33.47	1.755	MW
042	35.12	1.683	VW	35.09	1.684	W	34.84	1.694	VW
313	36.01	1.646	VW	35.95	1.649	W	35.86	1.652	VW
023	36.87	1.613	MW	36.87	1.613	MW	36.43	1.630	MW

TABLE 4 (continued)

Enstatite (continued)				Bronzite (continued)			Hypersthene (continued)		
D_{2h}^{15} hkl	θ_{Fe}	d(Å)	Relative Intensity	θ_{Fe}	d(Å)	Relative Intensity	θ_{Fe}	d(Å)	Relative Intensity
902	37.13	1.604	MW	37.03	1.607	MW	36.56	1.625	MW
840	37.51	1.589	MW	37.51	1.590	MW	37.22	1.600	W
1030	38.59	1.552	VW	38.30	1.560	VW	38.18	1.566	VW
650	39.29	1.529	MW	39.26	1.530	MW	38.88	1.542	MW
1200	39.55	1.520	M	39.58	1.519	M	39.33	1.527	MW
1031	40.63	1.486	S	40.62	1.487	S	40.25	1.498	S
060	41.11	1.472	SM	41.08	1.474	SM	40.57	1.488	SM
1220	42.32	1.438	VW	41.94	1.448	VW	41.78	1.453	VW
061	43.02	1.419	VW	42.32	1.438	VW	42.35	1.437	W
1040	43.40	1.409	VW	43.30	1.411	VW	42.86	1.423	VW
460	43.75	1.400	VW	43.49	1.407	VW	—	—	—
1131	44.10	1.391	SM	44.04	1.392	SM	43.72	1.401	SM
361	44.45	1.382	VW	44.48	1.382	VW	44.45	1.382	VW
043	45.37	1.360	VW	45.34	1.361	VW	44.93	1.371	VW
1400	47.76	1.307	MW	47.70	1.309	MW	47.35	1.316	MW
004	48.21	1.298	W	48.17	1.299	W	47.79	1.307	W
104	48.30	1.296	W	48.49	1.293	W	47.95	1.304	W
304	49.19	1.278	VW	49.10	1.281	VW	48.46	1.293	VW
1050?	49.70	1.269	MW	49.73	1.269	MW	49.10	1.281	MW
1240	50.53	1.254	W	50.47	1.255	W	49.77	1.268	W
404	50.75	1.250	W	50.69	1.251	VW	49.92	1.265	W
024	51.07	1.244	VW	51.13	1.243	VW	50.34	1.257	VW
860	51.87	1.231	W	51.87	1.231	W	51.33	1.239	VW
861?	—	—	—	—	—	—	52.44	1.221	VW
134	54.73	1.186	W	54.76	1.185	W	54.09	1.195	W
1600	58.36	1.137	MW	57.79	1.144	W	58.39	1.137	VW
044	59.82	1.120	VW	59.15	1.127	VW	60.33	1.114	VW
080	61.13	1.105	VW	60.75	1.109	VW	61.32	1.103	VW
081?	63.48	1.082	W	63.83	1.079	W	63.17	1.085	W
480?	—	—	—	—	—	—	64.34	1.074	W
381	65.65	1.062	VW	65.46	1.064	W	65.74	1.062	VW
1260	66.09	1.059	VW	66.16	1.058	VW	—	—	—
1450	67.30	1.049	MW	67.30	1.050	MW	66.89	1.052	W
205	70.30	1.028	VW	70.36	1.028	VW	70.23	1.029	VW
681?	71.32	1.022	W	71.32	1.022	W	71.35	1.022	W
1640?	72.91	1.013	W	72.81	1.013	W	72.98	1.012	VW
582?	80.93	0.980	VW	80.64	0.981	W	80.61	0.981	VW

Hypersthene No. 12

$$\left.\begin{array}{l} d\,(10\,3\,1) = 1.498\ \text{Å} \\ d\,(0\,6\,0) = 1.488\ \text{Å} \end{array}\right\} > \text{difference: } 0.010\ \text{Å}.$$

Here it appears also that the difference indeed is present. The connection with the chemical composition is shown in Table 6.

CLAVAN, MCNABB and WATSON (1954) state that there is no difference in the spacing between hypersthene with a low iron content and that with a high iron content. We cannot agree with this statement, as the above data do indicate a slight difference.

In fig. 7 the relative distance Δ (in mm and in Å) between 10 3 1 and 0 6 0 for different orthopyroxenes has been plotted against the chemical

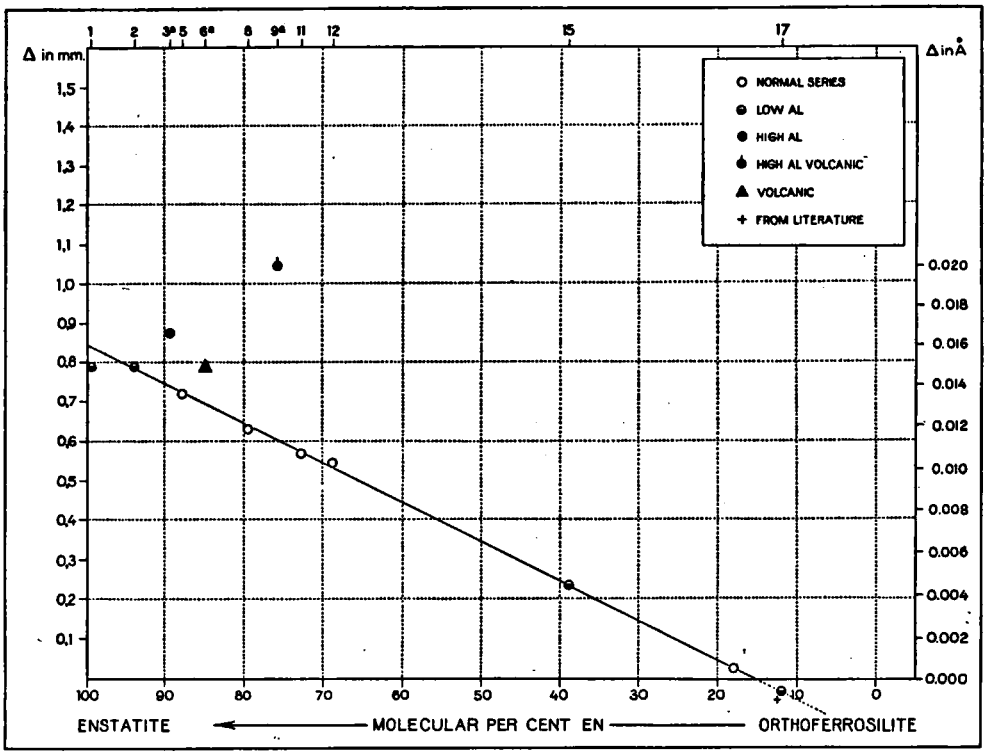

Fig. 7. Δ is relative distance in millimeters and Å between 10 3 1 and 0 6 0 for various orthopyroxenes, mentioned in HESS's paper 1952. The numbers in the upper part of the diagram refer to those in Table 5. The curve is calculated from the data of HESS about the unit cell dimensions of these orthopyroxenes. The point symbols are the same as in HESS's fig. 1. (Camera diameter 9 cm; $FeK\alpha_1$ radiation).

composition. There can be observed a linear function between Δ and this composition. This figure has been made up from the results of HESS (1952) and the sample numbers in the upper part of the diagram correspond with those of HESS. From those specimens, from which the unit cell dimensions were calculated by HESS, we have calculated the relative distance Δ (in mm)

between 10 3 1 and 0 6 0 for FeKα_1-radiation and a Camera diameter of 9 centimeters. This calculation has been carried out by deriving θ_{Fe} of 10 3 1 and 0 6 0 from given cell dimensions with the aid of the formula for the Orthorhombic Crystal system:

$$Q = \frac{H^2}{a^2} + \frac{K^2}{b^2} + \frac{L^2}{c^2}$$

in which

$$Q = \frac{4 \sin^2 \theta}{\lambda^2}$$

By these means the result has been obtained which is stated in Table 5. The Δ data in this table, as has already been mentioned, were plotted against the

TABLE 5

Relative distance Δ (in millimeters) between 10 3 1 and 0 6 0 calculated for orthopyroxenes, mentioned in HESS's paper 1952.

Sample No.	a (in Å)	b (in Å)	c (in Å)	% R_2O_3	mg	Δ in Å	Δ in mm
1 Sh	18.230	8.815	5.177	No	99.5	0.015	0.79
2 W 26	18.240	8.820	5.189	Low	94	0.015	0.79
3a R Fl	18.250	8.812	5.192	4	89.5	0.017	0.88
5 7666	18.253	8.836	5.194	Normal	88	0.014	0.72
6a Bonia	18.285	8.843	5.198	Normal	85	0.015	0.78
8 EB 38	18.270	8.857	5.200	Normal	79.75	0.012	0.63
9a Al-Hy	18.300	8.807	5.201	8.5	76	0.020	1.05
11 EB 130	18.283	8.874	5.205	Normal	73	0.011	0.57
12 EB 41	18.293	8.887	5.208	Normal	69	0.010	0.55
15 K 9	18.353	8.960	5.229	Low	39	0.005	0.24
17 K 11	18.408	9.029	5.249	Low	12	— 0.000	— 0.03

$$mg = \frac{100\ Mg^{+2}}{Mg^{+2} + Fe^{+2} + Fe^{+3} + Mn^{+2}}$$

λ FeKα_1 = 1.93597 Å
Camera diameter 9 cm.

chemical composition in fig. 7. The samples which belong to the Bushveld type lie on or close to one straight line. This line thus gives the relation by which it is possible to determine the chemical composition from the relative distance of these strong reflections. It is evident, however, that the specimens Nos. 3a, 6a and 9a do not fit in with the remaining orthopyroxenes. Remarkably enough these are Al rich orthopyroxenes. Besides the fact that these samples show an abnormal relative distance Δ between 10 3 1 and 0 6 0, HESS also indicates abnormal unit cell dimensions for these orthopyroxenes, which might have been expected.

Hitherto all data on the relative distance between 10 3 1 and 0 6 0 have been calculated only and although it appears from this theoretical study that the "relative distance method" for determining chemical composition will be feasible, there are various practical difficulties.

In order to test this hypothesis on all the investigated powder diagrams of orthopyroxenes, the relative distance between 10 3 1 and 0 6 0 has been measured by us correct to within 0.01 mm. From these data, which are stated in Table 6 the relation between Δ and the chemical composition has been given in fig. 8. From this it turns out that the samples Nos. 1, 3,

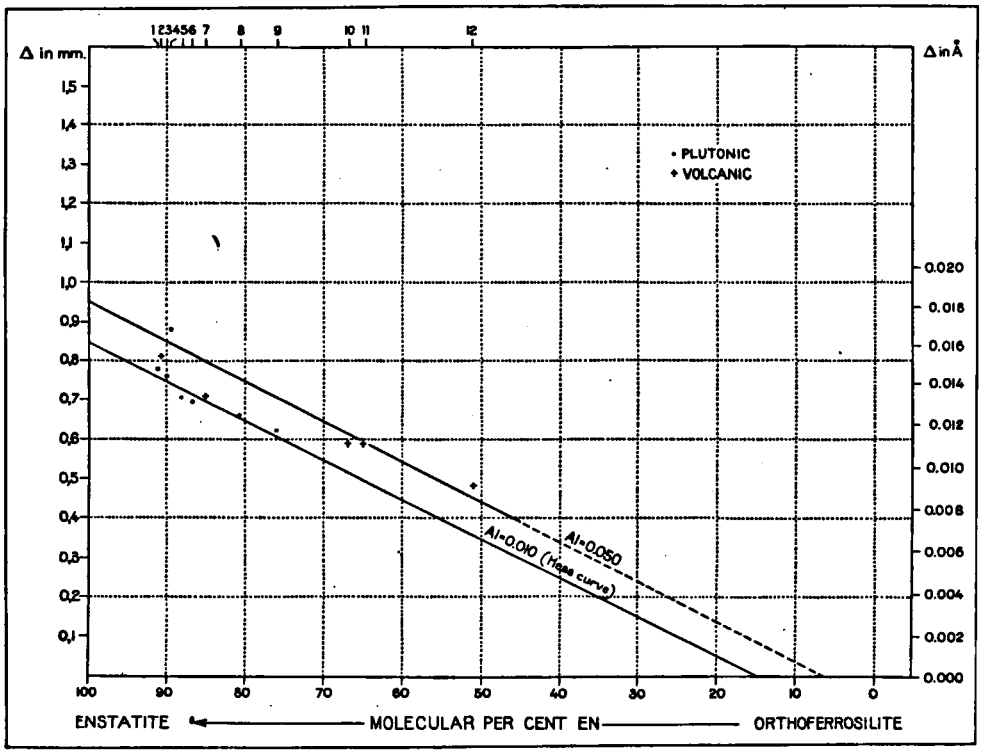

Fig. 8. Δ is relative distance in millimeters and Å between 10 3 1 and 0 6 0 for various orthopyroxenes. The numbers in the upper part of the diagram refer to those in Table 6. The curves are calculated from the data of HESS (1952) and KUNO (1954) about the unit cell dimensions of orthopyroxenes with Al is about 0.010 and Al is about 0.050 in B^{VI} position respectively. The dots and crosses refer to measurements on X-ray powder photographs. The molecular percent enstatite of the specimens is obtained from chemical analysis or N_x. (Camera diameter 9 cm, $FeK\alpha_1$ radiation).

5, 6, 7, 8 and 9 almost give the same idea as do the specimens of HESS. They lie practically on the HESS curve and are all, except for sample No. 7, orthopyroxenes of the Bushveld type. Sample No. 7 is a volcanic orthopyroxene with a low Al content (Al = 0.001 in B^{VI} position).

The remaining specimens that were examined Nos. 2, 4, 10, 11 and 12 appear to behave in a different way; they lie, except for samples No. 2 and 4, more or less on a second curve, about parallel with the HESS curve. These samples are volcanic orthopyroxenes, while specimen No. 4 has a very high proportion of Al and is a plutonic orthopyroxene.

It turns out that not all plutonic specimens lie on the HESS curve and

TABLE 6

Relative distance Δ (in millimeters) between 10 3 1 and 0 6 0 of some orthopyroxenes. Camera diameter 9 cm; FeKα_1 radiation (λ = 1.93597 Å).

Sample Number	Δ(mm)	mol % Enstatite	
		from chem. analysis	from N_z curve Kuno (1954)
1 Enstatite, Great Dyke	0.78	91 (see Table 2)	
2 Enstatite, Finkenberg	0.81		90.6
3 Enstatite, Bonn	0.76		90
4 Bronzite, No. 3a (Hess)	0.88	89.5 (Hess 1952)	
5 Bronzite, Austria	0.71	88 (see Table 2)	
6 Bronzite, Kupferberg	0.70		86.7
7 Bronzite, Bonin Islands	0.71	85 (Hess 1952)	
8 Bronzite, Harz	0.66		80.6
9 Bronzite, Labrador	0.62	76 (Hess 1940)	
10 Hypersthene, Odawara	0.59	67	
11 Hypersthene, Sitisei-zan	0.59	65 (Kuno 1954)	
12 Hypersthene, Kaziya	0.48	51	

not all volcanic specimens on the other one. The Hess curve is suitable for determining the Mg percentage of orthopyroxenes with Al about 0.010 in B^{VI} (Mg) position. The other curve serves for determining the chemical composition of orthopyroxenes with Al about 0.050 in B^{VI} (Mg) position. This curve has been calculated from the data of Kuno (1954) about the unit cell dimensions of orthopyroxenes with Al is about 0.050 in B^{VI} position.

The following may be noted in view of these statements: It is not yet possible to determine the chemical composition of orthopyroxenes with the aid of the relative distance method, because one cannot know beforehand what will be the proportion of Al. In order to know to this, however, we have employed a somewhat more complicated method, which will be described below. One might determine the Al content by deriving the Mg percentage from the N_z curve; this is almost accurate at all, because N_z only slightly depends upon the Al content, but we will still try to determine the Al- and Ca content of orthopyroxenes by means of the X-ray method mentioned above. Before passing on to this subject, we will first discuss some results of the investigation.

It turned out to be impossible to infer simply the plutonic or volcanic character of orthopyroxenes from the X-ray powder diagram. The volcanic or plutonic character can be determined, however, by means of an optical examination, for the volcanics have a zonal structure while the plutonics have a lamellar structure.

Hess and Philips (1938) state that the lamellae which occur in plutonic orthopyroxenes consist of exsolved diopside; we could not establish the presence of an admixture of diopside in the usual X-ray powder diagrams of the plutonic orthopyroxenes but with the aid of a Nonius-Guinier camera (see

foot-note 5) also X-ray powder photographs were made. In the diagrams of samples Nos. 3, 5, 6, 8 and 9 the presence of an admixture of diopside could be seen, these are plutonics with a high atomic proportion of Ca, according to chemical analysis (see Table 3). Therefore we are inclined to support the hypothesis of HESS and PHILIPS. The matter in question should be solved if one made use of a precession-camera, making a photograph of one crystal.

Since the relative distance depends on:

a. the wavelength (λ) of the used radiation,
b. the camera diameter,

it is useful to give a tabulation of the distance between 10 3 1 and 0 6 0 for different radiations and for a few types of camera. This distance will also be given in Å units.

In Table 7a the above mentioned distances are recorded for orthopyroxenes with Al = 0.010 in B^{VI} position and those with Al = 0.050 in B^{VI} position respectively.

Comparison of Both Methods

Since both HESS (1952) and we have proposed a method for determining the chemical composition of certain orthopyroxenes without making a chemical analysis, it is useful to compare these two methods. The method of KUNO (1954). may be considered as an elaboration of the HESS method, so that we will only look at the HESS method.

HESS calculates the unit cell dimensions of each specimen, as already said and from these data he concludes what is the Mg percentage.

With our method, which we will call "the relative distance method", only the relative distance between certain reflections is measured. This distance depends on the size and shape of the unit cell and consequently on the chemical composition and it is possible to calculate the molecular percentage of enstatite from this measurement.

The HESS method requires intricate calculations, that require exact corrections so that errors can be made easily. Our method is quick and practically needs no corrections.

In order to test both methods as to their accuracy, we have calculated the unit cell dimensions of two specimens by means of the reflections 12 0 0, 0 6 0 and 0 0 4. The results have been compared with the measured relative distance (Δ) between 10 3 1 and 0 6 0 on the X-ray powder photographs of these samples.

This gave the following:

	Enstatite No. 1		Bronzite No. 9	
a_0	18.243 Å		18.262 Å	
b_0	8.823 Å	→ 93 mol % En (HESS)	8.865 Å	→ 78 mol % En (HESS)
c_0	5.193 Å		5.205 Å	
Δ	0.78 mm → 93.3 mol % En		0.62 mm → 77.4 mol % En	
Chemical composition from chemical analysis	91.		76.	

TABLE 7a

Distances between 10 3 1 and 0 6 0 for orthopyroxenes with atomic proportion of Al = 0.010 in B^{VI} position.

	θ(0 6 0)–θ(10 3 1) in Hundredths of Degrees* used X-radiation				Δ:(10 3 1)–(0 6 0) in mm for CuKα_1 radiation Camera diameter			Δ:(10 3 1)–(0 6 0) in mm for FeKα_1 radiation Camera diameter			d(10 3 1)–d(0 6 0)
mol % En.	Cu	Fe	Cr	Co	9 cm	11.4 cm	19 cm	9 cm	11.4 cm	19 cm	in Å
100	0.38	0.53	0.76	0.47	0.59	0.74	1.24	0.85	1.06	1.75	0.016
90	0.33	0.47	0.67	0.42	0.52	0.66	1.10	0.74	0.94	1.55	0.014
80	0.28	0.41	0.58	0.36	0.45	0.57	0.95	0.64	0.82	1.34	0.012
70	0.24	0.35	0.49	0.31	0.38	0.48	0.80	0.54	0.69	1.14	0.010
60	0.19	0.28	0.40	0.25	0.31	0.39	0.65	0.44	0.56	0.92	0.009
50	0.15	0.22	0.31	0.19	0.24	0.30	0.50	0.34	0.44	0.72	0.007
40	0.10	0.15	0.22	0.14	0.17	0.21	0.35	0.24	0.31	0.51	0.005
30	0.06	0.09	0.13	0.08	0.10	0.12	0.20	0.14	0.19	0.30	0.003
20	0.02	0.03	0.04	0.03	0.03	0.04	0.06	0.04	0.06	0.10	0.001
10	—	—	—	—	—	—	—	—	—	—	—
0	—	—	—	—	—	—	—	—	—	—	—

Distances between 10 3 1 and 0 6 0 for orthopyroxenes with atomic proportion of Al = 0.050 in B^{VI} position.

	θ(0 6 0)–θ(10 3 1) in Hundredths of Degrees* used X-radiation				Δ:(10 3 1)–(0 6 0) in mm for CuKα_1 radiation Camera diameter			Δ:(10 3 1)–(0 6 0) in mm for FeKα_1 radiation Camera diameter			d(10 3 1)–d(0 6 0)
mol % En.	Cu	Fe	Cr	Co	9 cm	11.4 cm	19 cm	9 cm	11.4 cm	19 cm	in Å
100	0.42	0.60	0.84	0.51	0.67	0.84	1.41	0.94	1.21	1.98	0.018
90	0.38	0.54	0.75	0.46	0.60	0.75	1.25	0.84	1.08	1.76	0.016
80	0.33	0.47	0.66	0.40	0.53	0.66	1.10	0.74	0.95	1.55	0.014
70	0.28	0.40	0.56	0.34	0.46	0.57	0.94	0.64	0.81	1.34	0.012
60	0.24	0.34	0.47	0.28	0.38	0.48	0.79	0.54	0.68	1.12	0.010
50	0.20	0.27	0.37	0.23	0.30	0.39	0.63	0.44	0.55	0.91	0.008
40	0.15	0.20	0.28	0.17	0.24	0.30	0.48	0.34	0.41	0.70	0.006
30	0.10	0.14	0.19	0.12	0.16	0.21	0.32	0.24	0.28	0.49	0.004
20	0.06	0.07	0.09	0.06	0.09	0.12	0.17	0.14	0.15	0.28	0.002
10	0.02	0.01	0.00	0.01	0.02	0.03	0.02	0.04	0.02	0.07	0.000
0	—	—	—	—	—	—	—	—	—	—	—

* θ is given in hundredths of degrees (circumference of a circle = 360°).

TABLE 7b

Distances between quartz reflection $2\,1\,\bar{3}\,1$ and pyroxene reflection $0\,6\,0$ for orthopyroxenes with atomic proportion of Al = 0.010 in B^{VI} position.

	$\theta(0\,6\,0)-\theta(2\,1\,\bar{3}\,1)$ in Hundredths of Degrees used X-radiation				$\Delta:(2\,1\,\bar{3}\,1)-(0\,6\,0)$ in mm for $CuK\alpha_1$ radiation Camera diameter			$\Delta:(2\,1\,\bar{3}\,1)-(0\,6\,0)$ in mm for $FeK\alpha_1$ radiation Camera diameter			$d(2\,1\,\bar{3}\,1)-d(0\,6\,0)$
mol % En.	Cu	Fe	Cr	Co	9 cm	11.4 cm	19 cm	9 cm	11.4 cm	19 cm	in Å
100	1.66	2.34	3.27	2.05	2.60	3.30	5.49	3.72	4.67	7.78	0.074
90	1.56	2.20	3.08	1.94	2.45	3.10	5.17	3.49	4.40	7.31	0.070
80	1.46	2.06	2.88	1.81	2.29	2.91	4.84	3.26	4.12	6.86	0.065
70	1.36	1.92	2.68	1.69	2.14	2.72	4.52	3.03	3.84	6.37	0.061
60	1.26	1.78	2.48	1.57	1.99	2.53	4.20	2.80	3.56	5.91	0.057
50	1.16	1.64	2.28	1.45	1.84	2.34	3.88	2.58	3.28	5.46	0.053
40	1.07	1.50	2.09	1.33	1.68	2.14	3.56	2.36	3.00	4.99	0.048
30	0.97	1.36	1.89	1.21	1.53	1.95	3.24	2.13	2.72	4.53	0.044
20	0.87	1.22	1.69	1.09	1.38	1.76	2.92	1.92	2.44	4.06	0.040
10	0.78	1.08	1.49	0.97	1.22	1.56	2.60	1.70	2.17	3.60	0.036
0	0.68	0.94	1.29	0.85	1.07	1.37	2.28	1.48	1.91	3.16	0.032

Distances between quartz reflection $2\,1\,\bar{3}\,1$ and pyroxene reflection $0\,6\,0$ for orthopyroxenes with atomic proportion of Al = 0.050 in B^{VI} position.

	$\theta(0\,6\,0)-\theta(2\,1\,\bar{3}\,1)$ in Hundredths of Degrees used X-radiation				$\Delta:(2\,1\,\bar{3}\,1)-(0\,6\,0)$ in mm for $CuK\alpha_1$ radiation Camera diameter			$\Delta:(2\,1\,\bar{3}\,1)-(0\,6\,0)$ in mm for $FeK\alpha_1$ radiation Camera diameter			$d(2\,1\,\bar{3}\,1)-d(0\,6\,0)$
mol % En.	Cu	Fe	Cr	Co	9 cm	11.4 cm	19 cm	9 cm	11.4 cm	19 cm	in Å
100	1.71	2.44	3.38	2.14	2.67	3.40	5.65	3.83	4.85	8.09	0.076
90	1.61	2.29	3.18	2.01	2.52	3.20	5.33	3.60	4.56	7.59	0.071
80	1.51	2.14	2.98	1.88	2.36	3.00	5.00	3.36	4.27	7.09	0.066
70	1.41	1.99	2.77	1.75	2.21	2.80	4.67	3.12	3.95	6.59	0.062
60	1.31	1.84	2.57	1.62	2.06	2.61	4.34	2.89	3.66	6.09	0.058
50	1.21	1.69	2.36	1.49	1.90	2.41	4.01	2.66	3.36	5.60	0.053
40	1.11	1.54	2.16	1.36	1.75	2.21	3.68	2.43	3.07	5.11	0.049
30	1.01	1.40	1.96	1.24	1.59	2.01	3.35	2.19	2.77	4.62	0.045
20	0.91	1.25	1.76	1.11	1.44	1.82	3.02	1.96	2.48	4.13	0.041
10	0.81	1.10	1.56	0.99	1.29	1.62	2.69	1.72	2.18	3.64	0.036
0	0.71	0.95	1.36	0.86	1.14	1.42	2.37	1.48	1.89	3.15	0.031

TABLE 7c

Distances between quartz reflection $(2\,0\,\bar{2}\,3)\,(3\,0\,\bar{3}\,1)$ and pyroxene reflection 11 3 1 for orthopyroxenes with atomic proportion of Ca = 0.020.

	$\theta(2\,0\,\bar{2}\,3)(3\,0\,\bar{3}\,1)$–$\theta(11\,3\,1)$ in Hundredths of Degrees used X-radiation				Δ:(11 3 1)–$(2\,0\,\bar{2}\,3)(3\,0\,\bar{3}\,1)$ in mm for $CuK\alpha_1$ radiation Camera diameter			Δ:(11 3 1)–$(2\,0\,\bar{2}\,3)(3\,0\,\bar{3}\,1)$ in mm for $FeK\alpha_1$ radiation Camera diameter			$d(11\,3\,1)$–$d(2\,0\,\bar{2}\,3)(3\,0\,\bar{3}\,1)$ in Å
mol % En.	Cu	Fe	Cr	Co	9 cm	11.4 cm	19 cm	9 cm	11.4 cm	19 cm	
100	0.43	0.64	0.95	0.56	0.70	0.88	1.38	1.00	1.26	2.10	0.016
90	0.49	0.72	1.06	0.62	0.78	0.98	1.58	1.13	1.42	2.36	0.018
80	0.54	0.80	1.18	0.69	0.86	1.09	1.76	1.25	1.57	2.63	0.020
70	0.60	0.88	1.30	0.76	0.94	1.19	1.95	1.38	1.73	2.90	0.022
60	0.65	0.96	1.42	0.82	1.02	1.30	2.14	1.51	1.89	3.16	0.024
50	0.71	1.04	1.54	0.89	1.10	1.41	2.33	1.63	2.05	3.44	0.026
40	0.76	1.12	1.66	0.96	1.19	1.52	2.52	1.76	2.22	3.72	0.028
30	0.82	1.20	1.79	1.03	1.28	1.63	2.72	1.89	2.38	3.98	0.030
20	0.88	1.28	1.91	1.10	1.36	1.75	2.91	2.02	2.54	4.25	0.032
10	0.93	1.37	2.03	1.17	1.45	1.86	3.11	2.14	2.71	4.52	0.034
0	0.99	1.45	2.15	1.24	1.54	1.97	3.31	2.27	2.87	4.77	0.036

Distances between quartz reflection $(2\,0\,\bar{2}\,3)\,(3\,0\,\bar{3}\,1)$ and pyroxene reflection 11 3 1 for orthopyroxenes with atomic proportion of Ca = 0.060.

	$\theta(2\,0\,\bar{2}\,3)(3\,0\,\bar{3}\,1)$–$\theta(11\,3\,1)$ in Hundredths of Degrees used X-radiation				Δ:(11 3 1)–$(2\,0\,\bar{2}\,3)(3\,0\,\bar{3}\,1)$ in mm for $CuK\alpha_1$ radiation Camera diameter			Δ:(11 3 1)–$(2\,0\,\bar{2}\,3)(3\,0\,\bar{3}\,1)$ in mm for $FeK\alpha_1$ radiation Camera diameter			$d(11\,3\,1)$–$d(2\,0\,\bar{2}\,3)(3\,0\,\bar{3}\,1)$ in Å
mol % En.	Cu	Fe	Cr	Co	9 cm	11.4 cm	19 cm	9 cm	11.4 cm	19 cm	
100	0.48	0.69	1.09	0.63	0.80	0.99	1.66	1.11	1.39	2.31	0.018
90	0.53	0.78	1.20	0.69	0.88	1.10	1.82	1.23	1.55	2.57	0.020
80	0.59	0.86	1.31	0.76	0.96	1.20	1.99	1.36	1.71	2.84	0.022
70	0.64	0.94	1.42	0.82	1.03	1.30	2.16	1.48	1.86	3.10	0.024
60	0.70	1.02	1.53	0.89	1.11	1.40	2.32	1.60	2.02	3.36	0.026
50	0.75	1.10	1.64	0.95	1.19	1.50	2.49	1.72	2.18	3.63	0.028
40	0.81	1.18	1.75	1.02	1.27	1.60	2.67	1.84	2.35	3.91	0.030
30	0.86	1.26	1.86	1.08	1.35	1.70	2.84	1.97	2.51	4.17	0.032
20	0.92	1.34	1.97	1.15	1.43	1.80	3.01	2.09	2.67	4.44	0.034
10	0.98	1.42	2.08	1.22	1.51	1.91	3.18	2.21	2.83	4.70	0.036
0	1.03	1.50	2.22	1.28	1.59	2.01	3.35	2.34	2.99	4.97	0.038

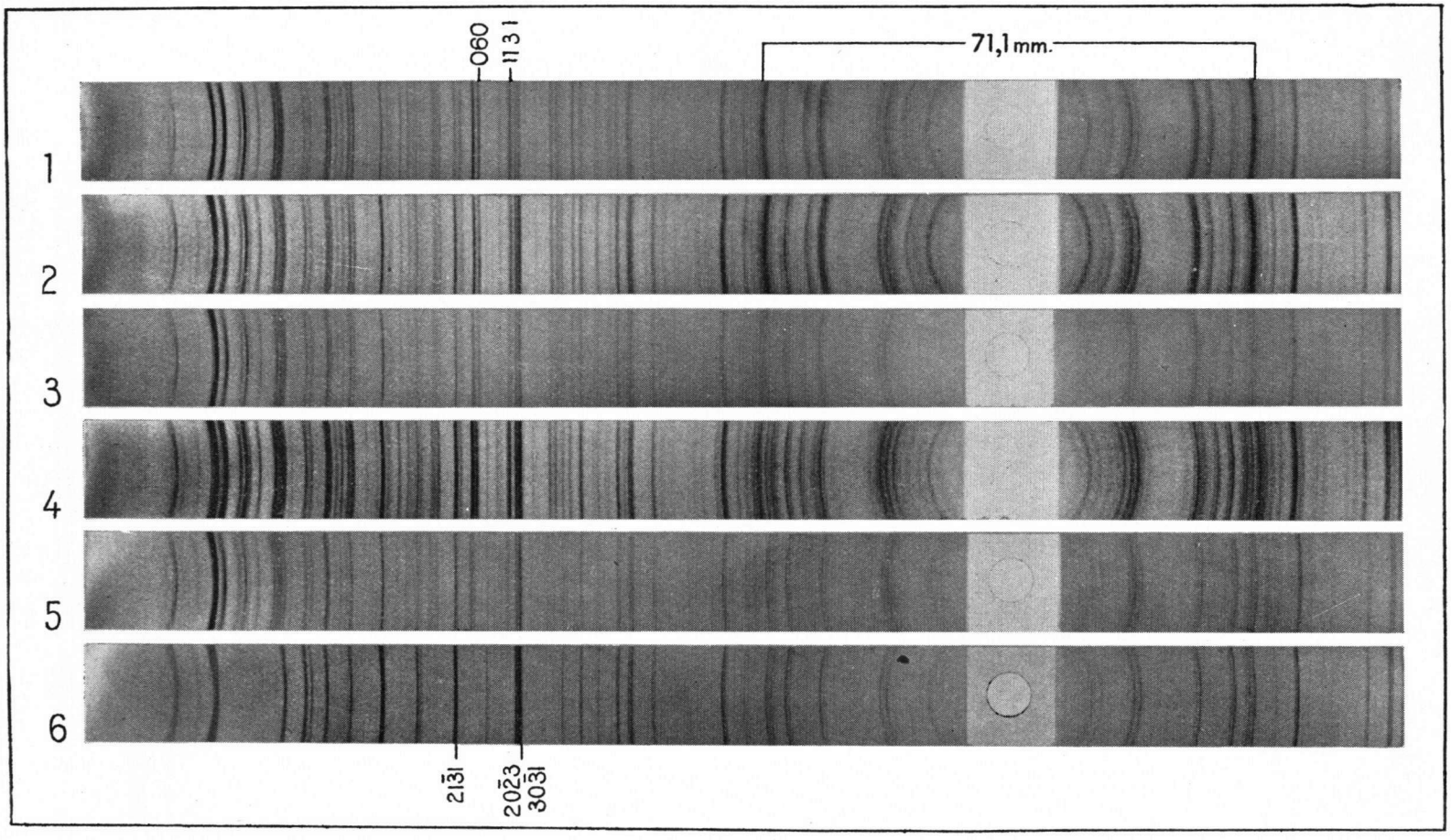

Fig. 9. X-ray powder photographs of a mixture of 70 % orthopyroxene and 30 % quartz. ($FeK\alpha_1$ radiation, Camera diameter 9 cm).

No. 1	Enstatite No. 1, Southern Rhodesia, st. 28685	m* 1331	No. 4	Hypersthene No. 11, Sitisei-zan, Japan	m 1333
No. 2	Bronzite No. 5, Kraubat, Austria	m 1332	No. 5	Hypersthene No. 12, Kaziya, Japan	m 1340
No. 3	Bronzite No. 7, Bonin Islands, Japan	m 1350	No. 6	Quartz	m 956

* Number X-ray photograph.

It is seen from these data that both methods are about equal in accuracy because the difference between the results amounts to less than 1 percent, while the difference with the chemical analyses for both methods is 2 to 3 %. One may say therefore in conclusion that both methods are useful for determining the chemical composition of certain orthopyroxenes, but as the HESS method is time consuming the relative distance method is preferable, because the procedure is particularly quick and as already proved, is equally accurate.

Extension of the Relative Distance Method

In order to determine the Al and Ca content of orthopyroxenes by means of a röntgenographic method exclusively, we have used a method which will be described here now. X-ray powder diagrams were made of orthopyroxenes mixed with ± 30 % quartz. In these mixed diagrams the distance between

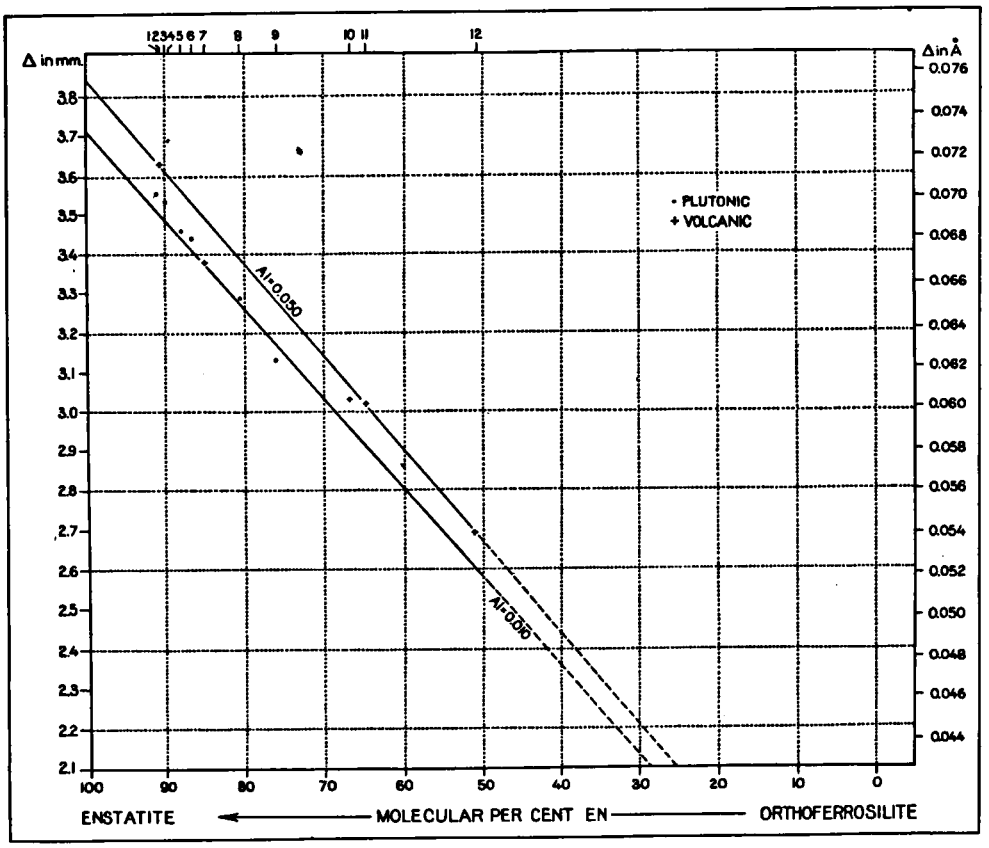

Fig. 10. Δ is relative distance in millimeters and Å between quartz reflection $2\,1\,\bar{3}\,1$ and orthopyroxene reflection 0 6 0 for various orthopyroxenes. The numbers in the upper part of the diagram refer to those in Table 8. The curves are calculated from the data of KUNO (1954) about the unit cell dimensions of orthopyroxenes with Al is about 0.010 and Al is about 0.050 in B^{VI} position. The dots and crosses refer to measurements on X-ray powder photographs. (Camera diameter 9 cm; $FeK\alpha_1$ radiation).

quartz reflection 2 1 $\bar{3}$ 1 and orthopyroxene reflection 0 6 0 has been measured, together with the distance between quartz line (2 0 $\bar{2}$ 3) (3 0 $\bar{3}$ 1) and orthopyroxene line 11 3 1. Since both quartz reflections have a fixed place in the pattern, the variation of these distances will depend on the positions of the orthopyroxene reflections. The lines 0 6 0 and 11 3 1 were selected for this purpose, because they prove to be very sensitive as regards changes in position, the more so as 0 6 0 is under the influence of the changeable b dimension, while 11 3 1, as appeared from a theoretical calculation, seems

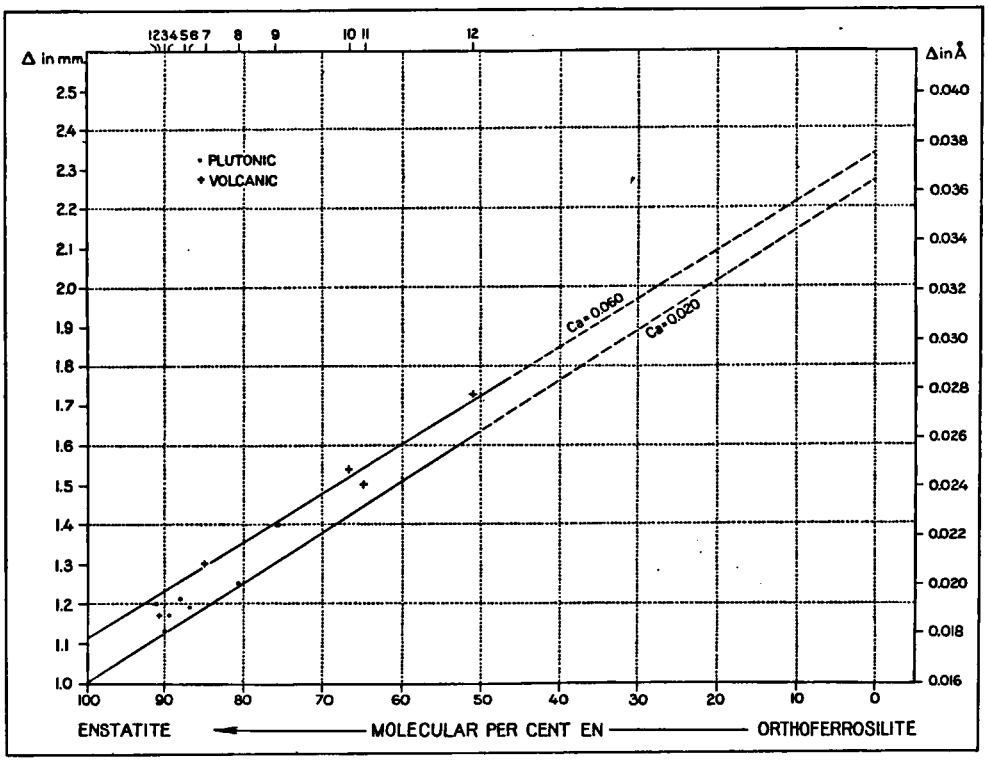

Fig. 11. Δ is relative distance in millimeters and Å between quartz reflection (2 0 $\bar{2}$ 3) (3 0 $\bar{3}$ 1) and orthopyroxene reflection 11 3 1 for various orthopyroxenes. The numbers in the upper part of the diagram refer to those in Table 8. The curves are calculated from the data of KUNO (1954) about the unit cell dimensions of orthopyroxenes with Ca is about 0.020 and Ca is about 0.060. The dots and crosses refer to measurements on X-ray powder photographs. (Camera diameter 9 cm; Fe$K\alpha_1$ radiation).

to be mainly under the influence of the variable a dimension. In fig. 9 some of these mixed diagrams are reproduced and by careful examination of the distance between quartz reflection 2 1 $\bar{3}$ 1 and orthopyroxene reflection 0 6 0, together with the distance between quartz reflection (2 0 $\bar{2}$ 3) (3 0 $\bar{3}$ 1) and orthopyroxene reflection 11 3 1, distinct changes can be seen. The former distance becomes smaller going from enstatite No. 1 to hypersthene No. 12, while the latter distance becomes greater. These distances were measured on all mixed diagrams; the data are given in Table 8. The distance between

quartz reflection $2\,1\,\bar{3}\,1$ and orthopyroxene reflection 0 6 0 is plotted against the chemical composition in fig. 10; the distance between quartz reflection $(2\,0\,\bar{2}\,3)$ $(3\,0\,\bar{3}\,1)$ and orthopyroxene reflection 11 3 1 was also plotted against the chemical composition in fig. 11.

TABLE 8

Relative distance $\Delta 1$ (in millimeters) between $2\,1\,\bar{3}\,1$ (quartz) and 0 6 0 (pyroxene) and $\Delta 2$ (in millimeters) between $(2\,0\,\bar{2}\,3)(3\,0\,\bar{3}\,1)$ (quartz) and 11 3 1 (pyroxene). Camera diameter 9 cm; $FeK\alpha_1$ radiation ($\lambda = 1.93597$ Å).

Sample Number	$\Delta 1$	$\Delta 2$	mol % Enstatite	
			from chem. analysis	from N_z curve KUNO (1954)
1. Enstatite, Great Dyke	3.56	1.20	91 (see Table 2)	
2. Enstatite, Finkenberg	3.63	1.17		90.6
3. Enstatite, Bonn	3.54	1.13		90
4. Bronzite, No 3a (HESS)	3.69	1.17	89.5 (HESS 1952)	
5. Bronzite, Austria	3.46	1.21	88 (see Table 2)	
6. Bronzite, Kupferberg	3.44	1.19		86.7
7. Bronzite, Bonin Islands	3.38	1.30	85 (HESS 1952)	
8. Bronzite, Harz	3.29	1.25		80.6
9. Bronzite, Labrador	3.13	1.40	76 (HESS 1940)	
10. Hypersthene, Odawara	3.03	1.54	67	
11. Hypersthene, Sitisei-zan	3.02	1.50	65 (KUNO 1954)	
12. Hypersthene, Kaziya	2.69	1.73	51	

It turns out from fig. 10 that the specimens Nos. 1, 3, 5, 6, 7, 8 and 9 lie more or less on a straight line. According to the chemical analyses these samples have a low to moderate Al content; this line in fig. 10 has been calculated from data, given by KUNO (1954), about the unit cell dimensions of orthopyroxenes with Al is about 0.010 in B^{VI} position and indicates orthopyroxenes with Al about 0.010 in B^{VI} position. The remaining specimens Nos. 2, 4, 10, 11 and 12 lie approximately on a second line; these are orthopyroxenes with a high proportion of Al. This curve, also calculated from data given by KUNO (1954), indicates orthopyroxenes with Al about 0.050 in B^{VI} position. It may be noted, that sample No. 4 lies far above this second line; this orthopyroxene has according to HESS (1952) an abnormally high Al content. Further it may be seen from the diagram that there exists a linear function between the relative distance Δ (from quartz reflection $2\,1\,\bar{3}\,1$ and pyroxene reflection 0 6 0) and the chemical composition, for both Al rich and Al poor orthopyroxenes.

It is seen here again that the b dimension is strongly under the influence of the Al content and therefore also the reflection 0 6 0; this agrees with the results of HESS and KUNO. In fig. 11, where the distance between the quartz line (2 0 $\bar{2}$ 3) (3 0 $\bar{3}$ 1) and the orthopyroxene line 11 3 1 has been plotted against the chemical composition, there are also two linear functions noticeable. According to the chemical investigation the samples lying close to the lower line, have a low Ca content while the other specimens have a high proportion of Ca. These two curves indicate orthopyroxenes with Ca about 0.020 and orthopyroxenes with Ca about 0.060. They are calculated from data, given by KUNO (1954), about the unit cell dimensions of pyroxenes with an atomic proportion of Ca is 0.020 and 0.060 respectively.

It appears now from diagram that the position of reflection 11 3 1 strongly depends upon the Ca content and with that the a dimension as has already been mentioned on p. 207. This also agrees with the results of KUNO (1954).

In the Tables 7b and 7c a tabulation of the above mentioned distances is given for different radiations and for a few types of camera.

Conclusions — With some reserve it is possible to determine the Mg percentage of orthopyroxenes by means of X-ray study; this can be worked out with the aid of the relative distance method. At the same time it can be determined whether the proportions of Al and Ca are high or low, in most cases these proportions may even be determined.

Technique of Investigation

These determinations can be carried out as follows: one prepares an X-ray powder diagram of a mixture of ± 70 % orthopyroxene material and ± 30 % quartz. Three relative distances must be measured on the resulting diagrams; 1°. the distance between quartz reflection 2 1 $\bar{3}$ 1 and orthopyroxene reflection 0 6 0; 2°. the distance between quartz reflection (2 0 $\bar{2}$ 3) (3 0 $\bar{3}$ 1) and orthopyroxene reflection 11 3 1; 3°. the relative distance between orthopyroxene reflections 10 3 1 and 0 6 0.

With the aid of these data one may trace in the respective figures, what is the Mg percentage. In each figure two values result, one for high and one for low proportions of Al or Ca. Of these six values, three will be practically equal to each other. The average of these three will indicate the Mg percentage, while at the same time the Al and Ca contents can be read off.

For illustration we may take for this purpose sample No. 7 (Bronzite, Bonin Islands).

Δ (relative distance) between quartz reflection 2 1 $\bar{3}$ 1 and orthopyroxene reflection 0 6 0 is 3.38 mm → (see fig. 10) mg = 85 or 80.5.

Δ (relative distance) between quartz reflection (2 0 $\bar{2}$ 3) (3 0 $\bar{3}$ 1) and orthopyroxene reflection 11 3 1 is 1.30 mm → (see fig. 11) mg = 84.8 or 76.5.

Δ (relative distance) between orthopyroxene reflections 10 3 1 and 0 6 0 is 0.71 mm → (see fig. 8) mg = 86.5 or 77.

It is evident now from these data that the Mg percentages 86.5, 85 and 84.8 practically correspond with each other; their average value is 85.4, which

is the Mg percentage of this specimen. From chemical analysis is calculated an Mg percentage of 85 (HESS 1952 and KUNO 1954).

Considering the figures 8, 10 and 11 for Mg = 85.4 it turns out now

from fig. 10 → Al is about 0.005
from fig. 8 → Al is about 0.015
and from fig. 11 → Ca is about 0.065.

The average proportions for Al and Ca are 0.010 and 0.065 respectively. From chemical analysis (KUNO 1954) were calculated Al = 0.001 and Ca = 0.068 (see Table 3). In this example surprisingly good results were obtained; the utility of the relative distance method has been demonstrated very clearly in this case.

At the same time it is shown once more in this example that one cannot simply distinguish between plutonic and volcanic orthopyroxenes as regards their proportions of Al and Ca, for this volcanic specimen turns out to have a low Al and a high Ca content. We can agree with KUNO when he states: "The only difference between the volcanic orthopyroxenes and those of Bushveld type is found in the variation of 2 V according to Mg per cent." (1954)

Essential Difficulties Attending the Relative Distance Method.

When employing this method to all the described orthopyroxenes it turns out, that in certain cases it is impossible to determine exactly the molecular percentage of enstatite; in such cases one obtains more than one combination of mg's, which lie close to each other. In order to illustrate this, here follow the results of the application of this method and at the same time are listed, for comparison, the results of the chemical analyses and the optical investigation. To simplify the matter we suppose that:

Δ_1 is the relative distance between the pyroxene reflections 10 3 1 and 0 6 0 (see fig. 8 and Table 6),

Δ_2 is the relative distance between quartz reflection $2\,1\,\bar{3}\,1$ and pyroxene reflection 0 6 0 (see fig. 10 and Table 8),

Δ_3 is the relative distance between quartz reflection $(2\,0\,\bar{2}\,3)$ $(3\,0\,\bar{3}\,1)$ and pyroxene reflection 11 3 1 (see fig. 11 and Table 8).

$$mg = \frac{100\,Mg^{+2}}{Mg^{+2} + Fe^{+2} + Fe^{+3} + Mn^{+2}}$$

Al and Ca are the atomic proportions of these elements on the basis of six oxygen atoms (Al only in B^{VI} position).

Enstatite No. 1.

		According to chemical analysis.
$\Delta_1 = 0.78 \rightarrow 93$ or 84 $\Delta_2 = 3.56 \rightarrow 93.5$ or 88.5 $\Delta_3 = 1.20 \rightarrow 92.5$ or 84.5	Al = 0.012 Ca = 0.060	0.030 0.019
$mg = \frac{93 + 93.5 + 92.5}{3} = 92.8$		91

For this orthopyroxene it is almost possible to determine exactly the value of mg but the Al- and Ca content do not line up with those calculated from the chemical analysis.

Enstatite No. 2.

According to optical investigation.

$\Delta_1 = 0.81 \rightarrow 96$ or 86.5
$\Delta_2 = 3.63 \rightarrow 96$ or 91.5
$\Delta_3 = 1.17 \rightarrow 95$ or 86.5

Al = 0.012 or 0.050
Ca = 0.065 or 0.030

$$mg = \frac{96+96+95}{3} = 95.6 \text{ or } mg = \frac{86.5+91.5+86.5}{3} = 88.2 \quad 90.6$$

Here it is not possible to determine the molecular percentage of enstatite unequivocally by this method.

Enstatite No. 3.

According to optical investigation.

$\Delta_1 = 0.76 \rightarrow 91$ or 81.5
$\Delta_2 = 3.54 \rightarrow 92.5$ or 88
$\Delta_3 = 1.13 \rightarrow 98.5$ or 89.5

Al = 0.010
Ca = 0.025

$$mg = \frac{91 + 92.5 + 89.5}{3} = 91 \qquad 90$$

It is evident that in this case the method does make possible an exact determination of mg.

Bronzite No. 4.

According to chemical analysis.

$\Delta_1 = 0.88 \rightarrow > 100$ or 93
$\Delta_2 = 3.69 \rightarrow 98.5$ or 94
$\Delta_3 = 1.17 \rightarrow 95$ or 86.5

Al = 0.050
Ca = 0.050

very high (4.00%)

$$mg = \frac{93 + 94 + 95}{3} = 94 \qquad 89.5$$

The method fails for this orthopyroxene, this is a consequence of the fact that it is a bronzite with an abnormally high Al content (4.00 %, Hess, 1952). But the optical method indicates an mg-value more in correspondence with that calculated from chemical analysis. A combination of the optical method with the X-ray method would be preferable therefore. In that case it can be seen that there is something abnormals forward.

Bronzite No. 5.

According to chemical analysis.

$\Delta_1 = 0.71 \rightarrow 86.5$ or 77
$\Delta_2 = 3.46 \rightarrow 89$ or 84.5
$\Delta_3 = 1.21 \rightarrow 92$ or 83.5

Al = 0.005 — 0.002
Ca = 0.045 — 0.063

$$mg = \frac{86.5 + 89 + 92}{3} = 89.2 \qquad 88$$

Here the value of mg agrees rather well with that calculated from chemical analysis and the same is the case for the Al content. The value of Ca is not so good, but the Ca content calculated from the chemical analysis is very high for an orthopyroxene of the Bushveld type. It is quite possible that a part of this Ca content (according to chemical analysis) is present in exsolved diopside lamellae and therefore not affects the cell dimensions of the bronzite itself.

Bronzite No. 6.

		According to chemical analysis.
$\Delta_1 = 0.70 \rightarrow 85.5$ or 76 $\Delta_2 = 3.44 \rightarrow 88$ or 83.5 $\Delta_3 = 1.19 \rightarrow 93.5$ or 85	Al = 0.012 Ca = 0.025	0.005 0.056
$mg = \frac{85.5 + 88 + 85}{3} = 86.2$		86.7

In this case the method works well again. The Ca content which is calculated from a chemical analysis by HINTZE (1897) for a bronzite of the same locality is very high; probably the value as determined by röntgenographic method is even more exact than the chemical value, because presence of lamellae renders it possible that a part of this Ca content, as calculated from chemical analysis, is present in exsolved diopside.

Bronzite No. 7.

		According to chemical analysis.
$\Delta_1 = 0.71 \rightarrow 86.5$ or 77 $\Delta_2 = 3.38 \rightarrow 85$ or 80.5 $\Delta_3 = 1.30 \rightarrow 84.8$ or 76.5	Al = 0.010 Ca = 0.065	0.001 0.068
$mg = \frac{86.5 + 85 + 84.8}{3} = 85.4$		85

For this bronzite of volcanic origin, the method gives results practically the same as those calculated from chemical analysis.

Bronzite No. 8.

		According to optical investigation.
$\Delta_1 = 0.66 \rightarrow 81.5$ or 72 $\Delta_2 = 3.29 \rightarrow 81.5$ or 77 $\Delta_3 = 1.25 \rightarrow 88.5$ or 80.5	Al = 0.010 Ca = 0.025	
$mg = \frac{81.5 + 81.5 + 80.5}{3} = 81.2$		81

In this case the method gives an excellent result.

Bronzite No. 9.

		According to chemical analysis.
$\Delta_1 = 0.62 \rightarrow 77$ or 68 $\Delta_2 = 3.13 \rightarrow 74.5$ or 70.5 $\Delta_3 = 1.40 \rightarrow 76$ or 68.5	Al = 0.007 or 0.050 Ca = 0.055 or 0.020	0.000 0.076
$mg = \frac{77+74.5+76}{3} = 75.8$ or $mg = \frac{68+70.5+68.5}{3} = 69$		76

An exact determination of the mg value is impossible for this orthopyroxene. A part of the Ca content (according to chemical analysis) may be present in exsolved diopside lamellae.

Hypersthene No. 10.

		According to chemical analysis.
$\Delta_1 = 0.59 \rightarrow 74$ or 65 $\Delta_2 = 3.03 \rightarrow 70$ or 66 $\Delta_3 = 1.54 \rightarrow 65$ or 57	Al = 0.045 Ca = 0.060	0.021 0.049
$mg = \frac{65 + 66 + 65}{3} = 65.3$		67

The method works well as regards the determination of mg and Ca. The determination of Al does not fit in with that calculated from the chemical analysis.

Remarkably enough this is also the case in the paper of KUNO (1954). He observed for the b dimension 8.884 Å which, according to his diagram, corresponds with Al = 0.050. Thus the method of KUNO and our method practically give the same result.

Hypersthene No. 11.

		According to chemical analysis.
$\Delta_1 = 0.59 \rightarrow 74$ or 65 $\Delta_2 = 3.02 \rightarrow 69.5$ or 65.5 $\Delta_3 = 1.50 \rightarrow 68$ or 60.5	Al = 0.045 Ca = 0.040	0.000 0.034
$mg = \frac{65 + 65.5 + 68}{3} = 66.2$		65

Here again, the Al determination is considerably different from that calculated from chemical analysis. The method of KUNO indicates Al = 0.050, thus corresponding again with the relative distance method.

Hypersthene No. 12.

		According to chemical analysis.
$\Delta_1 = 0.48 \rightarrow 63$ or 54 $\Delta_2 = 2.69 \rightarrow 55$ or 51 $\Delta_3 = 1.73 \rightarrow 49.5$ or 42	Al = 0.055 Ca = 0.070	0.069 0.072
$mg = \frac{54 + 51 + 49.5}{3} = 51.5$		51

For this orthopyroxene the method serves well again.

TABLE 9

Chemical composition of the investigated orthopyroxenes.

Sample Number	Determined by chemical method			Determined by optical method	Determined by the relative distance method			
	mg	Al	Ca	mg	mg	Al	Ca	range of mg*
1. Enstatite	91	0.030	0.019	(91)	92.8	0.012	0.060	
2. Enstatite				90.6	95.6 or 90.6	0.012 or 0.050	0.065 or 0.030	96 to 86.5
3. Enstatite				90	91	0.010	0.025	
4. Bronzite	89.5	very high (± 4%)		(91)	94!	0.050	0.050	
5. Bronzite	88	0.002	0.063	(89)	89.2	0.005	0.045	
6. Bronzite	86.7	0.005	0.056	(87)	86.2	0.012	0.025	
7. Bronzite	85	0.001	0.068	(84.8)	85.4	0.010	0.065	
8. Bronzite				81	81.2	0.010	0.025	
9. Bronzite	76	0.000	0.076	(76.5)	75.8 or 69	0.007 or 0.050	0.055 or 0.020	77 to 68
10. Hypersthene	67	0.021	0.049	(66)	65.3	0.045	0.060	
11. Hypersthene	65	0.000	0.034	(65.5)	66.2	0.045	0.040	
12. Hypersthene	51	0.069	0.072	(51)	51.5	0.055	0.070	

* Extreme values (for dubious cases) between which mg is situated, when exact values could not be determined.

From the above mentioned data, which are conveniently arranged in Table 9, it is seen that the relative distance method only functions if the values for Al and Ca correspond with values of our curves. This means that one obtains good results if the Al- and Ca contents are high or low i. e. Al content is about 0.010 or about 0.050 and Ca content is about 0.020 or about 0.060. For some plutonic samples the determination of the Ca content would be good if one accepts that lamellae which are present consist of diopside.

In all other cases one finds a certain range for mg, the average of which approximates rather closely the mg value calculated from chemical analysis. It may be pointed out that in such cases the optical method of investigation functions better. Let us now discuss such a case:

When comparing the usual relative distances of bronzite No. 9 and hypersthene No. 11, only small differences can be observed, although according to their chemical analyses their molecular percentages of enstatite are quite different (76 and 65 respectively). So although the relative distances will be measured by means of an exact measuring instrument, which, after all, always is a requisite for this method, in this case an exact determination is practically impossible because the selection of three mg's which lie close to each other cannot be determinative for bronzite No. 9. Exactly in such cases the optical method of investigation gives a much better result, for these orthopyroxenes show great differences in their optical properties (see Table 1). The reason for this is, of course, that the substitution of Fe for Mg has a great influence on the refractive indices. These are dependent on the molecular refractions of the ions; with the above mentioned substitution this changes greatly. On the other hand the substitution of Fe for Mg has little effect on the shape of the unit cell. The three unit cell dimensions all do become greater with a higher Fe content, but not so much that the shape of the cell changes importantly.

With a restricted substitution of Al and Ca for Mg the unit cell dimensions do change greatly and therefore also the shape of the cell. This may be seen from the following example:

For a hypersthene with 38 mol % Fe, 3 mol % Ca and 2 mol % Al (sample No. 13 in KUNO's paper, 1954), the following unit cell dimensions were observed: a = 18.340 Å, b = 8.893 Å and c = 5.220 Å. If there had only been present 1 % Ca and 1 % Al then would be a = 18.306 Å, b = 8.902 Å and c = 5.213 Å.

To obtain the original unit cell dimensions for 1 % Ca and 1 % Al, there would be necessary for the a dimension 54.4 % Fe, for the b dimension 34.5 % Fe and for the c dimension 48 % Fe. This proves that:

a. substitution of 2 % Ca for Mg has as much influence on the a dimension as substitution of 16.4 % Fe for Mg.
b. substitution of 1 % Al for Mg has as much influence on the b dimension as substitution of 3.5 % Fe for Mg.
c. substitution of 2 % Ca for Mg has as much influence on the c dimension as substitution of 10 % for Mg.

So it is seen, that the molecular percentage of enstatite can best be determined by optical investigation while the Al- and Ca contents best can be roughly estimated with the aid of the relative distance method.

A rough approximation of the value of mg, however, is always possible

with the X-ray method, so that in those cases, in which the optical method is impossible for practical reasons, as for instance with extrusives with very dense groundmasses, the relative distance method can be applied as a second choice.

Explanation of the Behaviour of the Characteristic Reflections

When HESS (1952) and KUNO (1954) found out the chemical composition of orthopyroxenes by means of the measurement of the unit cell dimensions, they both tried to explain the cause of the changes in these unit cell dimensions.

HESS says that when Fe is substituted for Mg, all three dimensions increase regularly, although the c dimension changes to a less extent. These increases are so regular that he even gives equations on certain conditions, from which one may calculate the three dimensions if mg is known. These equations apply only for orthopyroxenes of the Bushveld type, which, according to HESS, as already was mentioned on p. 191, contain a certain percentage of R_2O_3 (about 2.75 percent by weight) in which R consists predominantly of Al_2O_3.

For Al rich orthopyroxenes the b dimension appears to be considerably smaller than that for normal specimens, while the a- and c dimensions are practically the same as for normal series. According to HESS the b dimension decreases regularly with the substitution of the smaller Al^{+3} or other R^{+3} ions. The b dimension of an enstatite from a meteorite, which did not contain Al, was larger than that of a normal enstatite with the same Mg percentage, so that it is seen that the Al^{+3} ion does exert an influence on the b dimension.

It turns out according to HESS, that the substitution of the larger Al^{+3} ion for the smaller Si^{+4} ion first increases the length of the SiO_3-chains, but larger amounts of Al^{+3} possibly cause the SiO_3-chains to zigzag in the (0 1 0) plane.

Further the b dimension of highly aluminous orthopyroxenes turns out to be approximately equal to b for pure $MgSiO_3$. Therefore HESS suggests, that this value of the b dimension (8.810 Å) perhaps is the minimum value for the b dimension for such an orthopyroxene structure and that this may represent the maximum amount of R_2O_3 which the structure can accomodate for a given Mg/Fe ratio. To investigate this further, more analyses of orthopyroxenes with a high Al content are needed, says HESS.

HESS cannot evaluate the effect of Cr^{+3} and Fe^{+3} because both occur to a much lesser extent in the orthopyroxene structure than Al^{+3}.

The Ca^{+2} ion cannot fit into the orthopyroxene structure at low temperature judging from the exsolution effects observed, according to HESS. At the high temperature of crystallization of magmas it enters the structure in small amounts. If the large Ca^{+2} ion is retained in the structure then it seems that the a dimension increases considerably, so that the Ca ion strongly influences the a dimension.

KUNO (1954) states in the discussion of his results that the effects of Fe^{+2}, Ca and Al on the unit cell dimensions can be explained as due to the difference of their ionic radii from the ionic radius of Mg for which they are substituted. This agrees with the explanation of HESS (1952).

KUNO traces the three dimensions individually as regards to the effect of increase in these ions. He states that the a dimension increases when Fe^{+2}

is substituted for Mg; this effect is more marked when Ca is substituted for Mg. This is due to the fact that the Fe^{+2} ion is larger than the Mg ion while Ca is larger than Fe^{+2}. This is the reason that a Ca rich orthopyroxene has a larger a dimension than a Ca poor orthopyroxene with the same percentage of Mg.

The b dimension increases with substitution of Fe^{+2} for Mg but decreases with Al being substituted for Mg. KUNO explains this as follows: the Fe^{+2} ion is larger than the Mg ion, but Al is smaller than Mg.

The c dimension also increases with Fe^{+2} and Ca substituting for Mg but the rate of change is not so large as for the a dimension. It is seen again from KUNO's results that Ca exerts an influence on the a and c dimensions while Al only changes the b dimension.

In order to give a distinct idea of the changes in the unit cell we have made use of a crystal model of enstatite ($MgSiO_3$). This crystal model was constructed by means of the data given by WARREN and MODELL in 1930, who describe the arrangement of the atoms and give a projection on the plane (0 1 0). At the same time use was made of a projection on the plane (0 0 1), which is represented in a paper by the same authors in 1930 on the structure of anthophyllite. It turns out that the enstatite structure has much in common with the structure of diopside.

TAKANÉ described the structure of a bronzite in 1932 and stated that this structure is the same as that of enstatite.

ITO redetermined the crystal structure of enstatite in 1950 and indicated the following difference with the determination of WARREN and MODELL; according to WARREN and MODELL each Si ion is surrounded by four O ions arranged approximately at the corners of a regular tetrahedron. There are two kinds: the Si_I and the Si_{II} tetrahedron with different Si-O distances. The Si_I tetrahedra form endless chains parallel to the c axis of the crystal and the Si_{II} tetrahedra form similar chains in the same direction. The Si-O chains are held together by Mg ions. Again there are two kinds of Mg ions, that is Mg_I and Mg_{II}. The Mg_I ions are surrounded by six O ions arranged approximately at the corners of an octahedron while the Mg_{II} ions also are surrounded by six O ions but these form a rather irregular octahedron. The Si-O chains thus are not directly connected with each other which is a characteristic difference with the crystal structure of the amphiboles. The orthorhombic cell of enstatite is essentially two monoclinic cells joined on (1 0 0) through a glide plane of reflection. Thus there are Si-O chains differing considerably from each other and from those occurring in diopside.

According to ITO the orthorhombic cell of enstatite represents a regular repetition in juxtaposition of a monoclinic cell, which contains the same SiO_3 group as found in diopside but is different from it in the space group. The extent of necessary correction to be made to the parameters given by WARREN and MODELL is surprisingly small. The x- and z parameters are little changed while the y parameters are the same.

Construction of the crystal model of enstatite. — For the construction of the crystal model use was made of wooden balls with a diameter of two centimeters and iron wire with a diameter of 2.8 millimeters.

The balls representing Si are black, the O balls gray and the Mg balls white (figs. 12 and 13). The model was made on a scale of 1:250.000.000, or 1 Å = 2.5 centimeters. The whole model has about the size of four unit

cells, the limits of one unit cell are indicated with four brass rods connected with each other by thin wire. The model was constructed after the data of WARREN and MODELL. It may be noted, however, that the Si-O chains consist of true tetrahedra which are linked together by oxygen ions, which is

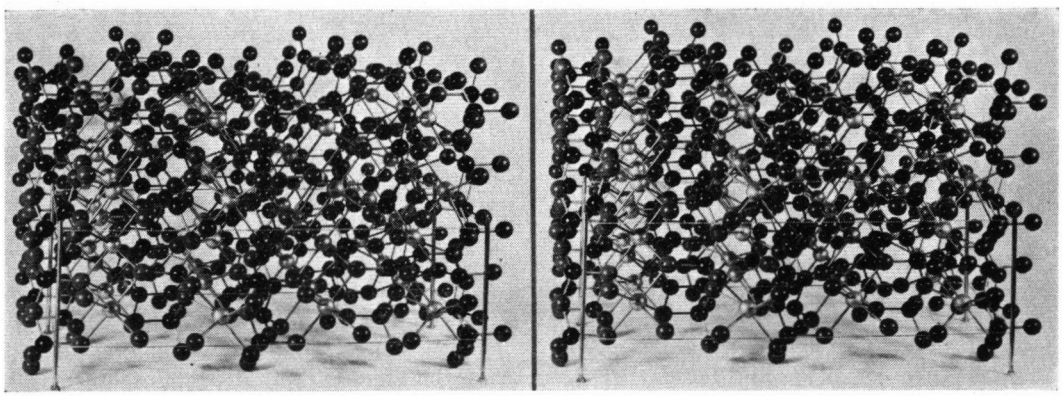

Fig. 12. Crystal structure of enstatite, looking at (0 1 0). Black balls in fourfold coordination = Si, white balls in sixfold coordination = Mg, gray balls = O.

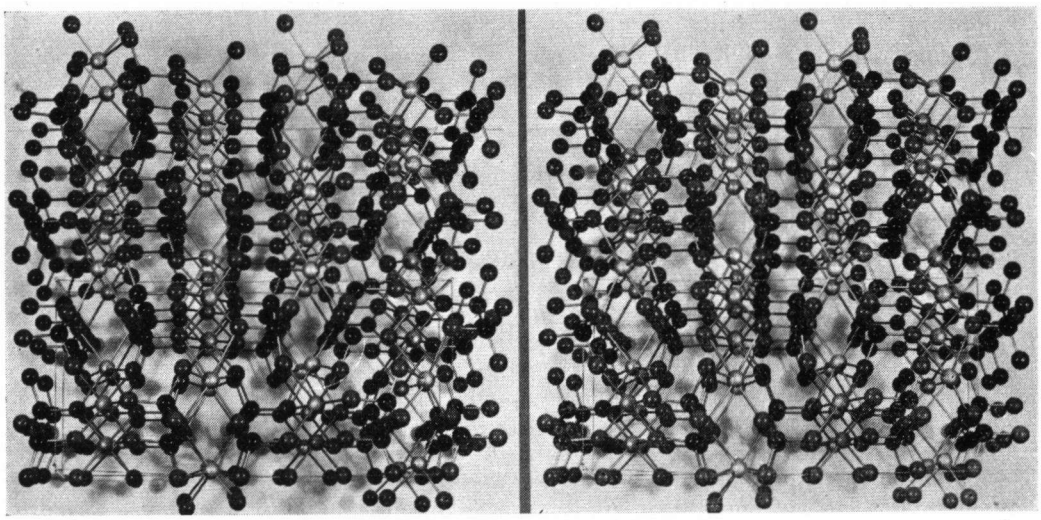

Fig. 13. Crystal structure of enstatite, looking at (0 0 1). Black balls in fourfold coordination = Si, white balls in sixfold coordination = Mg, gray balls = O.

not really the case according to these authors. The mounting of this same kind of tetrahedra is in accordance with the data of ITO. In the model it is clearly seen that the Si-O chains are oriented parallel to the c axis and are held together by the Mg ions. The Mg_I ions are surrounded by six O ions arranged at the corners of an octahedron while around the Mg_{II} ions the

six O ions form very irregular octahedra. The mounting of these "Mg_{II} octahedra" caused the greatest difficulty in the construction of this model. One can hardly speak in this case of octahedra because of the great irregularity. All this makes one think that the structure of enstatite might still be different from what was supposed up to now.

Discussion of the structure and the changes which arise by substitution of Fe, Al and Ca for Mg and of Al for Si. — In fig. 12 the crystal model of enstatite is seen, looking at (0 1 0); this figure consists of a stereo pair to be able to observe the model in three dimensions. It is clearly seen that there occurs a "layer" structure in the direction of (1 0 0), tetrahedra "layers" with black (Si) and gray (O) balls are alternated with octahedra "layers" with white (Mg) balls. However, there is no cleavage along these "layers". In fig. 13 the structure is shown, looking at (0 0 1); this figure also can be seen in three dimensions. In this case, the directions of cleavage can be observed to follow the direction of the open spaces between the Mg_{II} balls and can be indexed as (2 1 0). It can also be seen that these directions of cleavage make angles of about 92° with each other. This is in accordance with the statement of WINCHELL in 1951.

The changes of the unit cell dimensions by substitution of Fe^{+2}, Al^{+3} and Ca^{+2} for Mg^{+2} and of Al^{+3} for Si^{+4} can be studied accurately in this model. One can observe the following:

The Mg_I ions are oriented in a certain way and are connected with O ions of different tetrahedra. When these Mg_I ions are replaced by the slightly greater Fe ions, the Si-O chains are widely separated in the direction of the b dimension, in a lesser degree in the direction of the a dimension and only slightly in the direction of the c dimension. All dimensions thus increase, only slightly, however, but the b dimension is altered most strongly. This agrees on the whole with the results of HESS and KUNO. When supposing now that the Mg_{II} ions are replaced by Fe, then one cannot explain the increase of the three dimensions in this way. We think, therefore, that only the Mg_I ions can be replaced by Fe and since in each unit cell there occur as many Mg_I ions as Mg_{II} ions this probably explains why orthopyroxenes with more than 50 % Fe only rarely are found in nature.

On the other hand we can accept that only the Mg_{II} ions can be replaced by Ca; according to WARREN and MODELL the Mg_I ion corresponds directly to the Mg in diopside, while the Mg_{II} ion occupies very nearly the position of Ca in diopside. When these Mg_{II} ions now are replaced by the much larger Ca ion, the following occurs: the Mg_{II} ions are connected with O ions in such a way that twice two ions of one tetrahedron are held. Because of this special connection of the Mg_{II} ions, the Si-O chains are widely separated from each other in the direction of the a dimension, in a lesser degree in the direction of the c dimension and hardly in the direction of the b dimension, by replacement by Ca. The Ca ion thus mostly influences the a- and the c dimensions, which agrees with the results of KUNO (1954).

The influence of Al on the cell dimensions can only be explained by supposing that only the Mg_I ions can be replaced by Al at the same time with the substitution of Al for Si. Then the following happens:

$$Mg^{+2} + Si^{+4} \rightarrow Al^{+3} + Al^{+3}.$$

By substitution of the much smaller Al ion for Mg_I the Si-O chains are compressed strongly in the direction of the b dimension, in a much lesser degree in the direction of the a dimension and hardly in the direction of the c dimension. On the other hand the decrease of the a and c dimensions is partly compensated by the replacement of the Si ions by the much larger Al ions. These Al ions namely cause the Si-O chains to increase first but with larger quantities of Al in B^{IV} position to zigzag in the (0 1 0) plane. The substitution of Al thus causes a decrease in the b dimension. Again this is in accordance with the results of HESS and KUNO. Since only the Mg_I ions can be replaced by Al it is to be expected that orthopyroxenes with an Fe content of more than 50 % will contain hardly any Al in the B^{VI} position.

Recapitulating one may say that the substitution of Fe for Mg has little influence on the shape of the unit cell, that substitution of Al strongly changes the b dimension and that substitution of Ca strongly influences the a- and c dimensions. These changes can be explained in the first place by the fact that the substituting ions all have a different size and in the second place that there occur two different kinds of Mg ions in the structure which have different positions and are connected with the tetrahedra in altogether different ways.

The behaviour of the characteristic reflections. — The reflections 10 3 1 and 0 6 0 are under the influence of the a- and the b dimensions respectively. By substitution of Fe for Mg, therefore, mainly the reflection 0 6 0 will change in position, because this substitution influences the b dimension most strongly. The relative distance between 10 3 1 and 0 6 0 will vary therefore with the above-mentioned replacement. The variation of this distance will become greater, however, when Al enters into the structure; this ion strongly influences the b dimension so that the reflection 0 6 0 will change still more in position. It may be noted that the Ca ion may affect the reflection 10 3 1 somewhat but the influence of Al is considerably greater with this relative distance.

The distance between quartz reflection $2\,1\,\bar{3}\,1$ and pyroxene reflection 0 6 0 will mainly depend on the proportion of Al which occurs in the structure, for the above reasons. The position of the quartz reflection of course is not influenced. It is self-evident that this distance will also vary somewhat with the substitution of Fe or Mg.

The distance between quartz reflection $(2\,0\,\bar{2}\,3)$ $(3\,0\,\bar{3}\,1)$ and pyroxene reflection 11 3 1 will vary strongly with the proportion of Ca which is present. The reflection 11 3 1 is mainly under the influence of the a dimension. This a dimension strongly changes by substitution of Ca. The variation of the relative distance between these reflections thus is chiefly a result of the above-mentioned substitution, besides of the substitution of Fe for Mg and of Al for Mg or Si.

The high sensitivity of the characteristic reflections, for a change in the chemical composition has been demonstrated clearly now.

Finally it may be noted, that X-ray determination methods may result troublesome if more than two atoms have been substituted in the crystal structure. This is also the case for the orthopyroxenes. For instance when definite reflections change in position through the influence of the Al ion, one should remember, that a strange ion can exert the same influence on

these reflections. This means that the effect which can be ascertained röntgenographically does not always need to have the same cause so that one can never say with certainty that a certain ion causes a definite effect. It is necessary to conclude this chapter on the orthopyroxenes with the stress on that restriction.

THE CLINOPYROXENES

Introduction

The fact that the monoclinic pyroxenes are important rock-forming minerals and the large variety in its members are the reason that many publications have already appeared on this subject. Although one may determine a clinopyroxene by optical means, in some cases this method fails, e. g. with a dense groundmass of volcanites. It is desirable therefore to carry out an X-ray investigation to distinguish the different components when there are difficulties with the optical method.

Although it was supposed originally that the distinction of the different clinopyroxenes by means of X-ray powder photographs would meet with great difficulties because the differences in the cell dimensions of these pyroxenes are rather small (MEHMEL 1939), it will become clear in this paper that these powder diagrams do show sufficient differences to be able to form groups of monoclinic pyroxenes, that have a similar reflection pattern, distinctly differing from the pattern of another group. We will investigate, moreover, whether these röntgenographically obtained groups are related to the groups which are distinguished on account of the chemical composition, just as OSTEN in 1951 succeeded to do for the alkali feldspars.

More or less the same has already been done by KUNO and HESS in 1953, who studied the variations in the unit cell dimensions and the correlation between them and the chemical composition of the different clinopyroxenes. I have made use of their data about the cell dimensions of the clinopyroxenes for calculating the relative distance between certain reflections. These calculated distances have been correlated with the chemical composition as will be described on p. 254.

Just as for the orthopyroxenes we will use the X-ray method for determining the clinopyroxenes by measuring the relative distance between reflections which are sensitive to changes in chemical composition. For that purpose we will first give a short account of the optical and chemical investigations and afterwards the results of the röntgenographic examination will be given.

This investigation of clinopyroxenes was made possible especially by important gifts of material made to the Museum. Especially I want to thank Professor Dr. B. G. ESCHER of Leiden, Holland; Professor Dr. H. H. HESS of Princeton, New Jersey, U.S.A.; Professor Dr. A. STRECKEISEN of Bern, Switzerland; Dr. H. KUNO of Tokyo, Japan; Dr. H. M. E. SCHÜRMANN of The Hague, Holland; Mr. H. KONING of Leiden, Holland; Mr. P. N. J. BODES and Mr. A. G. BODE of The Hague, Holland.

Finally it may be noted that the numbers of the clinopyroxenes are running sample numbers which are used throughout this thesis.

Optical Investigation

Introduction

The variation of the optical properties of the clinopyroxenes is connected with the chemical composition. The angle Z ∧ c is determinative for clinopyroxenes together with the optic axial angle 2 V, the double refraction and dispersion. Strong dispersion of the optic axial angles indicates the Ti content. The colour and pleochroism of aegirite-augite and titaniferous augite are welcome aids for identification. The strongly variable optic axial angle is of great importance to distinguish for instance between diopside (2 V = + 59°) and pigeonite (2 V very small). In addition the prismatic angle (93°) of pyroxene is characteristic; this is a very important property to distinguish between amphiboles and pyroxenes.

Many investigators have already made use of these properties for determination.

HINTZE (1897) gave already a detailed account of clinopyroxenes and measured these properties.

It appeared, that the volcanic orthopyroxenes are characterized by a zonal structure and this is also the case with the volcanic augites; KUNO and SAWATARI described in 1934 a number of augites of different localities in Japan and they paid especially attention to the zonal structure of these augites. We will return to this subject on p. 230.

HESS described in 1941 in a very detailed manner clinopyroxenes of different occurrence and discussed the possibilities of the occurrence together of different clinopyroxenes and the circumstances under which it might be possible that a certain pyroxene inverts to another one; at the same time the variation of the optical properties was examined.

By the same author (1949) a very valuable paper was published, in which about forty chemical analyses of clinopyroxenes were given while all possible optical properties were shown in diagrams and in addition the methods are mentioned by which it is possible to measure these properties as accurately as possible.

In 1950 YODER paid attention to one clinopyroxene especially, investigating the jadeite problem. He concluded that the temperature of formation is probably less than 800° C, it occurs with low-temperature albite (< 700° C) and in a reaction zone against serpentine (< 500° C). At the same time YODER concluded from structural analysis that jadeite is a pyroxene with the type structure of diopside, which agrees with our results, as will be seen on p. 266.

A classification of the pyroxenes, based on the chemical composition, was proposed by P. and E. NIGGLI in 1948 and was maintained in the English edition of their book (P. NIGGLI, 1954). This classification agrees almost exactly with the arrangement mentioned by FORD in 1949 and may be briefly stated as follows:

Group I: Ca-poor, Mg-Fe pyroxenes. — The pyroxenes belonging to this group can be both orthorhombic and monoclinic.

Group II: Ca-rich, Al-poor pyroxenes. — In this group diopside and hedenbergite may be considered for instance; these are metasilicates of calcium magnesium and calcium iron respectively. Further all varieties of diopside occur in this group, together with pigeonite.

Group III: Alkali-poor, Silica-poor and Al-rich pyroxenes. — Augite and Ti-augite are arranged in this group. The chemical composition of the members of this group may vary strongly.

Group IV: Alkali pyroxenes. — In this group coupled atomic substitutions occur: AlNa in place of MgCa and AlLi in place of $Fe^{+3}Na$ or MgMg. The pyroxenes which belong to this group are: omphacite, jadeite, aegirite (acmite), aegirite-augite and spodumene.

We will arrange the monoclinic pyroxenes in a different way, disregarding the alumina content; this classification will be based on the relative molecular percentages of $CaSiO_3$, $MgSiO_3$ and $FeSiO_3$. By disregarding the alumina content, as was done by HESS in 1941, the augites fall also in this field; this is more or less a drawback of this classification because Al and Na substitute Si, Mg and Ca in the crystal structure so that the calculation of the molecular percentages of $CaSiO_3$, $MgSiO_3$ and $FeSiO_3$ for Al-rich and alkali-rich pyroxenes will cause trouble. This has already been mentioned by P. NIGGLI in 1943 when he classified the pyroxenes according to the base calculation.

Our classification in accordance with the classification of HESS (1941) may be stated as follows:

Group I: Mg-Fe pyroxenes. — The pyroxenes belonging to this group are both orthorhombic and monoclinic, although the latter are very rare. In preceding chapters of this thesis, the orthorhombic members have already been dealt with in detail.

Group II: Ca-Mg-Fe and Ca-Mg-Fe-Al pyroxenes. — In this group all clinopyroxenes must be placed, except the alkali pyroxenes and the rare members mentioned in Group I. Therefore, diopside, hedenbergite, pigeonite, augite and Ti-augite may be considered in this group.

Group III: Alkali pyroxenes. — In this group occur jadeite, omphacite, aegirite and spodumene for instance. Coupled atomic substitutions are possible.

Methods of Determination

The way in which the optical properties of the clinopyroxenes are measured, is the same as that which is used for the orthopyroxenes so for the methods of determination of these monoclinic pyroxenes can be referred to those which were described in the chapter on the orthopyroxenes on p. 175. The measurement of the angle Z ∧ c was carried out in the usual way by means of the Universal Rotating Stage.

Macroscopic and Optical Description of the Röntgenographically Investigated Samples

Group II: Ca-Mg-Fe and Ca-Mg-Fe-Al pyroxenes

No. 13 *Diopside from Zillertal, Tyrol, Austria.* (St 24594) [4]) — Fine

[4]) Registration number of the Rijksmuseum van Geologie en Mineralogie, Leiden, Holland.

dark green opaque to pale bottle green transparent crystals have been examined macroscopically, a fine striation on crystal faces could be observed; some of these crystals were definitely of gem quality. They were made available for investigation by Professor Dr. B. G. ESCHER.

A microscopic inspection indicated fine diopside with the characteristic pyroxene cleavage parallel to (1 1 0); no pleochroism could be observed because the mineral is practically colourless in thin section. The mineral has some liquid and ore inclusions.

With the aid of a Double Variation Equipment after EMMONS, Mr. A. C. TOBI determined the following optical properties: $N_z = 1.706 \pm 0.002$; $N_y = 1.676 \pm 0.001$ and $N_x = 1.670 \pm 0.0005$. Further $2V = +61°$ and $Z \wedge c = 38.5°$. The chemical composition according to analysis made in our Laboratory, is $Ca_{49.5}\ Mg_{46.5}\ Fe_4$ (see Table 11).

No. 14 *Malacolite from Björmyresweden, Dalarna, Sweden.* (St 24602) — The rock has a grayish green colour and appears to be monomineral, in some places, however, fine green needle shaped crystals can be observed, which resemble amphibole crystals. In thin section no amphibole was observed; only malacolite could be seen, this pyroxene has partly been altered to calcite; it turned out that $2V = +59.5°$ and $Z \wedge c = 39°$. In the X-ray powder diagram, reflections of amphibole were encountered besides the diffraction lines of the pyroxene in question.

No. 15 *Malacolite from Moravia, Czechoslovakia.* (St 24605) — The mineral occurs in large crystals in a pegmatite. The colour of the pyroxene is grayish green and large quantities of quartz and feldspar are present.

In thin section much malacolite can be found, often altered to calcite, epidote and chlorite. Also plagioclase feldspar (andesine with $\pm$ 48 mol % anorthite) and quartz occur. The whole rock has a holocrystalline, hypidiomorphic, granular structure. Apatite is met with as an accessory mineral.

The malacolite in question has the following optical properties: $2V = +58.5°$ and $Z \wedge c = 39.5°$. Sometimes the mineral is nearly idiomorphic in thin section (see fig. 14).

No. 16 *Coccolite from Arendal, Norway.* (St 24606) — Macroscopically the mineral has a dark green colour and on the crystal faces zones of weathering can be seen.

Under the microscope the mineral shows a weak pleochroism: X = green, Y = yellowish green and Z = green, and $2V = +58°$, $Z \wedge c = 39°$.

No. 17 *Sahlite from Sala, Vastmanland, Sweden.* (St 24600) — A greenish gray coloured mineral, showing distinct cleavage planes, can be seen macroscopically.

In thin section the characteristic pyroxene cleavage parallel to (1 1 0) can be observed; the mineral has been altered along veins to chlorite and calcite. The optical properties were measured to be $2V = +61°$ and $Z \wedge c = 44°$.

No. 18 *Schefferite from Ytterby, Sweden.* (St 69559) — Macroscopically a red brown grain mineral may be seen together with some calcite having perfect cleavage.

Under the microscope schefferite, calcite and epidote can be observed. The pyroxene has a very weak pleochroism in tones of pale yellow-brown and pale brown; $2V = +61°$ and $Z \wedge c = 45.5°$.

No. 19 *Fassaïte from Traversella, Brozo, Italy.* (St 24615) — Splendid black-green crystals with a high lustre can be observed together with a fine-grained yellow-green material.

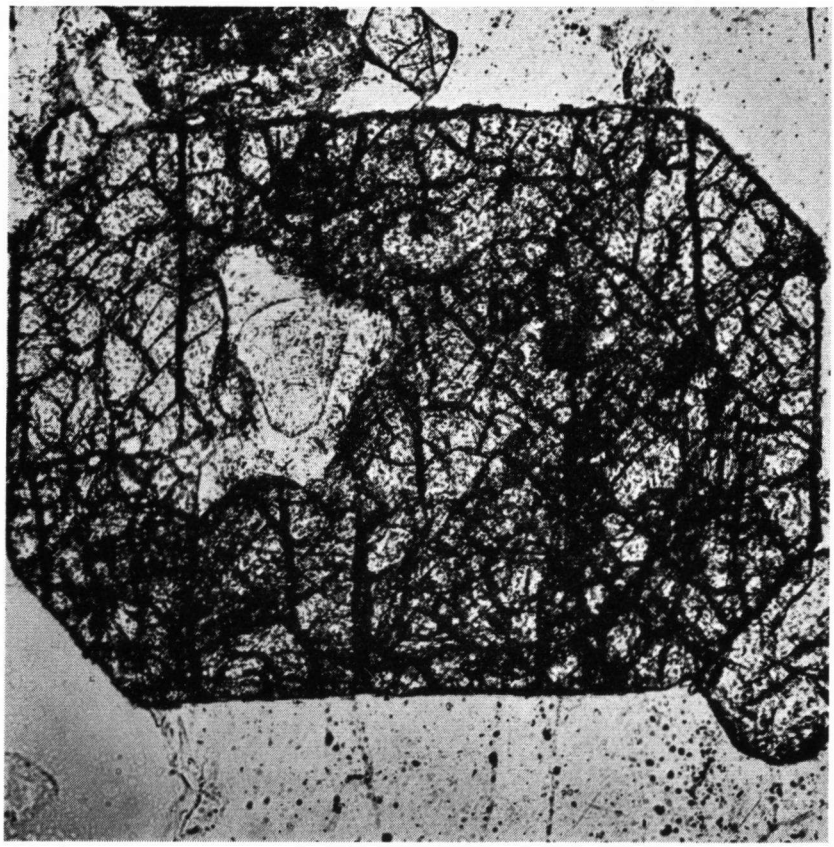

Fig. 14. Idiomorphic malacolite No. 15. Moravia, Czechoslovakia. (st. 24605) × 170.

In thin section the fassaïte has a distinct pleochroism: Y = brownish green and Z = grass green. The fine grained material is chlorite.

The pyroxene has the following optical properties: $2V = +58.5°$ and $Z \wedge c = 40.5°$.

No. 20 *Chrome-diopside in basalt from Finkenberg, Bonn, Germany.* (Number Fbg 150 of Dr. H. M. E. SCHÜRMANN.) — This sample has been made available for investigation by Dr. H. M. E. SCHÜRMANN.

In the hand specimen one may see a grass green mineral together with yellow-green olivine and a bronzy coloured mineral (bronzite) in a nodule-like inclusion of olivine in basalt. Some quartz is observable at the border of the nodule.

Under the microscope mainly olivine is seen, altered in veins to serpentine, further bronzite, almost entirely altered to bastite and in some places to calcite and finally chrome-diopside.

This pyroxene is nearly colourless in thin section and therefore practically no pleochroism can be observed. The measured optical properties are: $2V = +61°$ and $Z \wedge c = 38.5°$.

No. 21 *Diallage from La Barraca, Sestri, Levante, Italy.* (St 24590) — A grayish green mineral with a bronze lustre can be seen macroscopically. The mineral has perfect cleavage planes parallel to (1 0 0) with a very fine striation.

In thin section this striation is very distinct. The mineral also contains ore inclusions and does not show pleochroism. The observed optical properties are: $2V = +56°$ and $Z \wedge c = 40.5°$.

No. 22 *Diallage from Veltlin, Tyrol, Austria.* — Macroscopically a black-brown mineral can be seen, having a bronze lustre and fine striation on distinct cleavage planes parallel to (1 0 0). It is seen that this mineral occurs in a pegmatite for a gray-white mineral is also present which resembles a feldspar because of the distinct cleavage planes.

In thin section it turns out, that it is a plagioclase feldspar (andesine with $\pm$ 48 mol % anorthite) in some places altered to sericite and chlorite. In addition the diallage contains Schiller inclusions (see fig. 15), which according to WINCHELL (1948) not only may occur in bronzite but also in diallage. In thin section the rock has sometimes a red-brown colour, probably due to impurities of iron.

The pyroxene has the following optical properties: $2V = +58°$ and $Z \wedge c = 39.5°$.

No. 23 *Diallage in gabbro-pegmatite from Coverack, Lizard, Cornwall, England.* — This sample has been made available for investigation by Mr. H. KONING of Leiden.

The rock has a pegmatitic character; the diallage has a dark grey colour and a brown metallic lustre. In addition feldspar can be observed together with spots of red brown material.

Under the microscope plagioclase feldspar (labradorite with $\pm$ 57 mol % anorthite) can be seen, almost entirely altered to kaolin, epidote and chlorite. The red-brown spots are probably due to impurities of iron. The diallage has a fine striation on cleavage planes parallel to (1 1 0). $2V = +54°$ and $Z \wedge c = 42°$.

No. 24 *Diallage in gabbro-diorite from Lac Robert, Belledone, France.* (Number 117 of Collection H. KONING.) — This sample was kindly lent for investigation by Mr. H. KONING of Leiden.

In the hand specimen the diallage is black-brown and has a distinct cleavage parallel to (1 0 0) and (1 1 0); this mineral occurs irregularly in a white feldspar.

In thin section it shows the characteristic parting parallel to (1 0 0) and on outside edges is sometimes altered to uralite, furthermore bastite occurs as a secondary mineral.

The plagioclase feldspar is andesine with ± 48 mol % anorthite, but it is strongly altered to sericite, epidote, calcite, chlorite and kaolin. Since the molecular percentage anorthite was measured on altered plagioclase, the

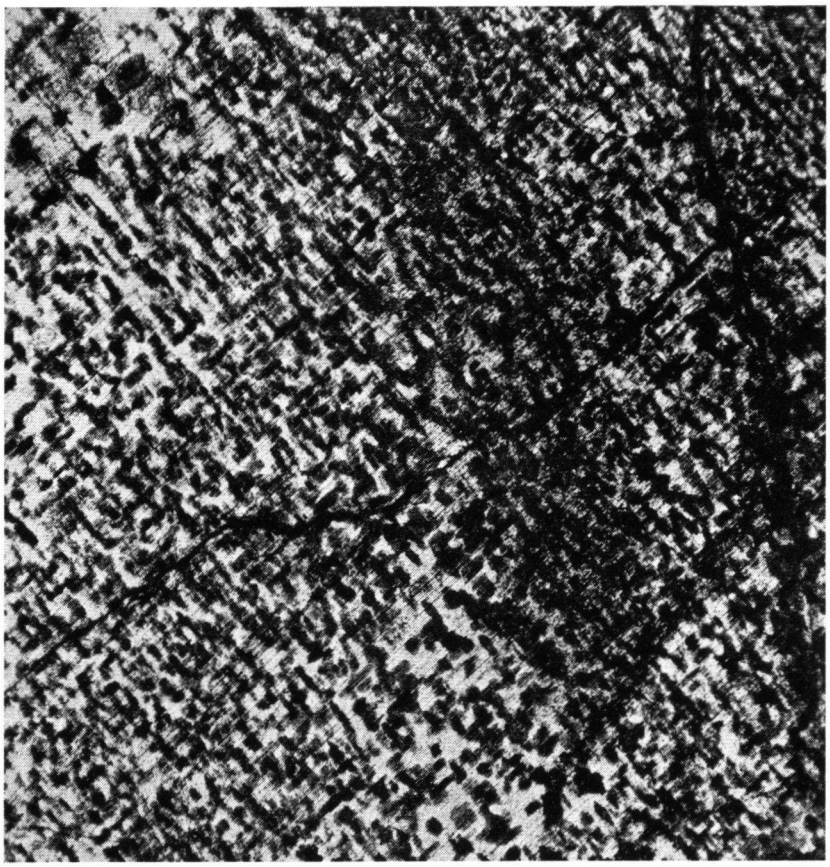

Fig. 15. Schiller inclusions in diallage No. 22. Veltlin, Tyrol, Austria. × 44.

original mol % anorthite is probably somewhat higher. Accessory minerals are apatite, carbonate and ore.

DEN TEX (1949), who has also described this rock, stated the following optical properties for the diallage: $2V = +52°$ and $Z \wedge c = 40°—44°$. This agrees quite well with our results: $2V = +51°$ and $Z \wedge c = 43°$.

No. 25 *Pigeonite from Usugoya-zawa, Hakone volcano, Japan.* (No. 2 in KUNO and HESS 1953) — Dr. KUNO was so kind to send this material, described as sample No. 2 in his paper 1953.

With the naked eye only a greyish powder can be seen, without any definite characteristics. In the grain preparation colourless grains appear mainly, some of them have a very weak pleochroism: X = brownish, Y = pale greenish and Z = pale greenish. $2V = +14°$ (average) and $Z \wedge c = 42°$ according to KUNO and NAGASHIMA (1952), which agrees well with our results: $2V = +13.5°$ and $Z \wedge c = 43°$. The composition from chemical analysis made from the same specimen is $Ca_8 Mg_{64} Fe_{28}$ (according to KUNO and HESS 1953).

No. 26 *Hedenbergite from Yxsjo Mine, Sweden.* (St 69562) — Macroscopically the mineral is greenish black and has distinct cleavage. One can observe quartz and calcite in the hand specimen.

In thin section the pyroxene is pale green coloured and has a weak pleochroism: X = pale green; Y = yellowish brown and Z = greenish.

Ore inclusions are observable together with the secondary mineral epidote. In addition quartz and carbonate occur, partly in veins.

The optical properties of the hedenbergite were measured as follows: $2V = +59.5°$ and $Z \wedge c = 47.5°$.

No. 27 *Hedenbergite from Herault, California.* (No. 6 in KUNO and HESS 1953) — Professor Dr. H. H. HESS kindly sent this material, described as sample No. 6 in his paper 1953.

The mineral has a greenish black colour and distinct cleavage; a fine striation on the cleavage plane can be observed.

In thin section the pyroxene is nearly colourless, therefore no pleochroism can be detected. The mineral contains opaque inclusions and in places some carbonate may be seen. This hedenbergite also possesses the characteristic pyroxene cleavage parallel to (1 1 0).

The measured optical properties are $N_z = 1.752$, $N_x = 1.721$, $2V = +62°$ and $Z \wedge c = 47°$. The chemical composition of the same specimen is $Ca_{48} Mg_3 Fe_{49}$ (according to KUNO and HESS 1953).

No. 28 *Augite from Vesuvius, Italy.* (St 15106) — Macroscopically individual black crystals, sometimes entirely idiomorphic can be observed. The size of crystals varies up to a few centimeters; often penetration twinning occurs.

In thin section the pyroxenes show strong zoning (see fig. 16) and have a greenish colour. A rather distinct pleochroism can be seen: X = pale green, Y = yellowish brown and Z = green. The mineral contains many ore inclusions and has the characteristic pyroxene cleavage parallel to (1 1 0). The optical properties were determined as follows: $2V = +58°$ (average) and $Z \wedge c = 43.5°$.

No. 29 *Augite in dacite pumice from Odawara, Eastern foot of Hakone volcano, Kanagawa Prefecture, Japan.* — This sample was made available by Dr. H. KUNO.

The sample contains individual black augite crystals which are often idiomorphic. Further a few other minerals occur which have already been described under hypersthene No. 10 on p. 181.

In thin section the pyroxene has a distinct pleochroism X = greenish, Y = brownish yellow and Z = green; in addition zoning may be observed

together with black inclusions. Here and there twinning is present in the augite.

The measured optical properties are $N_z = 1.710$, $N_x = 1.681$, $2V = +58°$ (average) and $Z \wedge c = 42°$. The chemical composition of this sample is $Ca_{48} Mg_{40} Fe_{12}$ (see Table 11).

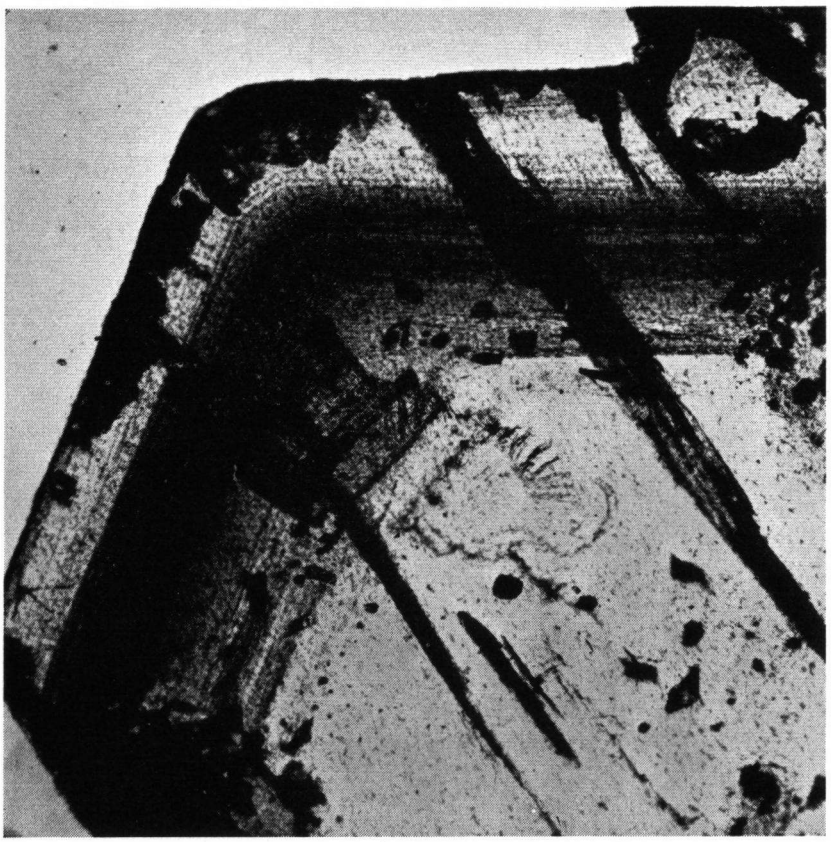

Fig. 16. Sharply defined zoning in augite No. 28. Vesuvius, Italy. (st. 15106) × 44.

No. 30 *Augite from Wadaki, Shizuoka Prefecture, Japan.* — This sample was made available by Dr. H. KUNO.

Black, sometimes idiomorphic augite crystals can be detected macroscopically. According to KUNO and SAWATARI (1934) these augite crystals occur as phenocrysts in a basalt tuff. They have described this augite in detail and give the values: $2V = +59.3°$ and $Z \wedge c = 42.6°$.

In thin section this augite has a pale green colour, showing only a weak pleochroism: X = greenish; Y = brownish green and Z = greenish brown. The mineral contains opaque inclusions and has perfect cleavage parallel to (1 1 0).

We measured the optical properties as follows: $N_z = 1.708$, $N_x = 1.681$,

$2V = +59.5°$ (average) and $Z \wedge c = 41.5°$, which agrees very well with the results of KUNO and SAWATARI. The chemical composition of this augite calculated from chemical analysis as communicated by Dr. H. KUNO is $Ca_{48}\ Mg_{45}\ Fe_7$.

No. 31 *Augite from Puy de la Vache, Auvergne, France.* (St 56363) — The individual, sometimes idiomorphic black crystals were collected from the rubble in the wall of the old crater. Corroded crystals are common.

In thin section the mineral has a greenish colour and weak pleochroism can be seen: X = greenish; Y = brownish green and Z = olive green. Inclusions of opaque minerals often occur. The augite has a zonal structure. The measured optical properties are: $2V = +55°$ (average) and $Z \wedge c = 49.5°$.

No. 32 *Augite from Nishigatake, Nagasaki Prefecture, Kynshu, Japan.* — This sample was also made available by Dr. H. KUNO.

These augite crystals are often idiomorphic and have a grayish green colour macroscopically; according to KUNO they occur as phenocrysts in a basalt tuff. Since we have only the augite crystals at our disposal, we cannot give further details about this tuff.

Microscopically the augite is greenish and contains a great number of opaque inclusions, which can be seen clearly in fig. 17.

According to WINCHELL (1948) is for an augite of the same locality $2V = +58°25'$ and $Z \wedge c = 41°36'$, which agrees quite well with our results: $2V = +59.5°$ (average) and $Z \wedge c = 41°$. Further is $N_z = 1.709$ and $N_x = 1.681$. The chemical composition according to a personal communication of Dr. H. KUNO is: $Ca_{44}\ Mg_{51}\ Fe_5$ (see Table 11).

No. 33 *Augite from Yone-yama, Niigata Prefecture, Japan.* — This sample again was made available for investigation by Dr. H. KUNO.

These augite crystals have a dull black colour and often show penetration twinning. According to KUNO and SAWATARI (1934) these crystals belong to the weathered part of an agglomerate tuff of hypersthene-bearing olivine-augite-basalt.

In thin section the augite is pale green coloured and a weak pleochroism can be seen: X = greenish; Y = brownish and Z = green. Inclusions of olivine, plagioclase feldspar, a black opaque mineral (probably magnetite) and glass occur. Twinning can be observed clearly.

According to KUNO and SAWATARI is $2V = +54°05'$ and $Z \wedge c = 43°$, while the chemical composition of the same specimen is $Ca_{44}\ Mg_{43}\ Fe_{13}$. We measured $2V = +55°$ (average) and $Z \wedge c = 44°$, which agrees very well with the results of KUNO and SAWATARI. Further is $N_z = 1.712$ and $N_x = 1.689$.

No. 34 *Augite from Monte Rossi, Etna, Italy.* (St 24627) — The material consists of individual, often idiomorphic crystals, having a black to brownish black colour; penetration twins are common. The size of the crystals varies from 8 to 14 millimeters.

In thin section a weak to distinct pleochroism can be seen: X = green; Y = yellowish brown and Z = greenish, further the mineral contains numerous magnetite inclusions and has a nice zonal structure due to difference of chemical composition. The optical properties were measured as: $2V = +56.5°$ (average) and $Z \wedge c = 46°$.

No. 35 *Titaniferous augite in syeno-diorite from Rongstock, Czechoslovakia.* (St 12630) — Macroscopically a typical plutonic igneous rock can be observed. In thin section the Ti-augite has a peculiar reddish violet colour and shows a weak pleochroism: X = reddish, Y = violet and Z = yellowish; further the mineral contains black opaque inclusions. Moreover there occur: plagioclase feldspar (andesine-labradorite with 40—60 mol % anorthite),

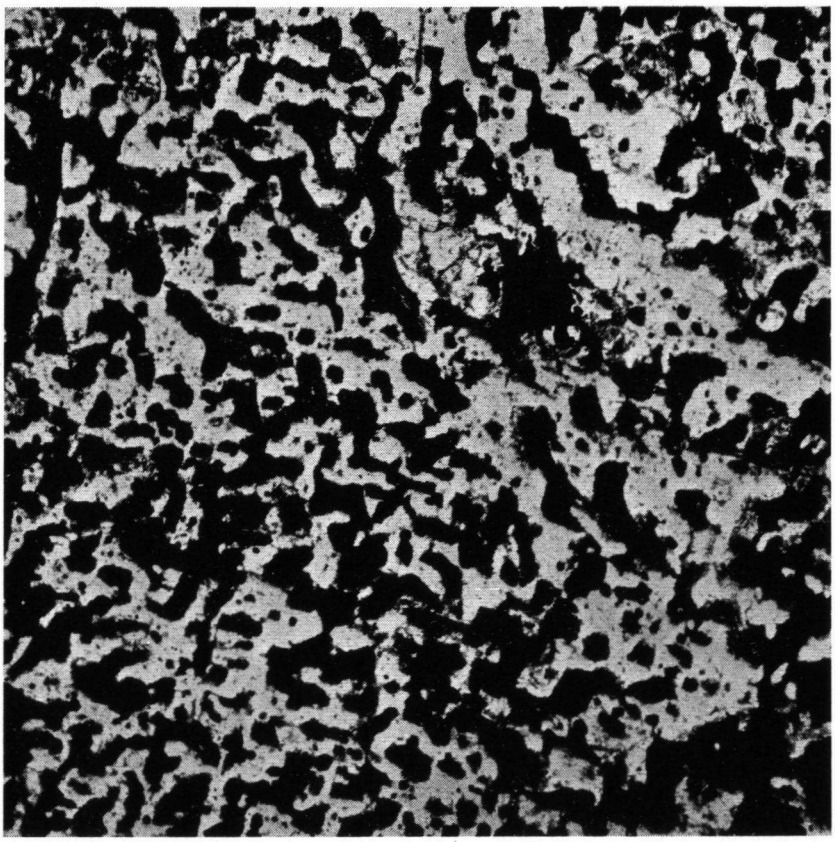

Fig. 17. Ore inclusions in augite No. 32. Nishigatake, Nagasaki Prefecture, Kyushu, Japan. × 44.

sometimes showing a fringe of orthoclase feldspar and altered to sericite and epidote; biotite; Na-K-feldspar, partly altered to sericite; nephelite altered to zeolites; barkevikite, sometimes grown parallel with titaniferous augite; olivine with magnetite, altered to iddingsite. As accessory minerals apatite, zircon, magnetite, ilmenite and titanite occur. It is seen from these data that the rock is a syeno-diorite. It has a holocrystalline, hypidiomorphic, medium-grained, granular structure.

The optical properties of the Ti-augite are: $2V = +58°$ and $Z \wedge c = 44°$.

No. 36 *Titaniferous augite in microfoid diorite from Babutzin Böhm Mittelgebirge, Czechoslovakia.* (St 12696) — A macroscopic examination indicates a black porphyritic rock with white phenocrysts and with black columnar crystals.

Under the microscope one may distinguish Ti-augite, reddish coloured with a weak pleochroism: X = reddish, Y = violet reddish, Z = reddish. The mineral has a strong extinction dispersion and twinning can be seen; it contains ore inclusions. In fig. 18 a thin section of the Ti-augite has been

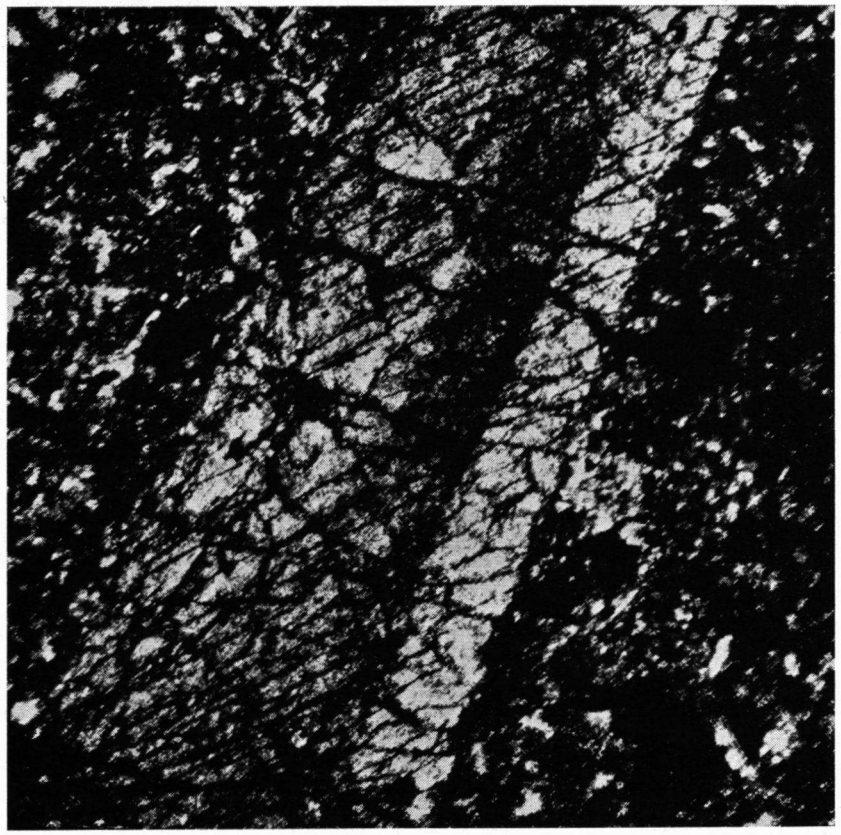

Fig. 18. Titaniferous augite No. 36 with strong dispersion in microfoid diorite. Babutzin, Czechoslovakia. (st. 12696) Crossed nicols × 55.

represented. Besides these phenocrysts of Ti-augite one may also observe phenocrysts of leucite, plagioclase feldspar and sodalite. In the groundmass feldspar, Ti-augite, hornblende, leucite and sodalite are present. Apatite and magnetite occur as accessory minerals. The rock has a holocrystalline, porphyritic structure, the groundmass is panxenomorphic, microcrystalline to cryptocrystalline.

The optical properties of the Ti-augite are: $2V = +58°$ and $Z \wedge c = 48.5°$.

Group III. Alkali pyroxenes

No. 37 *Acmite in acmite-granite from Eker, Norway.* (St 24642) — Macroscopically black columnar pyroxene crystals with well-developed crystal faces having a high lustre can be observed in a coarse-grained granite, in which quartz and feldspar can be easily recognized. One might call this granite also a pegmatite.

In thin section the characteristic brownish grass green colour of acmite is striking and a distinct pleochroism in tones of green and yellow. The optical properties are: $2V = -61°$ and $Z \wedge c = 92°$.

No. 38 *Aegirite in nephelite-alkali-syenite from Langesundfiord, Norway.* (St 52759) — Very large black crystals with good crystal faces having a fine striation occur in a nephelite rich rock.

In thin section the aegirite has a grass green colour with a characteristic pleochroism in tones of green and yellow. Besides there occur nephelite with cancrinite; Na-K-feldspar, partly altered to sericite; biotite with the secondary mineral chlorite and ore.

WINCHELL (1948) gives the following data for an aegirite from the same locality: $2V = -62°13'$ and $X \wedge c = +4°$; our measurements gave $2V = -63°$ and $Z \wedge c = 94°$, which agrees rather well with the data of WINCHELL.

No. 39 *Aegirite-augite in ijolite from Slöda, Alnö, Sweden.* (St. 12649) — Macroscopically a typical plutonic rock with reddish and black constituent minerals.

In thin section one may observe somewhat bleached aegirite-augite having a very weak pleochroism, further nephelite with the secondary minerals zeolite, cancrinite, carbonate and chlorite. Schorlomite or ivaarite also occurs together with biotite. Accessory minerals are apatite and hematite.

The rock has a holocrystalline, hypidiomorphic, coarse-grained granular structure.

The measured optical properties of the aegirite-augite are: $2V = +65°$ and $Z \wedge c = 69.5°$.

No. 40 *Aegirite-augite in leucite-rich hauyne-phonolite, from Rieden, Eifel, Germany.* (St 12766) — Phenocrysts of a green-coloured pyroxene, leucite and black garnet occur in this grey rock.

Under the microscope phenocrysts can be seen of green aegirite-augite, partly altered to zoisite; this pyroxene possesses a weak pleochroism in tones of green and yellowish green.

Phenocrysts of leucite, hauyne, Na-K-feldspar and melanite garnet are also present. In the groundmass the same minerals occur. Titanite, apatite and ore minerals (among others hematite) are the accessory minerals. The rock has a holocrystalline, porphyritic, granular structure, the groundmass is pilotaxitic.

In fig. 19 the aegirite-augite has been reproduced. The measured optical properties are: $2V = +61°$ and $Z \wedge c = 71.5°$.

No. 41 *Omphacite in eclogite from Silberbach (near Hoff), Fichtel Mountains, Germany.* — Macroscopically it is a dark yellowish green rock, in which pale pink garnet occurs.

Microscopically colourless omphacite can be seen, besides garnet, kyanite, quartz and muscovite; accessory minerals are magnetite, sphene and rutile.

According to WILLIAMS, TURNER and GILBERT (1954) one can distinguish omphacite only by its high optic axial angle ($2V = 70°—80°$; sign +). The optical properties of this mineral are: $2V = +66.5°$ and $Z \wedge c = 38.5°$; so this is almost in accordance with the statement of the above mentioned authors, because its optic axial angle is higher than that of all the diopside samples.

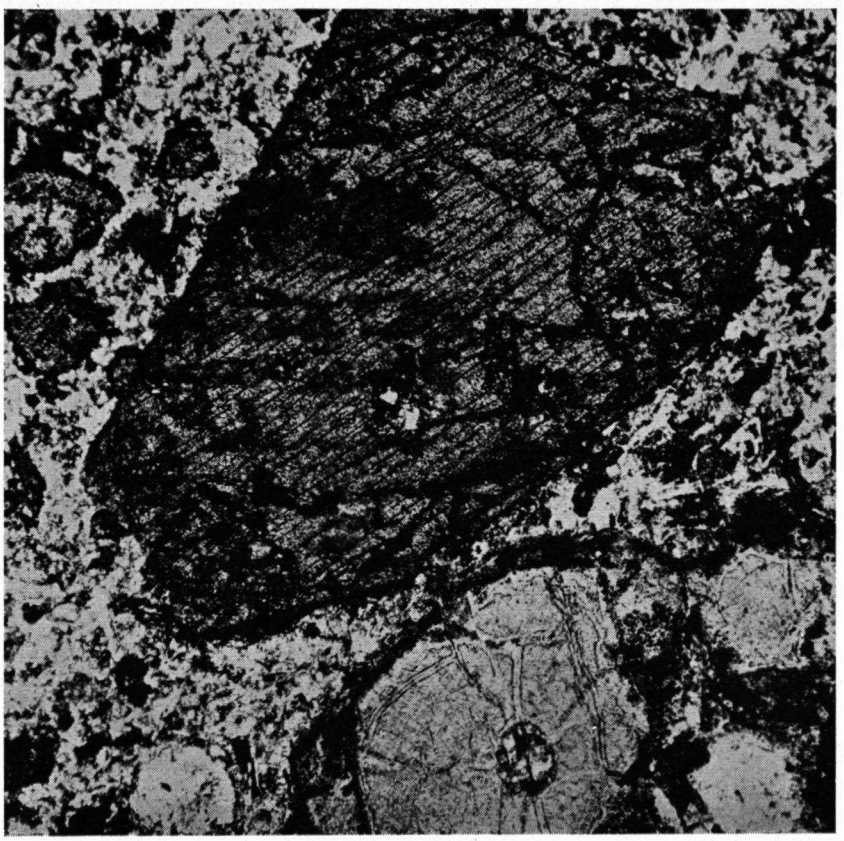

Fig. 19. Aegirite-augite No. 40, in leucite-rich hauyne phonolite. Rieden, Eifel, Germany. (st. 12766) × 55.

No. 42 *Omphacite in eclogite from Carinthia, Austria.* — In hand specimen an emerald green mineral with distinct cleavage is the main constituent. Moreover, a darker green mineral, also with cleavage planes and a pale pink mineral are present.

In thin section colourless omphacite can be observed together with an amphibole (smaragdite) having the usual amphibole extinction and a weak pleochroism in tones of yellowish green and colourless. Kyanite occurs, weakly

pleochroic (pale blue-colourless); the garnet which is present has a characteristic absorption spectrum: three broad bands centred at 5751 Å; 5272 Å and 5041 Å; a fourth band is observed at 4625 Å; from these data one may conclude, according to ANDERSON (1951), that this garnet belongs to the almandine-pyrope series. Accessory minerals are magnetite and a large quantity of rutile.

The optical properties of the omphacite are: $2V = +73°$ and $Z \wedge c = 39.5°$.

No. 43 *Jadeite from Upper Burma.* — This sample was made available by Mr. P. N. J. BODES and Mr. A. G. BODE of The Hague.

Macroscopically the specimen is green-gray and has apple green spots. In thin section a colourless pyroxene can be seen with perfect cleavage parallel to (1 1 0) and associated with serpentine.

The optical properties are: $2V = +79°$ and $Z \wedge c = 38°—43°$.

No. 44 *Spodumene in pegmatite from Varuträsk, Northern Sweden.* (St 44424 and St 37602) — In hand specimen large blue grayish white crystals of spodumene having a fine striation on cleavage planes and sometimes altered to a yellowish material, occur together with quartz and feldspar.

In thin section colourless spodumene with perfect prismatic cleavage can be seen. The optical properties are: $2V = +64.5°$ and $Z \wedge c = 24.5°$.

No. 45 *Spodumene in pegmatite from Boston, Massachusetts, U.S.A.* (St 64940) — Large opaque yellowish white crystals of spodumene with perfect cleavage planes can be seen in the hand specimen, together with quartz, feldspar and muscovite.

Microscopically one may observe plagioclase feldspar (andesine with ± 36 mol % anorthite) mainly, altered to kaolin and showing polysynthetic albite twinning. Besides quartz with undulatory extinction and Na-K-feldspar are present. The latter mineral is partly altered to kaolin. In the rock muscovite also occurs while large crystals of spodumene are present; the mineral is colourless in thin section and shows a perfect cleavage parallel to (1 1 0).

The optical properties are: $2V = +66°$ and $Z \wedge c = 27°$.

No. 46 *Aegirite in nephelite syenite pegmatite from Ditro, Siebenbürgen, Roumania.* — This sample is a gift of Professor Dr. A. STRECKEISEN of Bern, Switzerland.

Macroscopically large black columnar to short prismatic crystals of aegirite up to five centimeters in size can be seen, and white feldspar and on a fresh surface also gray nephelite.

Under the microscope one sees mainly Na-K-feldspar with the secondary minerals sericite, epidote and carbonate. A smaller quantity of plagioclase feldspar (oligoclase with about 28 mol % anorthite) occurs, in places altered to sericite. Nephelite is present with the secondary minerals cancrinite, muscovite and sodalite. Biotite and aegirite occur as dark components. The biotite is strongly pleochroic in tones of dark brown and pale brown-yellow.

The green aegirite has a distinct pleochroism: X = green, Y = yellowish green and Z = green-yellow.

The optical properties are: $2V = -71°$, $Z \wedge c = 91.5°$, $N_z = \pm 1.795$

and $N_x = \pm 1.755$. The chemical composition is 71 molecular percent $NaFe''' Si_2O_6$ (see Table 11). This analysis was made in the Petro-chemical Laboratory of Leiden by Mrs. Dr. C. M. DE SITTER—KOOMANS. Finally zircon, titanite and much ore occur as accessory minerals.

Discussion of the Optical Results (see Table 10 and fig. 20)

The Ca-Mg-Fe-pyroxenes have all about the same optic axial angle, except the diallage samples which have a slightly smaller optic angle and pigeonite with a very small 2 V.

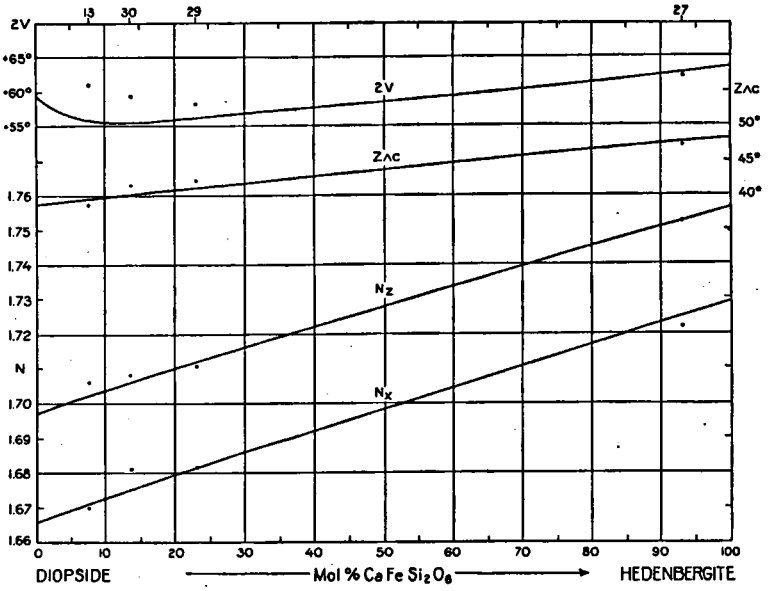

Fig. 20. Variation of optical properties of a few clinopyroxenes in the diopside-hedenbergite series. The numbers in the upper part of the diagram refer to those in Table 10. The dots in the diagram refer to measurements on the clinopyroxene specimens. Diagram after TRÖGER (1952).

The angle Z ∧ c is more variable and is largest for schefferite and hedenbergite. According to the value of Z ∧ c the schefferite is a manganiferous diopside with about 14 percent MnO + FeO (WINCHELL 1948). This agrees with the result of the röntgenographic investigation that schefferite gives an X-ray powder diagram which is practically identical to that of diopside.

The Ca-Mg-Fe-Al-pyroxenes vary rather strongly in 2 V and Z ∧ c.

Most of the augite specimens possess a zonal structure due to difference of chemical composition; the titaniferous augites are characterized by the typical colour and pleochroism and by the strong dispersion in the extinction.

For the specimens of Group III (Alkali pyroxenes) the diversity of 2 V and Z ∧ c is very large. The sign of 2 V is negative for aegirite; moreover this pyroxene has the highest value for Z ∧ c. In this group the pleochroism

TABLE 10

Optical properties of some clinopyroxenes

Group	Sample number	2 V	Z ∧ c	Chemical composition from chem. analysis
II	13. Diopside, Austria	+61°	38.5°	$Ca_{49.5}\,Mg_{46.5}\,Fe_4$ (see Table 11)
	14. Malacolite, Sweden	+59.5°	39°	
	15. Malacolite, Czechoslovakia	+58 5°	39.5°	
	16. Coccolite, Norway	+58°	39°	
	17. Sahlite, Sweden	+61°	44°	
	18. Shefferite, Sweden	+61°	45.5°	
	19. Fassaite, Italy	+58.5°	40.5°	
	20. Chrome-Diopside, Germany	+61°	38.5°	
	21. Diallage, Italy	+56°	40.5°	
	22. Diallage, Austria	+58°	39.5°	
	23. Diallage, England	+54°	42°	
	24. Diallage, France	+51°	43°	
	25. Pigeonite, Japan	+13.5°	43°	$Ca_8\ Mg_{64}\ Fe_{28}$ (KUNO & HESS 1953)
	26. Hedenbergite, Sweden	+59.5°	47.5°	
	27. Hedenbergite, California	+62°	47°	$Ca_{48}\,Mg_3\ Fe_{49}$ (KUNO & HESS 1953)
	28. Augite, Vesuvius	+58°	43.5°	
	29. Augite, Odawara, Japan	+58°	42°	$Ca_{48}\,Mg_{40}\,Fe_{12}$ (see Table 11)
	30. Augite, Wadaki, Japan	+59.5°	41.5°	$Ca_{48}\,Mg_{45}\,Fe_7$ (KUNO & SAWATARI 1934)
	31. Augite, France	+55°	49.5°	
	32. Augite, Nishigatake, Japan	+59.5°	41°	$Ca_{44}\,Mg_{51}\,Fe_5$ (see Table 11)
	33. Augite, Yone-yama, Japan	+55°	44°	$Ca_{44}\,Mg_{43}\,Fe_{13}$ (KUNO & SAWATARI 1934)
	34. Augite, Etna, Italy	+56.5°	46°	
	35. Ti-augite, Rongstock, Czechoslovakia	+58°	44°	
	36. Ti-augite, Babutzin, Czechoslovakia	+58°	48.5°	
III	37. Acmite, Eker, Norway	—61°	92°	
	38. Aegirite, Langesundfiord, Norway	—63°	94°	
	39. Aegirite-augite, Sweden	+65°	69.5°	
	40. Aegirite-augite, Germany	+61°	71.5°	
	41. Omphacite, Germany	+66.5°	38.5°	
	42. Omphacite, Austria	+73°	39.5°	
	43. Jadeite, Upper Burma	+79°	38°–43°	
	44. Spodumene, N. Sweden	+64.5°	24.5°	
	45. Spodumene, U.S.A.	+66°	27°	
	46. Aegirite, Ditro, Siebenbürgen	—71°	91.5°	71 mol % $NaFe'''Si_2O_6$ (see Table 11)

of aegirite-augite is characteristic. The omphacite specimens have an optic axial angle which is considerably larger than that of diopside. In accordance with this difference in optical properties their X-ray powder diagrams show a reflection pattern which can be considered as a transition between that of diopside and that of the alkali pyroxenes (e. g. aegirite).

Finally it may be noted that the optical properties of the clinopyroxenes stated in Table 10 do not differ much from the values mentioned in the literature for the various pyroxenes. This can be seen in fig. 20 which is a diagram according to TRÖGER (1952). The optical properties of four clinopyroxenes for which the chemical composition is known, are plotted against the number of molecular percent $CaFeSi_2O_6$. The 2 V values differ somewhat from the 2 V curve and they agree better with the 2 V curve given by WINCHELL (1948). However, it is seen that the data agree rather well with the other curves according to TRÖGER.

Chemical Analyses

The chemical compositions of eight röntgenographically investigated clinopyroxenes are stated in Table 10. In Table 11 four chemical analyses are listed; two of them (Nos. 13 and 46) were made in the Mineralogical-Petrological Laboratory in Leiden, while the analyses Nos. 29 and 32 were communicated by Dr. H. KUNO. The remaining samples Nos. 25, 27, 30 and 33 were sent by Dr. H. KUNO and Professor Dr. H. H. HESS, while they indicated where I could find the analyses of the same specimens in the literature.

Considering the chemical compositions of these eight monoclinic pyroxenes in relation with the molecular percentages of $CaSiO_3$, $MgSiO_3$, $FeSiO_3$, and disregarding the alumina content (according to HESS 1941), the following may be seen:

Pyroxene No. 13 lies in the diopside field and is almost an end member of the diopside-hedenbergite series. Specimen No. 25 with its low Ca content lies in the pigeonite field. Pyroxene No. 27 belongs in the hedenbergite field, being nearly an end member in the diopside-hedenbergite series. The specimens Nos. 29, 30, 32 and 33 lie all in the augite field. The alkali pyroxene No. 46, with 71 mol % $NaFe'''Si_2O_6$ is a rather $NaFe'''$ rich member of the diopside-acmite series.

One may conclude from these data, that the nomenclature of the eight monoclinic pyroxenes is justified.

X-ray Investigation

Introduction

The X-ray method is used on clinopyroxenes both for determining crystal structures and determining minerals.

As was mentioned on p. 192, WARREN and BRAGG described in 1929 the structure of diopside $CaMg(SiO_3)_2$. They determined this structure by means of rotation photographs. Since we will not occupy ourselves with structure investigation in this thesis, we will only look at the determination of clinopyroxenes by X-rays.

In 1925 WYCKOFF, MERWIN and WASHINGTON made measurements on pyroxenes with X-ray diffraction. Commenting on the reflection pattern of the

TABLE 11

Chemical analyses of some clinopyroxenes

Sample	No. 13, Diopside, Austria	No.29, Augite, Odawara*	No.32, Augite, Nishigatake*	No. 46, Aegirite, Ditro
SiO_2	53.42	50.87	50.67	49.45
TiO_2	tr.	0.48	0.56	0.79
Al_2O_3	0.24	3.22	4.11	3.89
P_2O_5	tr.	n.d.	n.d.	n.d.
Fe_2O_3	1.72	0.49	1.94	23.18
FeO	2.56	7.51	3.17	2.92
MgO	16.82	14.14	17.13	2.31
MnO	0.18	0.07	n.d.	1.99
CaO	24.89	23.87	20.43	6.74
Na_2O	0.15	0.32	0.38	7.47
K_2O	tr.	0.10	0.25	0.81
H_2O+	0.06	n.d.	n.d.	0.58
H_2O-	0.00	0.05	0.06	
Total	100.04	101.12	99.32* * + 0.62 Cr_2O_3	100.13
NIGGLI-values				
si	69.3	91.6	93.1	117.2
al	0.2	3.4	4.4	5.4
fm	51.5	50.0	54.4	59.1
c	48.1	46.0	40.2	17.1
alk	0.2	0.6	1.	18.4
k	—	0.17	0.33	0.07
mg	0.87	0.76	0.86	0.14
Chemical composition:	$Ca_{49.5}Mg_{46.5}Fe_4$	$Ca_{48}Mg_{40}Fe_{12}$	$Ca_{44}Mg_{51}Fe_5$	71 mol% $NaFe'''Si_2O_6$
Analyzed by:	Miss B. HAGEMAN	K.Nagashima	T. Miyake	Mrs. Dr. C. M. DE SITTER—KOOMANS

* Analyses Nos. 29 and 32, H. KUNO, Personal communication.

investigated samples they pointed out that all available pyroxenes, with a few exceptions, gave patterns of one of four different groups, namely a diopside group, an enstatite group, a wollastonite group and a rhodonite group. Examples of pyroxenes belonging to each of the groups are given below. The diopside group includes for instance, acmite and jadeite; we can-

not agree with this, because both pyroxenes have an reflection pattern which can be clearly distinguished from that of diopside. Further it is seen, that enstatite and hypersthene belong to the enstatite group which is in accordance with our results. Besides the wollastonite and rhodonite group they propose a fifth group of minerals having a different reflection pattern not corresponding with one of the other four groups. One of the members of this latter group is spodumene. Finally WYCKOFF, MERWIN and WASHINGTON state that Fe and Mg may be substituted for each other with practically no change in shape or size of the resulting crystal. Mn in the divalent condition seems to have a slightly larger and Ca a much larger effective volume than Fe and Mg. This statement amounts to the same thing as that which is given for the orthopyroxenes as an explanation for the change of the unit cell dimensions.

ATLAS described the polymorphism of $MgSiO_3$ in 1952. He examined the stability of three different crystalline phases of $MgSiO_3$. Protoenstatite, for instance, is a modification which is stable above 990° C.; below this temperature the stable form is rhombic enstatite. The importance of this paper is that it gives the unit cell dimensions of rhombic enstatite, protoenstatite and clinoenstatite, in addition to the powder X-ray data for these pyroxenes. ATLAS concludes that protoenstatite is also orthorhombic. From this conclusions it is evident that ATLAS found differences between orthorhombic and monoclinic pyroxenes with the X-ray method.

KUNO and HESS came out in 1953 with an important publication. In this paper they give data about the unit cell dimensions of clinoenstatite, pigeonite, diopside, ferrosalite and hedenbergite. They conclude that the chemical composition of these pyroxenes may be determined rather accurately from the combined data about the optical properties and the unit cell dimensions. We will calculate the relative distance between certain reflections which are sensitive to a change of the chemical composition from their data about the unit cell dimensions. This will be done to show the connection between these relative distances and the chemical composition. The calculation will be described on p. 254. Further it appears on comparison of the X-ray powder diagrams of the above-mentioned minerals, that the structures of all clinopyroxenes are similar. We can agree with this result on the ground of this comparison.

KUNO devoted a publication to the diopside-ferropigeonite series of clinopyroxenes in 1955 paying special attention to the transition between augite and pigeonite which is called subcalcic augite. According to several investigators on pyroxenes as, for instance, HESS (1941) and POLDERVAART and HESS (1951), there is no continual transition between augite and pigeonite but an immiscibility gap exists. Now KUNO states that under ordinary conditions of crystallization of magmas, this subcalcic augite indeed does not form. Under certain exceptional conditions, however, this does happen, according to KUNO, namely when part of Si^{4+} in the Si-O chains is replaced by Fe^{3+}, making it possible for Ca^{2+}, Mg^{2+} and Fe^{2+} to enter the pyroxene structure in all proportions, also in those proportions which are necessary to form subcalcic augite. KUNO's data about the unit cell dimensions of a few pyroxenes were used to calculate the relative distances between certain reflections.

RAMDOHR (1954) states, that clinoenstatite is probably analogous to wollastonite; this mineral therefore should not have a pyroxene structure, which contradicts the ideas of KUNO and HESS (1953). Since we have no clino-

enstatite at our disposal we are not in a position to check either statement.

It is our intention to distinguish the different clinopyroxenes from each other by X-ray powder diagrams and afterwards we will try to show the relation between the relative distance of certain reflections and the chemical composition, as was done for the orthopyroxenes.

General Data About Photographic Techniques

The camera and radiation, the average exposure, the measurements on powder diagrams etcetera are the same for the monoclinic and the orthorhombic pyroxenes, so that one may find all details on p. 192.

Results of the X-ray Investigation

On the basis of the reflection pattern, i. e. the position and the intensity of the reflections, the X-ray powder diagrams were subdivided into two main groups, independently of the optical and chemical results.

A. Orthorhombic group (e. g. enstatite, bronzite, hypersthene).

B. Monoclinic group.

The latter group was subdivided in four subgroups, that is:

Group B 1 (e. g. hedenbergite, diopside, augite, diallage)
Group B 2 (e. g. pigeonite)
Group B 3 (e. g. aegirite, jadeite)
Group B 4 (e. g. spodumene).

From each group one powder photograph is given in fig. 21 while a diagram of θ_{Fe} is given in fig. 22 (the heights of the lines represent relative estimated intensities). It is evident from these diagrams, that the main groups A and B can be distinguished clearly from each other. The subgroups of group B also show some differences but here naturally transitions are possible between some groups as, for instance, between groups B 1 and B 2 and between groups B 1 and B 3, so that no sharp lines can be drawn here. Further it may be possible that some more groups can be distinguished for as we had no clinoenstatite or ferrosilite at our disposal, we could not check whether these pyroxenes have powder diagrams differing from the others.

First we will discuss the principal characteristics of the groups and afterwards we will describe each group separately.

Principal Characteristics of the Groups

Group A. *Orthorhombic group.* (figs. 6, 21 and 22) — This group is distinguished from group B by the position and the high intensity of the reflection (4 2 0) (2 2 1) ($\theta_{FeK\alpha}$ 17.77) [5].

[5]) This reflection is really a pair of reflections which cannot be seen using the normal photographic techniques described on p. 192. By using a NONIUS GUINIER camera with a diameter of 114.6 millimeters (as designed by Dr. P. M. DE WOLFF) and $FeK\alpha_1$ radiation ($\lambda = 1.93597$ Å) with a quartz filter, one can observe the reflections 420 and 221 separately. This camera was especially designed for reflections with a low glancing angle.

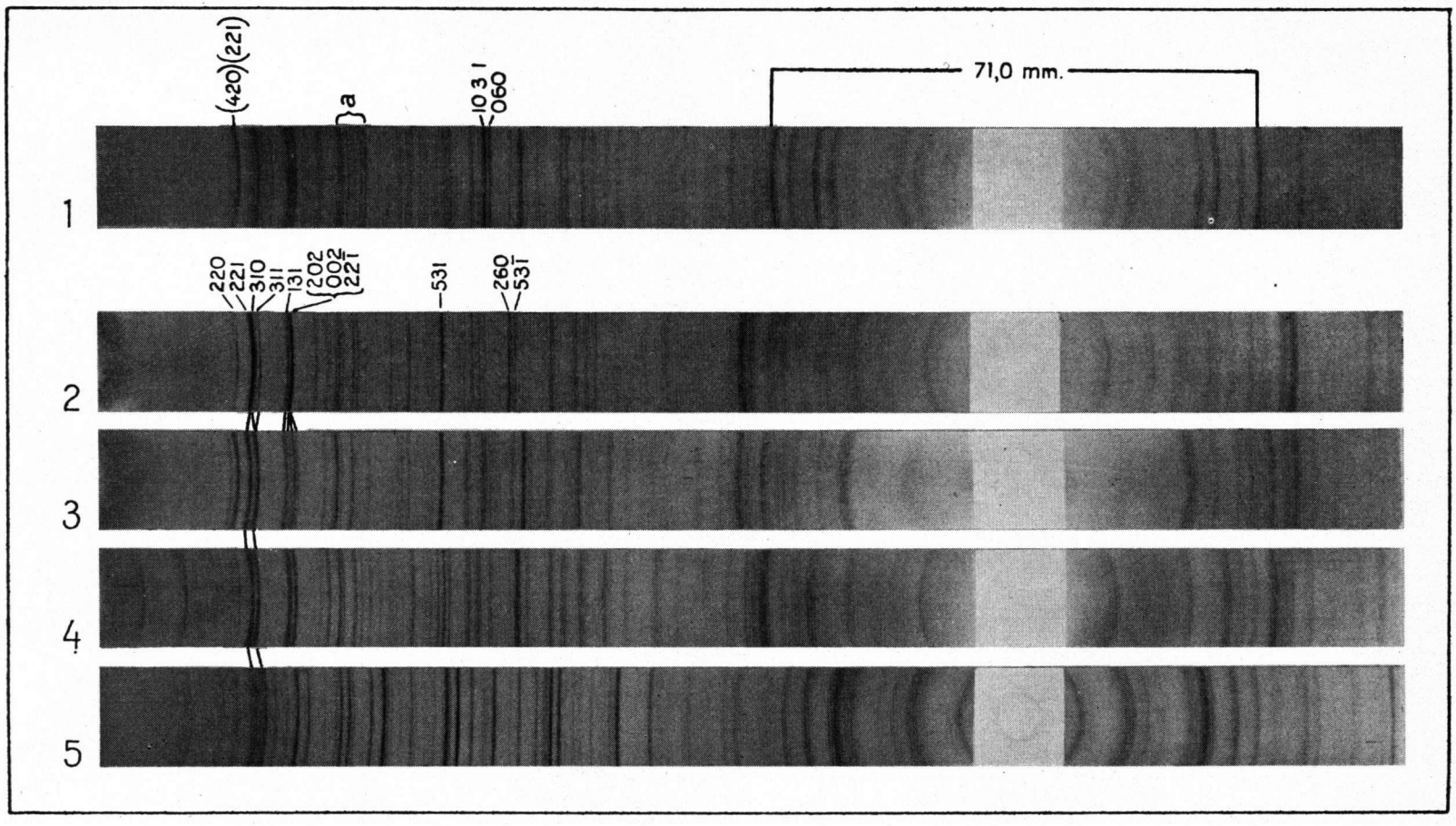

Fig. 21. X-ray powder photographs of some pyroxenes. (FeKα_1 radiation, Camera diameter 9 cm).

No. 1 Group A, Enstatite No. 3, Finkenberg, Germany m* 1253
No. 2 Group B 1, Diopside No. 13, Zillertal, Austria st. 24594 m 568
No. 3 Group B 2, Pigeonite No. 25, Hakone volcano, Japan m 1320
No. 4 Group B 3, Acmite No. 37, Eker, Norway st. 24642 m 572
No. 5 Group B 4, Spodumene No. 45, Massachusetts, U.S.A. st. 64940 m 1216

* Number X-ray photograph.

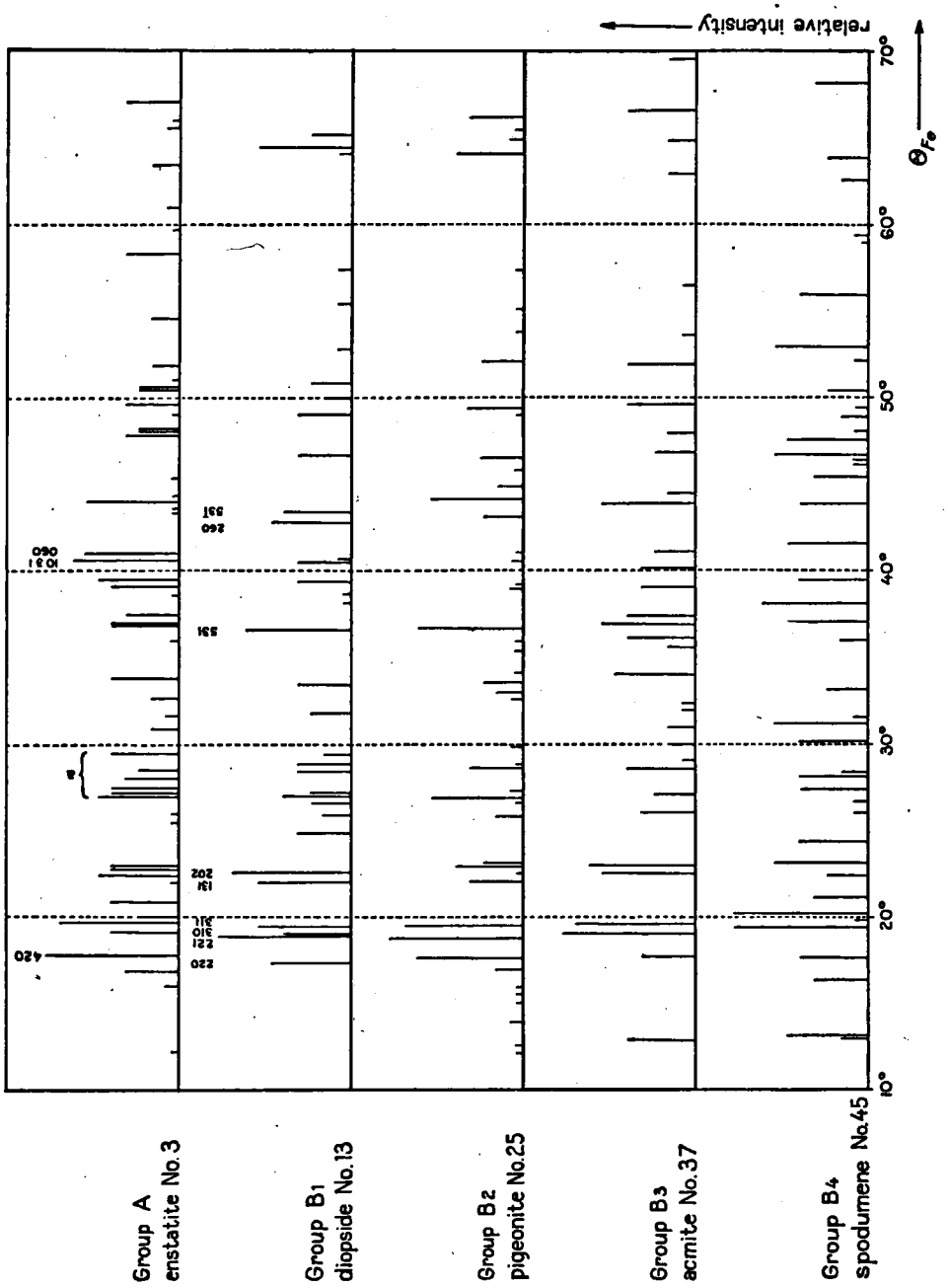

Fig. 22. θ diagrams of some pyroxenes ($FeK\alpha_1$ radiation).
Heights of lines represent estimated relative intensities.

A further characteristic is the group of reflections, indicated with "a", besides the strong pair of reflections 10 3 1 (θ 40.61) and 0 6 0 (θ 41.40). The specimens having a powder diagram in accordance with that of this group are all orthopyroxenes (enstatite, bronzite and hypersthene) so that the reader is referred to the chapter on the orthopyroxenes for details.

Group B. *Monoclinic group.* (figs. 21 and 22) — This group has a reflection pattern, altogether different from group A.

All subgroups have a strong reflection 2 2 1 ($\theta_{FeK\alpha}$ 18.90), while they show more or less differences in the position and the intensity of the reflection groups 2 2 1 (θ 18.90), 3 1 0 (θ 19.11), 3 1 1 (θ 19.53) and 1 3 1 (θ 22.20), 2 2 $\bar{1}$ (θ 22.65). We will therefore describe the characteristic properties of each subgroup separately.

Group B 1. (figs. 23 and 24) — The positions and intensities of the reflection groups 2 2 1 ($\theta_{FeK\alpha}$ 18.86), 3 1 0 (θ 19.11), 3 1 1 (θ 19.53) and 1 3 1 (θ 22.20), 2 2 $\bar{1}$ (θ 22.65) are characteristic for this group; the isolated strong reflection 5 3 1 (θ 36.59) moreover is important to distinguish this group from the other subgroups, as is the strong pair of reflections 2 6 0 (θ 42.79) and 5 3 $\bar{1}$ (θ 43.43). Hedenbergite, diopside, augite and diallage belong to this group.

Group B 2. (figs. 23 and 24) — The powder diagram of this group has a coincidence of the reflections 3 1 0 and 3 1 1 ($\theta_{FeK\alpha}$ 19.59) in contrast to that of group B 1, so that the reflections 2 2 1 (θ 18.83) and (3 1 0) (3 1 1) have about the same high intensity.

In addition one may observe the reflections 2 0 2 (θ 22.61), 0 0 2 (θ 23.03) and 2 2 $\bar{1}$ (θ 23.28) separately; the intensity of 0 0 2 is greater than that of the other two. These three reflections coincide in group B 1. Pigeonite can be included in this group.

Group B 3. (figs. 21 and 22) — The position and the intensity of the reflections 2 2 1 ($\theta_{FeK\alpha}$ 18.96), (3 1 0) (3 1 1) (θ 19.60), 1 3 1 (θ 22.59) and 2 2 $\bar{1}$ (θ 23.07) are characteristic for the X-ray powder diagrams belonging to this group, because the lines 2 2 1 and (3 1 0) (3 1 1) form a very strong pair of reflections; both have the highest intensity which can be observed on the reflections in the diagram. The lines 1 3 1 and 2 2 $\bar{1}$ likewise form a strong pair of reflections, their intensity, however, is somewhat lower than that of the other reflections. Aegirite and jadeite belong to this group.

Group B 4. (figs. 21 and 22) — The X-ray powder diagrams of the pyroxenes belonging to this group show such obvious differences in the reflection pattern with respect to those of the other pyroxenes (including the other alkali pyroxenes) that it seemed desirable to form a special group for them. The position and the intensity of the reflections 2 2 1 ($\theta_{FeK\alpha}$ 19.40) and 3 1 1 (θ 20.35) is characteristic for the members of this group. These lines form a very strong pair of reflections with a great relative distance between them in comparison with other pyroxenes. Although this pair of reflections is sufficient to recognize the diagrams of this group, it may be noted that a rather large number of isolated strong reflections occur over the whole powder diagram.

All spodumene specimens belong to this group.

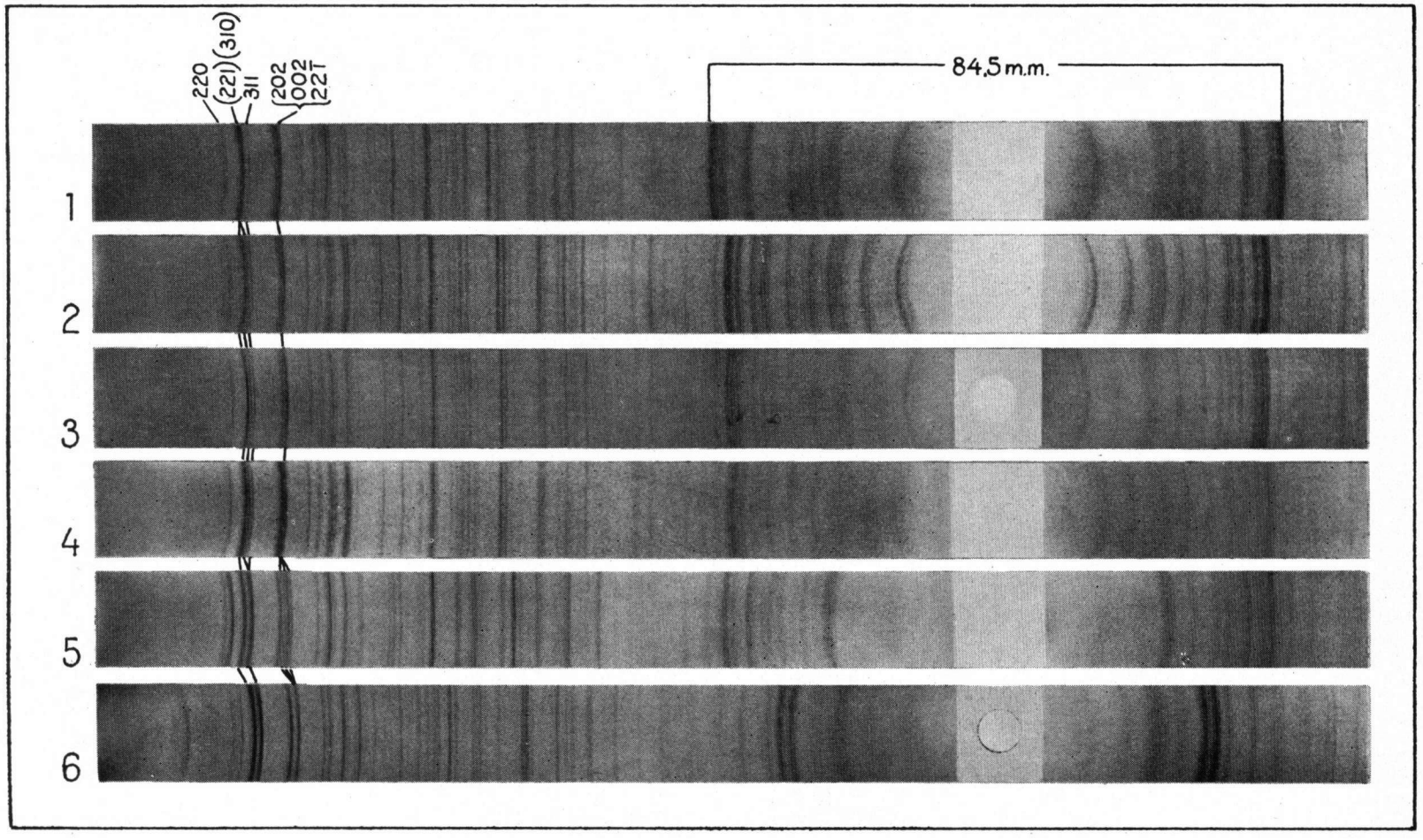

Fig. 23. X-ray powder photographs of a few pyroxenes. (FeK α, radiation, Camera diameter 9 cm).

No. 1	Hedenbergite No. 26, Sweden	st. 69562	m* 1252	No. 4	Ti-augite No. 36, Babutzin, Czechoslovakia	st. 12696	m	1214
No. 2	Fassaite No. 19, Italy	st. 24615	m 802	No. 5	Pigeonite No. 25, Hakone volcano, Japan		m	1320
No. 3	Augite No. 30, Wadaki, Japan		m 1203	No. 6	Jadeite No. 43, Upper Burma		m	1193

* Number X-ray photograph.

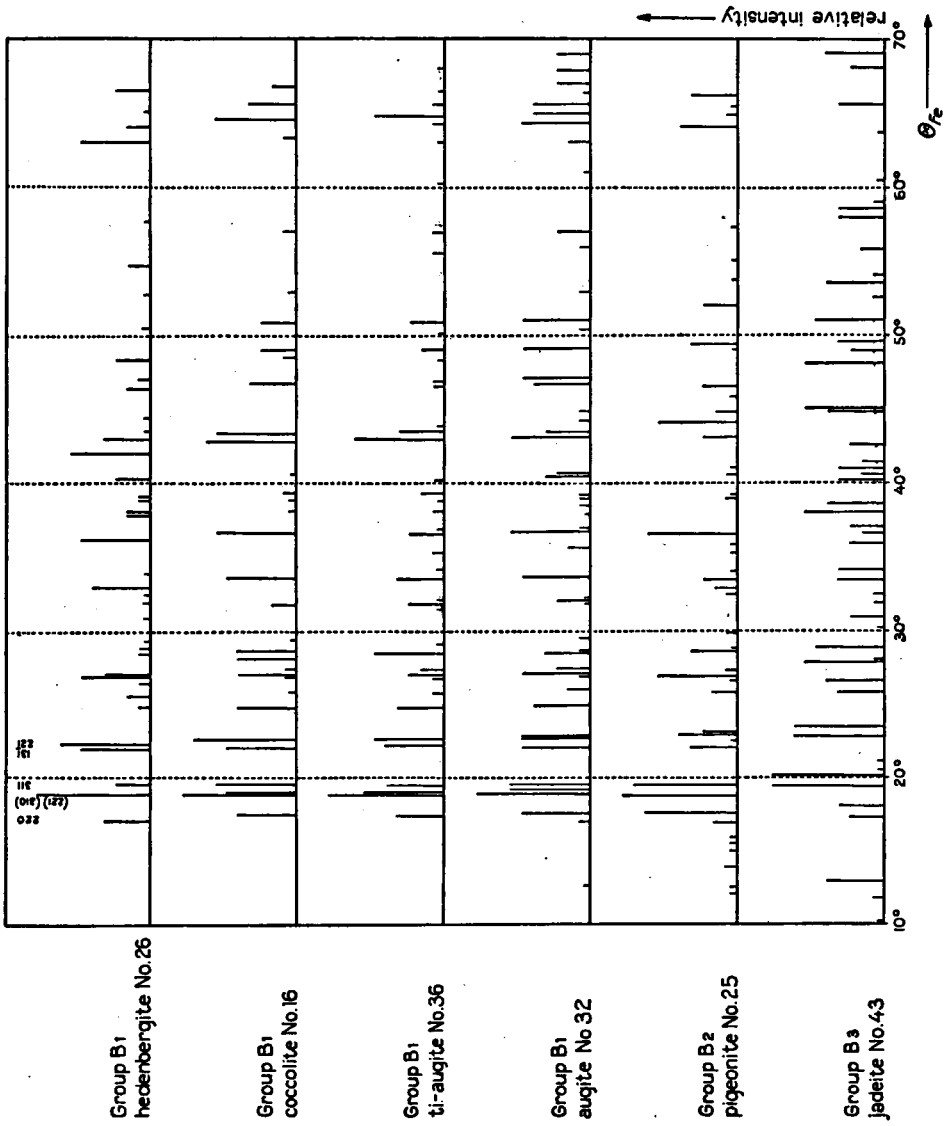

Fig. 24. β diagrams of some clinopyroxenes (FeKα_1 radiation). Heights of lines represent estimated relative intensities.

TABLE 12

X-ray powder patterns group B 1

Hedenbergite, Yxsjo Mine, Sweden (No. 26) 2 V = +59.5°; Z ∧ c = 47.5°				Diopside, Zillertal, Tyrol, Austria (No. 13) 2 V = +61°; Z ∧ c = 38.5° $Ca_{49.5}Mg_{46.5}Fe_4$			Ti-augite, Babutzin, Czechoslovakia (No. 36) 2 V = +58°; Z ∧ c = 48.5°			Diallage, Coverack, Lizard, Cornwall, England (No. 23) 2 V = +54°; Z ∧ c = 42°			Augite, Nishigatake, Nagasaki Pref, Kynshu, Japan (No. 32) 2 V = +59.5°; Z ∧ c = 41° $Ca_{44}Mg_{51}Fe_5$			
6 C_{2h} hkl	θ_{Fe}	d(Å)	Relative Intensity	θ_{Fe}	d(Å)	Relative Intensity	θ_{Fe}	d(Å)	Relative Intensity	θ_{Fe}	d(Å)	Relative Intensity	θ_{Fe}	d(Å)	Relative Intensity	hkl
110	8.54	6.52	VW	—	—	—	—	—	—	—	—	—	—	—	—	110
111	—	—	—	—	—	—	—	—	—	—	—	—	12.68	4.41	VW	111
021	—	—	—	—	—	—	—	—	—	—	—	—	17.08	3.30	VW	021
220	17.30	3.26	MW	17.43	3.23	M	17.39	3.24	MW	17.52	3.22	MW	17.55	3.21	M	220
221	18.95	2.980	VS	18.86	2.994	VS	18.83	2.999	VS	18.95	2.981	VS	18.92	2.985	VS	221
310				19.11	2.957	MW	19.11	2.957	SM	19.27	2.933	SM	19.27	2.933	SM	310
311	19.56	2.891	W	19.53	2.896	SM	19.49	2.901	MW	19.65	2.879	M	19.59	2.887	SM	311
131	22.07	2.576	M	22.20	2.562	SM	22.30	2.551	MW	22.29	2.551	MW	22.23	2.559	M	131
202													22.65	2.514	M	202
002	22.42	2.538	S	22.65	2.514	VS	22.68	2.510	M	22.68	2.510	M				002
$22\bar{1}$													22.77	2.501	M	$22\bar{1}$
400	24.91	2.298	VW	24.91	2.298	MW	24.84	2.304	MW	24.97	2.293	MW	24.87	2.302	MW	400
222	25.67	2.235	W	25.89	2.217	W	25.80	2.224	VW	26.02	2.207	VW	26.08	2.202	W	222
$11\bar{2}$	26.47	2.172	VW	26.66	2.157	W	26.78	2.148	VW	26.85	2.143	VW	26.88	2.141	VW	$11\bar{2}$
331	26.85	2.143	M	26.97	2.134	MW	27.04	2.129	W	27.04	2.129	MW	27.07	2.127	M	331
421	27.17	2.120	MW	27.29	2.111	W	27.36	2.106	W	27.36	2.106	W	27.39	2.104	W	421
420	28.53	2.027	VW	28.41	2.035	MW	28.47	2.031	M	28.47	2.031	VW	28.50	2.029	MW	420
240	28.82	2.008	VW	28.76	2.012	MW	—	—	—	28.76	2.012	VW	28.63	2.020	VW	240
132	29.36	1.974	VW	29.39	1.973	W	29.33	1.976	VW	29.46	1.968	VW	29.52	1.965	VW	132
422	31.40	1.858	VW	—	—	—	31.49	1.853	VW	—	—	—	31.75	1.840	VW	422
332	32.07	1.823	VW	31.84	1.835	W	31.78	1.838	W	31.97	1.828	MW	31.97	1.828	W	332
$33\bar{1}$	32.61	1.796	VW	—	—	—	32.19	1.817	VW	—	—	—	32.29	1.812	VW	$33\bar{1}$
150	33.18	1.769	MW	33.50	1.754	MW	33.66	1.746	MW	33.66	1.746	MW	33.63	1.748	M	150

42$\bar{1}$	*33.95*	*1.733*	*VW*	—	—	—	*34.26*	*1.720*	*VW*	—	—	—	—	—	—	*42$\bar{1}$*
313	—	—	—	—	—	—	35.38	1.672	VW	35.54	1.665	VW	35.57	1.664	W	313
531	36.30	1.635	M	36.59	1.624	S	36.59	1.624	W	36.62	1.623	M	36.68	1.621	SM	531
440	—	—	—	—	—	—	36.84	1.614	VW	—	—	—	36.94	1.611	VW	440
530	37.77	1.580	W	—	—	—	—	—	—	37.86	1.577	VW	37.80	1.579	VW	530
023	38.21	1.565	W	38.34	1.560	VW	38.31	1.562	VW	38.43	1.557	W	38.56	1.553	VW	023
51$\bar{1}$	38.82	1.544	VW	38.69	1.549	VW	38.82	1.544	VW	38.82	1.544	VW	38.85	1.543	VW	511
600	39.17	1.533	VW	39.39	1.525	MW	39.39	1.525	W	39.33	1.527	VW	39.29	1.529	VW	600
442	40.40	1.493	W	40.09	1.503	MW	40.25	1.498	W	40.50	1.491	W	40.38	1.494	VW	442
060	—	—	—	40.57	1.488	VW	—	—	—	40.76	1.483	VW	40.76	1.483	W	060
260	42.16	1.442	SM	42.79	1.425	M	42.89	1.422	S	43.08	1.417	SM	43.14	1.416	SM	260
53$\bar{1}$	43.11	1.416	MW	43.43	1.408	MW	43.46	1.407	MW	43.46	1.407	MW	43.43	1.408	MW	53$\bar{1}$
.....	43.69	1.401	VW	—	—	—	43.94	1.395	VW	44.29	1.386	VW	44.29	1.386	VW	.....
.....	44.64	1.378	VW	—	—	—	—	—	—	44.77	1.375	VW	44.83	1.373	VW	.....
.....	46.52	1.334	W	46.58	1.333	MW	46.58	1.333	VW	46.71	1.330	W	46.71	1.330	MW	.....
.....	47.28	1.318	VW	—	—	—	46.90	1.326	VW	47.12	1.321	W	47.19	1.320	M	.....
.....	48.49	1.293	W	49.00	1.283	MW	49.16	1.280	W	49.16	1.280	W	49.19	1.279	M	.....
.....	50.05	1.263	MW	49.96	1.264	W	50.18	1.260	VW	50.15	1.261	VW	50.43	1.256	VW	.....
.....	50.75	1.250	VW	50.82	1.249	W	50.91	1.247	W	51.04	1.245	W	51.13	1.243	M	.....
.....	52.76	1.216	VW	52.79	1.215	VW	—	—	—	52.98	1.212	VW	52.98	1.212	VW	.....
.....	54.67	1.187	W	55.53	1.174	VW	55.59	1.173	VW	55.94	1.168	W	56.04	1.167	VW	.....
800	57.69	1.145	VW	57.47	1.148	VW	57.02	1.154	VW	57.37	1.149	W	57.25	1.151	W	800
.....	59.92	1.119	VW	—	—	—	60.40	1.113	VW	61.06	1.106	VW	61.13	1.105	VW	.....
.....	—	—	—	—	—	—	63.20	1.085	VW	63.36	1.083	VW	63.33	1.083	W	.....
660	63.20	1.084	M	64.22	1.075	SM	64.38	1.074	VW	64.34	1.074	W	64.44	1.073	M	660
51$\bar{3}$	64.25	1.075	W	64.47	1.073	VW	64.76	1.070	M	64.82	1.070	W	65.01	1.068	MW	51$\bar{3}$
750	65.30	1.066	VW	65.24	1.066	W	65.68	1.062	VW	65.46	1.064	W	65.55	1.063	MW	750
.....	66.60	1.055	W	—	—	—	66.57	1.055	VW	66.19	1.058	VW	66.41	1.056	VW	.....
.....	—	—	—	—	—	—	—	—	—	66.92	1.052	W	67.05	1.051	W	.....
.....	—	—	—	68.23	1.042	W	68.23	1.042	VW	67.81	1.045	W	68.04	1.044	W	.....
.....	69.12	1.036	VW	—	—	—	—	—	—	68.80	1.038	W	69.02	1.037	W	.....
.....	70.55	1.027	VW	70.11	1.029	VW	70.26	1.028	VW	70.26	1.028	VW	70.42	1.027	W	.....
840	72.43	1.015	VW	72.21	1.017	VW	72.37	1.016	VW	72.56	1.015	W	72.75	1.014	MW	840
.....	73.64	1.009	VW	—	—	—	—	—	—	72.94	1.013	VW	73.07	1.012	VW	.....
.....	74.40	1.005	VW	76.44	0.996	W	74.30	1.005	VW	75.36	1.001	W	75.71	0.999	W	.....
.....	80.48	0.982	VW	81.56	0.979	W	80.04	0.983	VW	78.57	0.988	VW	78.95	0.986	W	.....
.....	—	—	—	—	—	—	—	—	—	81.92	0.978	W	81.76	0.978	MW	.....
.....	—	—	—	82.36	0.977	W	—	—	—	82.46	0.976	VW	82.65	0.976	W	.....

Description of the Groups

Group B 1 (figs. 23 and 24) — The variation in θ and the lattice spacings with accessory intensities for five clinopyroxenes, belonging to this group, are stated in Table 12, while in fig. 24 a diagram for θ_{Fe} can be seen, in which the heights of the lines represent estimated relative intensities.

In Table 13 the clinopyroxenes that were investigated with X-rays are shown. They have a powder pattern which is characteristic for this group. Except for hedenbergite and omphacite all the specimens mentioned in this table have an X-ray powder diagram which is almost the same as that of diopside No. 13. They may be considered therefore as clinopyroxenes which have a chemical composition in the isomorphous series diopside-hedenbergite and diopside-pigeonite close to that of diopside.

TABLE 13

Clinopyroxenes with the X-ray powder diagram of group B 1 arranged according to classification on p. 224.

Group	Sample Number	2 V	Z ∧ c	Chemical composition	Localities
II	13 Diopside	+61°	38.5°	$Ca_{49.5}\ Mg_{46.5}\ Fe_4$	Austria
	14 Malacolite	+59.5°	39°		Sweden
	15 Malacolite	+58.5°	39.5°		Czechoslovakia
	16 Coccolite	+58°	39°		Norway
	17 Sahlite	+61°	44°		Sweden
	18 Schefferite	+61°	45.5°		Sweden
	19 Fassaite	+58.5°	40.5°		Italy
	20 Chrome-diopside	+61°	38.5°		Germany
	21 Diallage	+56°	40.5°		Italy
	22 Diallage	+58°	39.5°		Austria
	23 Diallage	+54°	42°		England
	24 Diallage	+51°	43°		France
	26 Hedenbergite	+59.5°	47.5°		Sweden
	27 Hedenbergite	+62°	47°	$Ca_{48}\ Mg_3\ Fe_{49}$	California
	28 Augite	+58°	43.5°		Vesuvius
	29 Augite	+58°	42°	$Ca_{48}\ Mg_{40}\ Fe_{12}$	Odawara, Japan
	30 Augite	+59.5°	41.5°	$Ca_{48}\ Mg_{45}\ Fe_7$	Wadaki, Japan
	31 Augite	+55°	49.5°		France
	32 Augite	+59.5°	41°	$Ca_{44}\ Mg_{51}\ Fe_5$	Nishigatake, Japan
	33 Augite	+55°	44°	$Ca_{44}\ Mg_{43}\ Fe_{13}$	Yone-yama, Japan
	34 Augite	+56.5°	46°		Etna, Italy
	35 Ti-augite	+58°	44°		Rongstock, Czechoslovakia
	36 Ti-augite	+58°	48.5°		Babutzin, Czechoslovakia
III	39 Aegirite-augite	+65°	69.5°		Sweden
	40 Aegirite-augite	+61°	71.5°		Germany
	41 Omphacite	+66.5°	38.5°		Germany
	42 Omphacite	+73°	39.5°		Austria

Schefferite No. 18 probably is a manganiferous diopside, because its X-ray powder diagram practically is identical to that of diopside No. 13. Through lack of sufficient manganiferous pyroxene specimens we could not study the effect of Mn on the unit cell.

It is important to note, moreover, that both aegirite-augite specimens have an X-ray powder diagram also closely resembling that of diopside and quite unlike that of aegirite. Therefore they probably have the chemical composition of an $NaFe'''$-bearing diopside.

Both the hedenbergite samples show rather great differences in the powder pattern wih respect to the diopside diagram. Diopside No. 13 and hedenbergite No. 27 practically are the two end members of the diopside-hedenbergite series. The resemblance between the diagrams in question, however, is great enough to conclude, that they have a similar structure. The pattern of hedenbergite shows two coinciding reflections 2 2 1 and 3 1 0, the reflections (2 2 1) (3 1 0) and 3 1 1 can be observed, by that the former is very strong and the latter is weak. In the diagram of diopside, there occur three separate reflections, that is to say 2 2 1, 3 1 0 and 3 1 1 whose intensity decreases in the same order of succession.

In many other powder diagrams of clinopyroxenes given in Table 13, the reflection 3 1 0 has also another position with regard to the reflections 2 2 1 and 3 1 1 as in the diagram of diopside No. 13. The relative distance between 2 2 1 and 3 1 0 is considerably greater than with diopside. This can be seen in the powder diagrams of all augite, diallage, chrome-diopside, Ti-augite and omphacite samples. Although the augite specimens show distinct microscopic zoning, there cannot yet be seen a widening of certain reflections.

In addition it is important to note that both omphacite specimens have a reflection pattern which may be considered as a transition between that of diopside No. 13 and that of the alkalipyroxenes (group B 3).

This may be seen from the following tabulation:

Diopside No. 13

$d\,(2\,2\,0) = 3.232$ Å
$d\,(2\,2\,1) = 2.994$ Å $>$ difference: 0.238 Å
$d\,(3\,1\,0) = 2.957$ Å $>$ difference: 0.037 Å
$d\,(1\,3\,1) = 2.562$ Å
$d\,(2\,2\,\bar{1}) = 2.514$ Å $>$ difference: 0.048 Å

Omphacite No. 41

$d\,(2\,2\,0) = 3.205$ Å
$d\,(2\,2\,1) = 2.975$ Å $>$ difference: 0.230 Å
$d\,(3\,1\,0) = 2.923$ Å $>$ difference: 0.052 Å
$d\,(1\,3\,1) = 2.548$ Å
$d\,(2\,2\,\bar{1}) = 2.448$ Å $>$ difference: 0.060 Å

Omphacite No. 42

$d\,(2\,2\,0) = 3.205$ Å
$d\,(2\,2\,1) = 2.981$ Å $>$ difference: 0.224 Å
$d\,(3\,1\,0) = 2.923$ Å $>$ difference: 0.058 Å
$d\,(1\,3\,1) = 2.551$ Å
$d\,(2\,2\,\bar{1}) = 2.491$ Å $>$ difference: 0.060 Å

Aegirite No. 46

d (2 2 0) = 3.216 Å		
	>	difference: 0.211 Å
d (2 2 1) = 3.005 Å		
	>	difference: 0.082 Å
d (3 1 0) = 2.923 Å		
	>	difference: 0.050 Å
d (1 3 1) = 2.531 Å		
d (2 2 $\bar{1}$) = 2.481 Å		

Jadeite No. 43

d (2 2 0) = 3.091 Å		
	>	difference: 0.177 Å
d (2 2 1) = 2.914 Å		
	>	difference: 0.093 Å
d (3 1 0) = 2.821 Å		
	>	difference: 0.073 Å
d (1 3 1) = 2.488 Å		
d (2 2 $\bar{1}$) = 2.415 Å		

It is seen from above mentioned data that the relative distances between the reflections vary for the different pyroxenes and that these relative distances for the omphacite specimens lie between those of diopside and those of the alkali pyroxenes. It may be noted that the omphacite specimens also have an optic axial angle 2 V which is considerably larger than that of diopside, so that they can be distinguished from diopside both by optical- and X-ray investigation.

Besides the variation in the relative distance between 2 2 1 and 3 1 0 there are still other reflections which vary in separation for the different clinopyroxenes.

The relative distance between 2 2 0 and 2 2 1 is also strongly variable; e. g. this distance is much greater with hedenbergite No. 27 than with diopside No. 13.

The relative distance between 1 3 1 and 2 2 $\bar{1}$ is much greater with diopside No. 13 than with hedenbergite No. 27, while this distance also varies with other clinopyroxenes.

As also has been done with the orthopyroxenes, we have put these relative distances with the chemical composition of the different clinopyroxenes in a graph. Since this is also done for group B 2, we will first discuss this group.

Group B 2. (figs. 23 and 24) — As was mentioned, on p. 245, the reflections 3 1 0 and 3 1 1 coincide in the powder diagram of this group. The reflection 2 2 0 (θ 17.68) has a high intensity as compared with that of the clinopyroxenes of group B 1. In Table 14 the variation in θ and the lattice spacings with accessory intensities for pigeonite No. 25 are given, while in the figs. 22 and 24 a diagram for θ_{Fe} can be seen, in which the heights of the lines represent estimated relative intensities.

Comparing the relative distance between 2 2 1 and 3 1 0 in the diagram of this pigeonite with that of diopside, it can be seen that this distance is much greater with pigeonite than with diopside. A comparison of the relative distance between 2 2 0 and 2 2 1 indicates that this is greater with diopside than with pigeonite. The relative distance between 1 3 1 and 2 2 $\bar{1}$ is again greater with pigeonite than with diopside.

Although there are sufficient differences between the powder diagrams of groups B 1 and B 2, it may once more be noted that both pigeonite and

TABLE 14

X-ray powder pattern group B 2.
Pigeonite, Usugoya-zawa, Hakone volcano, Japan (No. 25)
$2V = +13.5°$; $Z \wedge c = 43°$
$Ca_8 Mg_{64} Fe_{28}$

C_{2h}^6 hkl	θ_{Fe}	d(Å)	Relative Intensity	hkl	θ_{Fe}	d(Å)	Relative Intensity
200	12.27	4.55	VW	$42\bar{1}$	34.30	1.718	VW
111	12.58	4.44	VW	313	35.41	1.671	VW
.....	13.96	4.01	VW	$31\bar{2}$	35.86	1.652	VW
.....	15.07	3.72	VW	531	36.68	1.621	S
.....	15.61	3.60	VW	$51\bar{1}$	38.97	1.539	VW
.....	16.02	3.51	VW	600	39.29	1.529	VW
021	17.04	3.30	W	060	40.73	1.484	VW
220	17.68	3.19	S	$40\bar{2}$	41.14	1.471	VW
221	18.83	2.999	VS	260	43.27	1.412	W
310 }	19.59	2.887	VS	$53\bar{1}$	44.26	1.387	SM
311 }				.....	44.86	1.372	W
131	22.20	2.562	MW	.....	45.82	1.350	VW
202	22.61	2.518	VW	.....	46.49	1.335	W
002	23.03	2.474	MW	.....	49.13	1.280	VW
$22\bar{1}$	23.28	2.449	W	.....	49.42	1.275	MW
222	25.80	2.224	W	.....	52.25	1.224	W
$11\bar{2}$	26.66	2.157	VW	.....	53.78	1.200	VW
331	26.94	2.137	SM	.....	55.27	1.178	VW
421	27.36	2.106	VW	800	57.44	1.149	VW
420	28.69	2.016	MW	660	64.15	1.076	MW
240	28.92	2.002	VW	$51\bar{3}$	64.88	1.069	VW
$20\bar{2}$	29.90	1.942	VW	750	65.52	1.064	VW
510	32.61	1.796	VW	.....	66.29	1.057	MW
$24\bar{1}$	32.99	1.778	W	840	73.80	1.008	MW
150	33.60	1.749	W				

hedenbergite will have a structure nearly corresponding with that of diopside. For the other clinopyroxenes mentioned in Table 13 it is evident that they have a similar structure as diopside.

Relation Between the Relative Distance of Certain Reflections and the Chemical Composition of Clinopyroxenes of Groups B 1 and B 2.

By a close examination of the relative distances between the reflections 2 2 1 and 3 1 0, the reflections 2 2 0 and 2 2 1 and the reflections 1 3 1 and $2\,2\bar{1}$ it turns out that there is a certain transition from hedenbergite over

diopside to pigeonite (figs. 23 and 24). The relative distance between 2 2 1 and 3 1 0 becomes greater when approaching the composition of pigeonite, the relative distance between 2 2 0 and 2 2 1 becomes smaller, while the relative distance between 1 3 1 and 2 2 $\bar{1}$ becomes greater at the same time.

We have measured accurately the relative distances between the reflections in question for all clinopyroxenes of the groups B 1 and B 2 for which the chemical composition is known. Moreover these distances are calculated for a number of clinopyroxenes which are described in the papers of KUNO and HESS (1953) and KUNO (1955) and for which they give the unit cell dimensions and the chemical compositions. These calculations were carried out for a camera with a diameter of 9 centimeters and FeKα_1 radiation (λ = 1.93597 Å). The results of these measurements and calculations are stated in Table 15.

TABLE 15

Relative distances (Δ) in millimeters between certain reflections of a few clinopyroxenes. Camera diameter 9 cm, FeKα_1 radiation ($\lambda = 1.93597$ Å).

Sample No. *	Δ(2 2 1-3 1 0) calc.	obs.	Δ(2 2 0-2 2 1) calc.	obs.	Δ(1 3 1-2 2 $\bar{1}$) calc.	obs.	Chemical composition	Atomic proportions of Al on the basis of six oxygen atoms
HESS 1	1.11		1.81		1.63		Mg_{100}	—
HESS 2 (25)	1.19	1.20	1.81	1.81	1.70	1.71	Ca_8 Mg_{64} Fe_{28}	0.018
HESS 3	1.45		1.81		1.73		Ca_7 Mg_{45} Fe_{48}	0.033
HESS 4	0.38		2.29		0.72		Ca_{49} Mg_{47} Fe_4	0.018
HESS 5	0.24		2.40		0.52		Ca_{50} Mg_{17} Fe_{33}	0.049
HESS 6 (27)	0.00	0.00	2.60	2.58	0.27	0.28	Ca_{48} Mg_3 Fe_{49}	0.015
KUNO 5	0.60		2.15		0.93		Ca_{41} Mg_{47} Fe_{12}	0.094
KUNO 6	0.77		2.09		1.15		Ca_{28} Mg_{49} Fe_{23}	0.113
KUNO 9	0.96		1.96		1.41		Ca_{19} Mg_{46} Fe_{35}	0.028
13		0.39		2.30		0.72	$Ca_{49.5}$ $Mg_{46.5}$ Fe_4	0.011
29		0.49		2.25		0.74	Ca_{48} Mg_{40} Fe_{12}	0.128
30		0.51		2.23		0.75	Ca_{48} Mg_{45} Fe_7	0.239
32		0.55		2.22		0.81	Ca_{44} Mg_{51} Fe_5	0.179
33		0.60		2.20		0.88	Ca_{44} Mg_{43} Fe_{13}	0.200

* The sample numbers of HESS and KUNO refer to those mentioned in the papers of KUNO and HESS (1953) and KUNO (1955) respectively.

The relation between these relative distances and the chemical composition can be seen in fig. 25 for the diopside-hedenbergite series. It is seen that all samples lie on the curves, except for the clinopyroxenes augite No. 30 and augite No. 29. These specimens have a higher Al content than the remaining specimens. According to Table 15 the latter all have an atomic proportion of Al < 0.050. One may conclude therefore that the curves in the diagram of fig. 25 indicate clinopyroxenes with Al < 0.050.

In fig. 25 at the same time the relation between the relative distances and the chemical composition can be seen for the diopside-pigeonite series. Here too, a few of the samples do not lie on the curves. The samples augite No. 30 and augite (KUNO No. 5) do not lie on the curve (2 2 0 — 2 2 1) which can be explained by their Al content. The higher Al content of augite No. 30 and augite No. 33 shows itself also in the curve (1 3 1 — 2 2 $\bar{1}$).

It seems strange, however, that the specimens of augite (KUNO No. 6) and subcalcic augite (KUNO No. 9) do not lie on the curve (2 2 1 — 3 1 0),

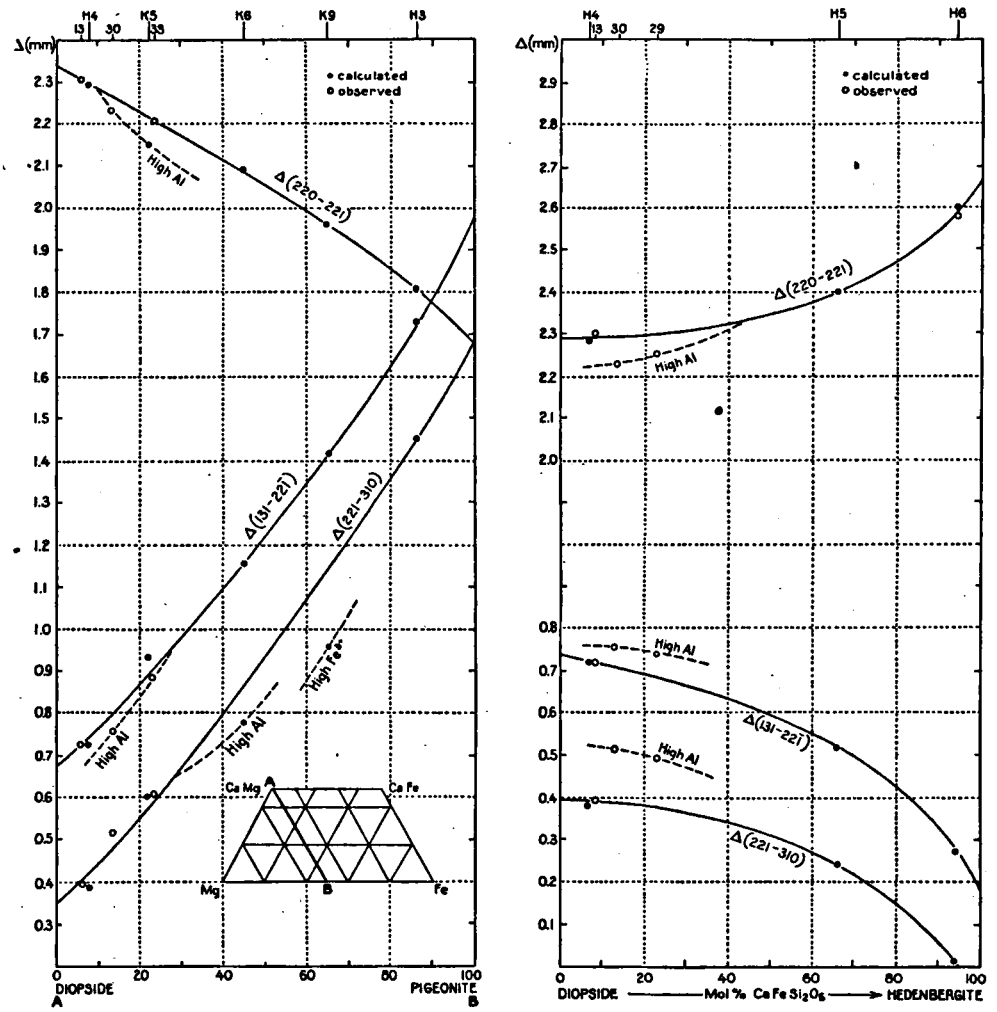

Fig. 25. Relation between relative distances in millimeters of certain reflections and the chemical composition for clinopyroxenes in the diopside-pigeonite series and the diopside-hedenbergite series. The numbers in the upper part of the diagram refer to those in Table 15. Camera diameter 9 cm, $FeK\alpha_1$ radiation, $\lambda = 1.93597$ A. The curves are calculated from the data of KUNO and HESS (1953 and 1955) about the unit cell dimensions of these clinopyroxenes. The open dots refer to real measurements on X-ray powder photographs of these specimens.

while they do lie on the other two curves. The Al content of specimen KUNO No. 9 especially is not at all high. This can only be explained by supposing that some strange ion can exercise the same influence as Al, for this sample contains high proportions of Fe^{3+} and Ti.

It is seen from fig. 25 and Table 15 that the observed relative distances on the X-ray powder photographs of our specimens agree surprisingly good with the relative distances as calculated from the data about the unit cell dimensions of HESS and KUNO of the same samples, which indicates the great accuracy of the measurements of HESS and KUNO.

The relation between the relative distances and the chemical composition for clinopyroxenes in the clinoenstatite — diopside — hedenbergite — ferrosilite field is shown in fig. 26. This is only a rough diagram. It is note

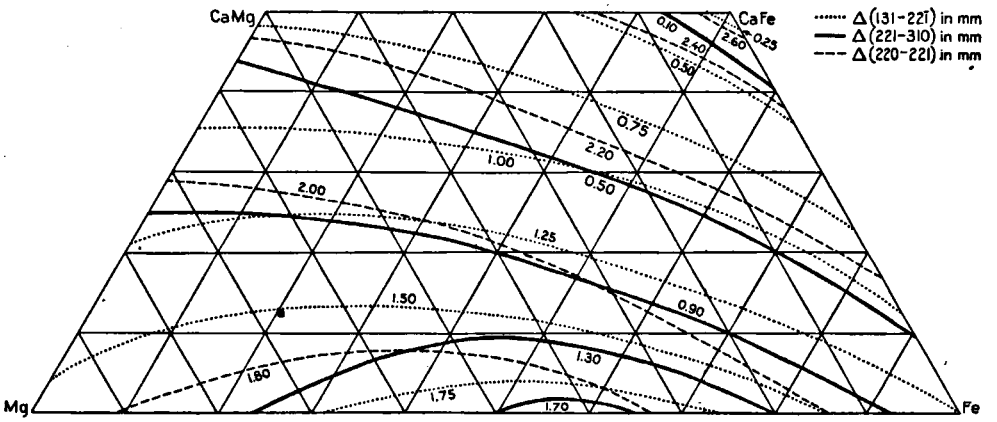

Fig. 26. Relation between relative distances in millimeters of certain reflections and the chemical composition for clinopyroxenes in the whole clinopyroxene field. Camera diameter 9 cm, $FeK\alpha_1$ radiation, $\lambda = 1.93597$ Å.

worthy, that all the curves coincide approximately with the straight line which can be drawn from diopside (CaMg) to ferrosilite (Fe), which indicates that the substitution of Fe for Mg has a relatively small influence on the unit cell dimensions or on the shape of the unit cell. This was also observed with the orthopyroxenes (see p. 215).

The curves for refractive indices are altogether different in a diagram after TRÖGER (1952). These curves are nearly vertical indicating that the substitution of Fe for Mg strongly influences the refractive indices. This is easily understood, because this substitution brings about a great change in the molecular refractions of the pyroxenes and the refractive indices change accordingly.

The substitution of Ca for Mg on the other hand does have a great influence on the unit cell dimensions which can be seen from the curves in fig. 26. This is also in accordance with the results obtained for the orthopyroxenes.

It is obvious now why the 2 V curves run in the direction of the straight line diopside (CaMg) — ferrosilite (Fe). This optical property depends on the shape of the unit cell, which strongly changes by substituting Ca for Mg as was mentioned above.

TABLE 16a

Distances between the reflections 2 2 0 and 2 2 1 for clinopyroxenes of the diopside-hedenbergite series.

mol % diopside	θ (2 2 1)–θ (2 2 0) in Hundredths of Degrees* used X-radiation				Δ:(2 2 0)–(2 2 1) in mm for CuKα_1 radiation Camera diameter			Δ:(2 2 0)–(2 2 1) in mm for FeKα_1 radiation Camera diameter			d(2 2 0)-d(2 2 1)
	Cu	Fe	Cr	Co	9 cm	11.4 cm	19 cm	9 cm	11.4 cm	19 cm	in Å
100	1.13	1.45	1.75	1.33	1.78	2.26	3.76	2.28	2.89	4.82	0.240
90	1.14	1.46	1.76	1.34	1.79	2.27	3.78	2.29	2.91	4.85	0.242
80	1.15	1.47	1.77	1.35	1.80	2.29	3.81	2.30	2.93	4.88	0.245
70	1.16	1.48	1.79	1.36	1.82	2.31	3.84	2.33	2.95	4.92	0.247
60	1.17	1.50	1.80	1.37	1.83	2.32	3.86	2.35	2.98	4.96	0.249
50	1.18	1.51	1.82	1.38	1.84	2.34	3.89	2.37	3.00	4.99	0.252
40	1.19	1.52	1.83	1.39	1.85	2.36	3.92	2.39	3.02	5.04	0.255
30	1.21	1.54	1.86	1.41	1.88	2.38	3.97	2.42	3.06	5.10	0.258
20	1.23	1.58	1.90	1.45	1.92	2.43	4.07	2.47	3.12	5.20	0.263
10	1.27	1.62	1.97	1.49	1.98	2.50	4.20	2.55	3.22	5.38	0.272
0	1.32	1.69	2.05	1.57	2.06	2.61	4.37	2.65	3.34	5.58	0.286

Distances between the reflections 2 2 0 and 2 2 1 for clinopyroxenes of the diopside-pigeonite series.

mol % diopside	θ (2 2 1)–θ (2 2 0) in Hundredths of Degrees used X-radiation				Δ:(2 2 0)–(2 2 1) in mm for CuKα_1 radiation Camera diameter			Δ:(2 2 0)–(2 2 1) in mm for FeKα_1 radiation Camera diameter			d(2 2 0)-d(2 2 1)
	Cu	Fe	Cr	Co	9 cm	11.4 cm	19 cm	9 cm	11.4 cm	19 cm	in Å
100	1.16	1.49	1.80	1.37	1.82	2.30	3.84	2.32	2.96	4.93	0.247
90	1.14	1.45	1.75	1.33	1.78	2.26	3.76	2.28	2.90	4.81	0.241
80	1.11	1.41	1.71	1.30	1.73	2.21	3.68	2.23	2.83	4.70	0.234
70	1.08	1.38	1.67	1.27	1.69	2.15	3.59	2.17	2.76	4.58	0.228
60	1.05	1.34	1.62	1.23	1.65	2.10	3.49	2.11	2.69	4.46	0.222
50	1.02	1.30	1.58	1.20	1.60	2.04	3.39	2.05	2.61	4.31	0.217
40	0.99	1.26	1.53	1.16	1.56	1.97	3.28	1.99	2.52	4.20	0.211
30	0.96	1.22	1.48	1.12	1.51	1.90	3.17	1.92	2.43	4.06	0.204
20	0.92	1.18	1.42	1.08	1.45	1.82	3.04	1.85	2.35	3.90	0.196
10	0.87	1.13	1.36	1.02	1.38	1.74	2.90	1.77	2.25	3.74	0.188
0	0.81	1.07	1.29	0.97	1.31	1.65	2.76	1.69	2.14	3.57	0.179

* θ is given in hundredths of degrees (circumference of a circle = 360°).

TABLE 16b

Distances between the reflections 1 3 1 and 2 2 $\bar{1}$ for clinopyroxenes of the diopside-hedenbergite series.

mol % diopside	θ (2 2 $\bar{1}$)–θ (1 3 1) in Hundredths of Degrees used X-radiation				Δ:(1 3 1)–(2 2 $\bar{1}$) in mm for CuKα_1 radiation Camera diameter			Δ:(1 3 1)–(2 2 $\bar{1}$) in mm for FeKα_1 radiation Camera diameter			d(1 3 1)-d(2 2 $\bar{1}$)
	Cu	Fe	Cr	Co	9 cm	11.4 cm	19 cm	9 cm	11.4 cm	19 cm	in Å
100	0.37	0.47	0.56	0.42	0.59	0.74	1.22	0.73	0.95	1.58	0.050
90	0.35	0.45	0.54	0.40	0.56	0.71	1.17	0.72	0.91	1.52	0.048
80	0.34	0.43	0.52	0.39	0.53	0.68	1.12	0.69	0.87	1.45	0.047
70	0.32	0.41	0.49	0.37	0.50	0.65	1.08	0.67	0.82	1.38	0.045
60	0.30	0.39	0.47	0.35	0.47	0.61	0.99	0.63	0.78	1.31	0.042
50	0.29	0.37	0.44	0.33	0.44	0.57	0.93	0.60	0.73	1.24	0.040
40	0.26	0.34	0.41	0.31	0.41	0.52	0.87	0.55	0.68	1.14	0.038
30	0.23	0.31	0.38	0.28	0.37	0.47	0.79	0.50	0.62	1.04	0.034
20	0.20	0.26	0.32	0.23	0.32	0.40	0.66	0.42	0.53	0.88	0.028
10	0.16	0.20	0.25	0.18	0.24	0.31	0.50	0.33	0.40	0.67	0.022
0	0.10	0.12	0.16	0.12	0.15	0.19	0.32	0.17	0.25	0.43	0.015

Distances between the reflections 1 3 1 and 2 2 $\bar{1}$ for clinopyroxenes of the diopside-pigeonite series.

mol % diopside	θ (2 2 $\bar{1}$)–θ (1 3 1) in Hundredths of Degrees used X-radiation				Δ:(1 3 1)–(2 2 $\bar{1}$) in mm for CuKα_1 radiation Camera diameter			Δ:(1 3 1)–(2 2 $\bar{1}$) in mm for FeKα_1 radiation Camera diameter			d(1 3 1)-d(2 2 $\bar{1}$)
	Cu	Fe	Cr	Co	9 cm	11.4 cm	19 cm	9 cm	11.4 cm	19 cm	in Å
100	0.33	0.41	0.49	0.36	0.52	0.64	1.09	0.64	0.82	1.40	0.044
90	0.37	0.48	0.57	0.42	0.58	0.74	1.22	0.74	0.94	1.60	0.051
80	0.41	0.55	0.66	0.48	0.67	0.84	1.39	0.86	1.08	1.82	0.058
70	0.46	0.62	0.74	0.55	0.75	0.94	1.56	0.98	1.22	2.04	0.066
60	0.52	0.69	0.84	0.61	0.83	1.05	1.76	1.09	1.37	2.28	0.073
50	0.58	0.76	0.94	0.69	0.92	1.15	1.94	1.20	1.52	2.51	0.081
40	0.65	0.83	1.04	0.77	1.03	1.25	2.15	1.32	1.68	2.79	0.089
30	0.73	0.92	1.15	0.85	1.14	1.37	2.38	1.45	1.85	3.08	0.098
20	0.80	1.03	1.26	0.93	1.26	1.54	2.64	1.60	2.04	3.40	0.108
10	0.88	1.13	1.39	1.03	1.38	1.74	2.93	1.78	2.24	3.77	0.119
0	0.97	1.24	1.52	1.12	1.51	1.94	3.24	1.98	2.42	4.18	0.130

TABLE 16c

Distances between the reflections 2 2 1 and 3 1 0 for clinopyroxenes of the diopside-hedenbergite series.

mol % diopside	θ (3 1 0)–θ (2 2 1) in Hundredths of Degrees used X-radiation				Δ:(2 2 1)–(3 1 0) in mm for CuKα_1 radiation Camera diameter			Δ:(2 2 1)–(3 1 0) in mm for FeKα_1 radiation Camera diameter			d(2 2 1)-d(3 1 0)
	Cu	Fe	Cr	Co	9 cm	11.4 cm	19 cm	9 cm	11.4 cm	19 cm	in Å
100	0.20	0.25	0.31	0.23	0.31	0.40	0.65	0.39	0.50	0.83	0.039
90	0.19	0.24	0.30	0.22	0.29	0.37	0.61	0.37	0.47	0.78	0.037
80	0.18	0.23	0.28	0.21	0.27	0.35	0.57	0.35	0.44	0.74	0.035
70	0.17	0.21	0.26	0.20	0.25	0.32	0.52	0.33	0.41	0.70	0.032
60	0.16	0.20	0.24	0.19	0.24	0.29	0.48	0.30	0.38	0.65	0.030
50	0.14	0.19	0.22	0.17	0.21	0.26	0.43	0.27	0.35	0.60	0.027
40	0.12	0.16	0.19	0.15	0.19	0.23	0.39	0.24	0.32	0.54	0.024
30	0.09	0.13	0.16	0.12	0.15	0.19	0.33	0.20	0.27	0.46	0.022
20	0.05	0.09	0.11	0.08	0.10	0.12	0.24	0.14	0.20	0.37	0.014
10	0.02	0.03	0.05	0.03	0.04	0.05	0.10	0.06	0.08	0.19	0.005
0	0.00	0.00	0.00	0.00	0.00	0.00	0.00	0.00	0.00	0.00	0.000

Distances between the reflections 2 2 1 and 3 1 0 for clinopyroxenes of the diopside-pigeonite series.

mol % diopside	θ (3 1 0)–θ (2 2 1) in Hundredths of Degrees used X-radiation				Δ:(2 2 1)–(3 1 0) in mm for CuKα_1 radiation Camera diameter			Δ:(2 2 1)–(3 1 0) in mm for FeKα_1 radiation Camera diameter			d(2 2 1)-d(3 1 0)
	Cu	Fe	Cr	Co	9 cm	11.4 cm	19 cm	9 cm	11.4 cm	19 cm	in Å
100	0.16	0.25	0.26	0.21	0.28	0.36	0.60	0.34	0.46	0.82	0.034
90	0.22	0.28	0.33	0.26	0.35	0.44	0.74	0.44	0.60	1.00	0.043
80	0.27	0.35	0.42	0.31	0.43	0.54	0.90	0.53	0.72	1.18	0.053
70	0.33	0.42	0.51	0.37	0.51	0.64	1.08	0.65	0.85	1.40	0.064
60	0.39	0.50	0.61	0.45	0.60	0.76	1.28	0.77	1.02	1.65	0.074
50	0.45	0.58	0.72	0.52	0.70	0.88	1.50	0.90	1.19	1.94	0.086
40	0.53	0.68	0.83	0.60	0.80	1.02	1.72	1.06	1.36	2.24	0.099
30	0.60	0.77	0.94	0.68	0.91	1.17	1.96	1.20	1.54	2.54	0.114
20	0.67	0.86	1.06	0.77	1.03	1.33	2.21	1.34	1.71	2.82	0.128
10	0.75	0.95	1.17	0.86	1.16	1.49	2.47	1.51	1.87	3.17	0.145
0	0.82	1.02	1.30	0.96	1.30	1.68	2.74	1.68	2.03	3.50	0.161

From these data it is clear that the chemical composition of these different clinopyroxenes may be determined fairly accurately by means of a combined optical and röntgenographic investigation.

Since the distance between certain reflections depends on the radiation

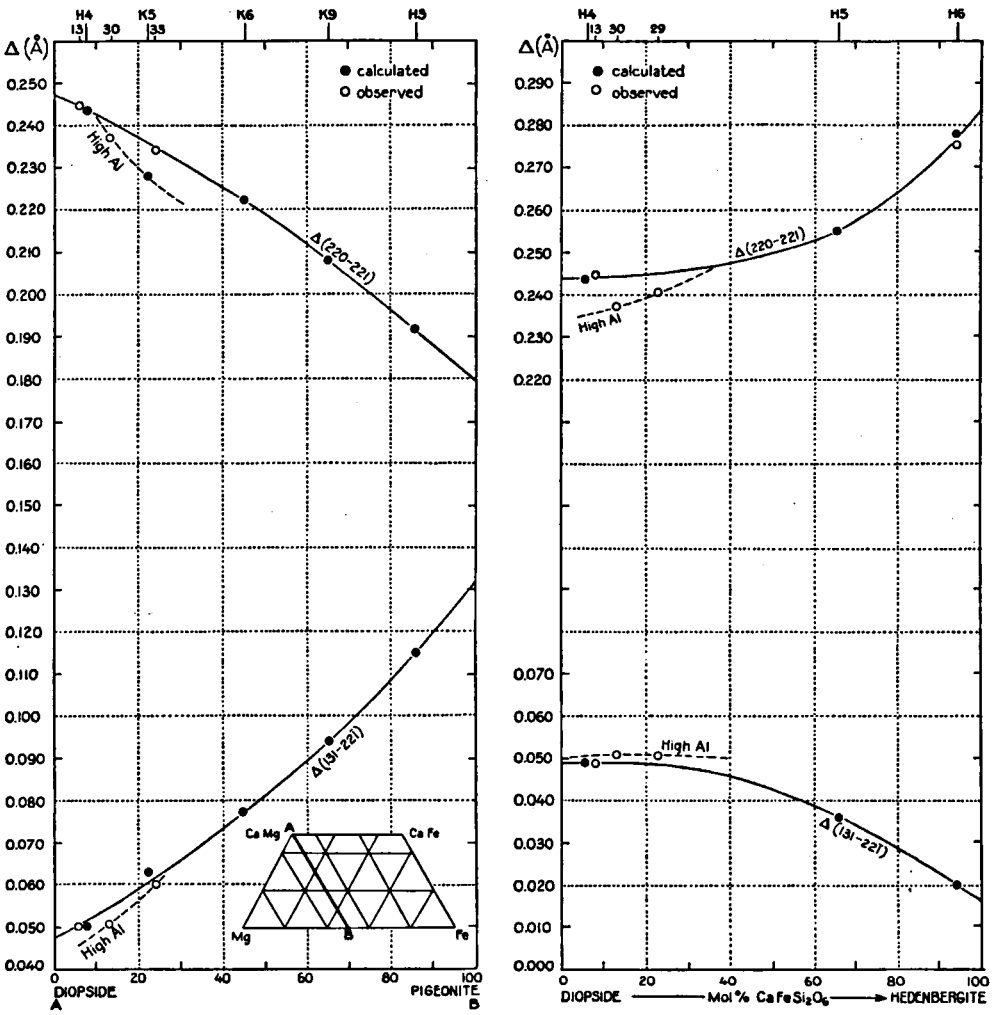

Fig. 27. Relation between relative distances in Å of certain reflections and the chemical composition for clinopyroxenes in the diopside-pigeonite series and the diopside-hedenbergite series. The numbers in the upper part of the diagram refer to those in Table 15. The curves are calculated from the data of KUNO and HESS (1953 and 1955) about the unit cell dimensions of these clinopyroxenes.

and camera employed, in Tables 16a, 16b and 16c these distances are stated for different radiations and for a few types of camera; moreover, the difference between the lattice spacings of the reflections is given in Ångström units.

Finally in figs. 27, 28 and 29 the relation is given between the distances between the reflections in Å and the chemical composition both for the diop-

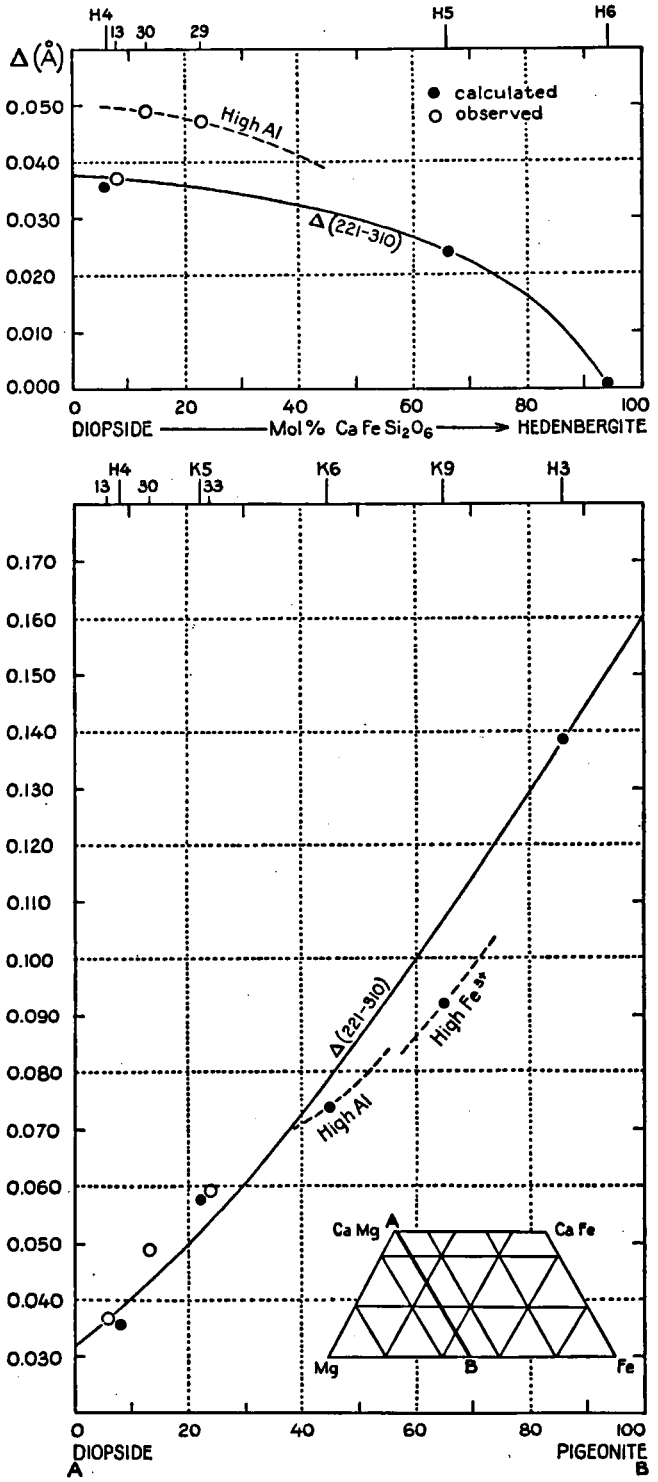

Fig. 28. Relation between relative distances in Å of the reflections 2 2 1 and 3 1 0 and the chemical composition for clinopyroxenes in the diopside-pigeonite series and the diopside-hedenbergite series. The numbers in the upper part of the diagram refer to those in Table 15. The curves are calculated from the data of KUNO and HESS (1953 and 1955) about the unit cell dimensions of these clinopyroxenes.

side-hedenbergite series and the diopside-pigeonite series and also for the whole clinopyroxene field.

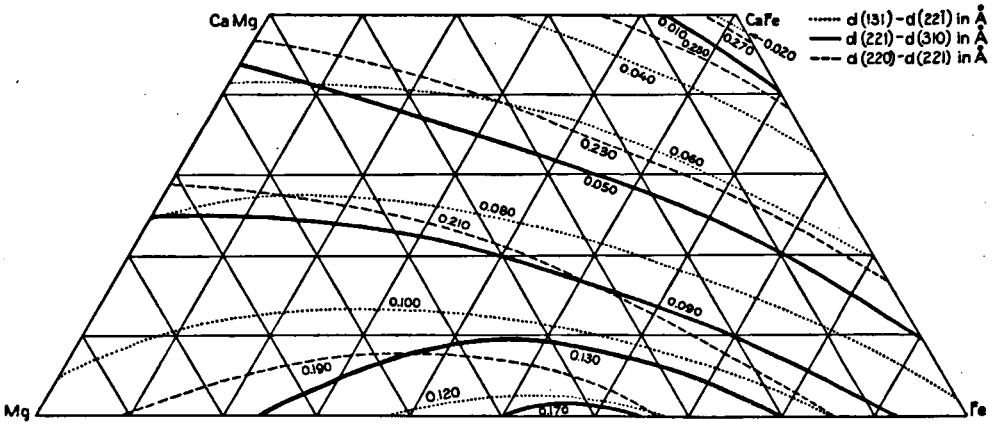

Fig. 29. Relation between relative distances in Å of certain reflections and the chemical composition for clinopyroxenes in the whole clinopyroxene field.

Group B 3. (figs 21 and 22) — In the X-ray powder diagrams of this group the position and the intensity of the reflections 2 2 1, (3 1 0) (3 1 1), 1 3 1 and $2\,2\,\bar{1}$ are characteristic, as was already mentioned in the description of the principal features of this group.

In Table 17 for three clinopyroxenes belonging to this group, the variation in θ and the lattice spacings with accessory intensities are given, while in fig. 21 a diagram of θ_{Fe} for acmite No. 37 and in fig. 24 for jadeite No. 43 can be seen.

The investigated pyroxenes, with a powder diagram in accordance with that of this group are:

Acmite No. 37, Eker, Norway $2V = -61°$, $Z \wedge c = 92°$.
Aegirite No. 38, Langesundfiord, Norway $2V = -63°$, $Z \wedge c = 94°$.
Aegirite No. 46, Ditro, Roumania $2V = -71°$, $Z \wedge c = 91.5°$, 71 mol % $NaFe'''Si_2O_6$.
Jadeite No. 43, Upper Burma $2V = +79°$, $Z \wedge c = 38—43°$.

The reflection patterns of the first three pyroxenes are nearly identical. The differentiation between acmite and aegirite mostly is made on the basis of the colour of the mineral in thin section (RAMDOHR 1954), but essentially there is no difference, and this is clearly shown in the powder diagrams. Jadeite has a corresponding powder diagram, but nearly all reflections have a greater glancing angle, from which may be concluded that the unit cell of jadeite is smaller than that of aegirite. Further it seems that the four pyroxenes included in this group are alkali pyroxenes according to the classification mentioned on p. 224. This means that one may distinguish these alkali pyroxenes from other pyroxenes by means of röntgenographic investigation (so far as they are practically end members of an isomorphous series) and this also counts for spodumene as will be seen when we describe group B 4. Practically pure alkali pyroxenes have sufficient differences in their reflection pattern to distinguish them from each other.

TABLE 17

X-ray powder patterns group B 3.

	Aegirite, Ditro, Siebenbürgen (No. 46) $2V = -71°$; $Z \wedge c = 91.5°$			Aegirite, Langesundfiord (No. 38) $2V = -63°$; $Z \wedge c = 94°$			Jadeite, Upper Burma (No. 43) $2V = +79°$; $Z \wedge c = 38°$—$43°$		
C_{2h}^6 hkl	θ_{Fe}	d(Å)	Relative Intensity	θ_{Fe}	d(Å)	Relative Intensity	θ_{Fe}	d(Å)	Relative Intensity
.....	—	—	—	—	—	—	8.74	6.37	VW
110	8.64	6.44	MW	8.70	6.40	MW	8.99	6.19	VW
.....	—	—	—	—	—	—	10.30	5.41	VW
.....	—	—	—	—	—	—	11.92	4.69	VW
111	12.59	4.44	MW	12.71	4.40	MW	13.00	4.30	MW
021	16.95	3.32	VW	17.14	3.28	W	17.43	3.23	W
220	17.52	3.22	W	17.62	3.20	W	18.25	3.09	MW
221	18.79	3.01	VS	18.95	2.981	VS	19.40	2.914	VS
310 311	19.34	2.923	S	19.49	2.901	S	20.07	2.821	VS
130	20.10	2.817	VW	20.26	2.795	VW	20.64	2.746	VW
.....	20.67	2.742	VW	20.64	2.746	VW	21.34	2.660	VW
131	22.49	2.531	S	22.55	2.524	SM	22.90	2.488	S
$22\bar{1}$	22.96	2.481	SM	22.96	2.481	SM	23.63	2.415	S
400	25.19	2.274	VW	25.22	2.272	VW	25.86	2.219	MW
222	26.02	2.207	MW	26.15	2.196	MW	26.69	2.155	MW
$11\bar{2}$	23.07	2.127	MW	27.17	2.120	M	27.93	2.067	SM
331	27.45	2.100	W	27.48	2.098	W	28.25	2.045	VW
420	28.66	2.018	MW	28.73	2.014	MW	28.88	2.004	M
240	29.04	1.994	VW	29.11	1.990	VW	30.19	1.925	VW
132	29.90	1.942	VW	30.03	1.934	VW	30.86	1.887	W
$20\bar{2}$	30.83	1.889	VW	30.99	1.880	VW	31.78	1.838	VW
422	31.69	1.843	VW	31.84	1.835	VW	32.55	1.799	VW
332	32.16	1.819	VW	32.42	1.806	VW	33.37	1.760	MW
150	33.82	1.739	MW	33.95	1.733	MW	34.23	1.721	MW
$42\bar{1}$	34.77	1.697	VW	34.84	1.694	VW	35.89	1.651	W
313	35.47	1.668	MW	35.60	1.663	W	36.62	1.623	W
$31\bar{2}$	36.30	1.635	MW	36.43	1.630	MW	37.00	1.608	W
531	36.78	1.617	MW	36.87	1.613	SM	38.02	1.572	SM
223	37.22	1.600	W	37.32	1.597	W	38.59	1.552	MW
023	38.72	1.548	VW	38.91	1.541	VW	40.28	1.497	MW
$51\bar{1}$	39.13	1.534	W	39.29	1.529	W	40.60	1.487	W
602	—	—	—	—	—	—	40.98	1.476	MW
600	39.99	1.506	M	40.06	1.504	MW	41.46	1.462	W
060	41.01	1.475	W	41.14	1.471	W	42.64	1.429	W
260	43.49	1.407	SM	43.65	1.402	SM	44.93	1.371	MW

TABLE 17 (continued)

C_{2h}^6 hkl	Aegirite No. 46 (continued) θ_{Fe}	d(Å)	Relative Intensity	Aegirite No. 38 (continued) θ_{Fe}	d(Å)	Relative Intensity	Jadeite No. 43 (continued) θ_{Fe}	d(Å)	Relative Intensity
$53\bar{1}$	44.45	1.382	W	44.61	1.378	W	45.31	1.362	SM
.....	46.71	1.330	W	46.77	1.329	MW	48.17	1.299	SM
.....	47.63	1.310	W	47.79	1.307	W	49.00	1.283	W
.....	48.27	1.297	W	48.33	1.296	MW	49.57	1.272	MW
.....	49.38	1.275	MW	49.57	1.272	M	51.13	1.243	M
.....	—	—	—	—	—	—	52.69	1.217	VW
.....	51.52	1.237	MW	51.61	1.235	MW	53.68	1.201	MW
.....	52.15	1.226	VW	—	—	—	54.32	1.192	VW
.....	53.52	1.204	VW	53.71	1.201	VW	55.88	1.169	W
.....	56.07	1.167	VW	—	—	—	58.01	1.141	MW
.....	56.80	1.157	VW	56.83	1.156	VW	58.65	1.134	MW
.....	—	—	—	—	—	—	59.25	1.126	VW
800	58.46	1.136	VW	58.39	1.137	VW	60.59	1.111	VW
.....	61.07	1.106	VW	60.94	1.107	VW	63.71	1.080	VW
.....	63.23	1.084	W	63.23	1.084	W	65.65	1.063	MW
660	64.63	1.071	W	64.89	1.070	W	68.04	1.044	W
$51\bar{3}$	65.84	1.061	W	66.13	1.059	MW	69.21	1.035	MW
.....	69.95	1.030	W	—	—	—	70.46	1.027	MW
750	70.77	1.025	W	70.74	1.025	W	72.49	1.015	VW
840	73.80	1.008	W	74.08	1.007	VW	74.78	1.003	VW
.....	76.25	0.997	VW	76.22	0.997	VW	77.75	0.995	VW
.....	77.39	0.992	VW	—	—	—	—	—	—
.....	80.93	0.980	W	81.02	0.980	W	80.45	0.982	VW

Group B 4. (figs. 21 and 22) — As regards position and intensity, the reflections 2 2 1 and 3 1 1 are characteristic; they occur in the powder diagram as very strong lines with a great mutual distance for pyroxenes. In addition many isolated strong reflections can be seen over the whole diagram.

The variations in θ with accessory lattice spacings and intensities for the two pyroxenes belonging to this group because of their reflection pattern are shown in Table 18. In fig. 22 a diagram of θ_{Fe} for spodumene No. 45 can be seen in which the heights of the lines represent estimated relative intensities.

The pyroxenes investigated röntgenographically having the typical powder diagram of this group are:

Spodumene No. 44, Northern Sweden $2V = +64.5°$, $Z \wedge c = 24.5°$.
Spodumene No. 45, U. S. A. $2V = +66°$, $Z \wedge c = 27°$.

These pyroxenes are alkali pyroxenes according to the classification of p. 224. This means that the nearly pure alkali pyroxenes can be distinguish-

TABLE 18

X-ray powder patterns group B 4.

Spodumene, Varuträsk, N. Sweden (No. 44) $2V = +64.5°$; $Z \wedge c = 24.5°$				Spodumene, Massachusetts, U.S.A. (No. 45) $2V = +66°$; $Z \wedge c = 27°$		
C_{2h}^6 hkl	θ_{Fe}	d(Å)	Relative Intensity	θ_{Fe}	d(Å)	Relative Intensity
110	8.77	6.35	VW	8.77	6.35	VW
.....	9.15	6.09	VW	9.15	6.09	VW
200	12.94	4.32	W	12.97	4.31	W
111	13.32	4.20	M	13.32	4.20	M
021	16.44	3.42	MW	16.44	3.42	MW
220	17.71	3.18	MW	17.71	3.18	MW
221	19.40	2.914	VS	19.40	2.914	VS
310	19.84	2.852	W	19.88	2.847	VW
311	20.35	2.784	VS	20.35	2.784	VS
130	21.31	2.664	W	21.34	2.660	MW
.....	22.36	2.545	W	22.36	2.545	W
131	23.31	2.446	SM	23.31	2.446	SM
202	24.33	2.350	MW	24.36	2.347	MW
.....	25.89	2.217	VW	25.89	2.217	VW
400	26.66	2.157	W	26.66	2.157	VW
222	27.39	2.104	MW	27.39	2.104	MW
$11\bar{2}$	28.12	2.054	MW	28.09	2.056	MW
331	28.47	2.031	W	28.44	2.033	W
421	30.13	1.928	MW	30.13	1.928	MW
132	31.34	1.861	M	31.34	1.861	SM
241	31.59	1.848	VW	31.62	1.846	VW
$20\bar{2}$	31.97	1.828	VW	—	—	—
422	32.86	1.784	VW	—	—	—
332	33.85	1.738	W	33.28	1.736	W
$42\bar{1}$	36.01	1.646	W	36.01	1.646	W
$31\bar{2}$	37.16	1.603	MW	37.13	1.603	M
531	38.21	1.565	S	38.18	1.566	S
223	39.52	1.521	MW	39.48	1.522	MW
602	41.55	1.459	MW	41.52	1.460	M
$40\bar{2}$	43.88	1.397	MW	43.81	1.398	MW
.....	45.44	1.359	W	45.40	1.360	MW
.....	46.07	1.344	VW	46.07	1.344	VW
.....	46.39	1.337	VW	46.39	1.337	VW
260	46.77	1.329	SM	46.74	1.329	SM
$53\bar{1}$	47.51	1.313	M	47.51	1.313	M
.....	48.08	1.301	VW	48.01	1.302	VW
.....	48.84	1.286	VW	48.81	1.286	W

TABLE 18 (continued)

Spodumene No. 44 (continued)				Spodumene No. 45 (continued)		
C_{2h}^6 hkl	θ_{Fe}	d(Å)	Relative Intensity	θ_{Fe}	d(Å)	Relative Intensity
.....	49.42	1.275	VW	49.42	1.275	VW
.....	50.53	1.254	W	50.43	1.256	W
.....	51.29	1.241	VW	—	—	—
.....	51.61	1.235	VW	—	—	—
.....	52.15	1.226	VW	52.22	1.225	VW
.....	52.92	1.213	M	52.89	1.214	SM
.....	55.97	1.168	MW	55.94	1.168	MW
.....	58.93	1.130	VW	58.96	1.130	VW
.....	59.44	1.124	W	59.44	1.124	VW
.....	62.66	1.090	W	62.66	1.090	W
800	63.80	1.079	W	63.80	1.079	W
.....	68.32	1.042	MW	68.26	1.042	MW
.....	70.20	1.029	MW	70.17	1.029	MW
660	72.43	1.015	W	72.36	1.016	W
513	73.00	1.012	MW	72.98	1.012	SM
750	73.35	1.010	W	73.32	1.010	W
.....	73.96	1.007	VW	73.89	1.008	VW
840	74.43	1.005	VW	74.43	1.005	W
.....	76.98	0.994	VW	76.89	0.994	VW
.....	78.32	0.988	W	78.25	0.989	W
.....	78.83	0.987	VW	—	—	—
.....	79.69	0.984	W	79.59	0.984	MW
.....	80.32	0.982	W	80.20	0.982	MW
.....	84.46	0.973	MW	84.37	0.973	MW

ed from each other by röntgenographic inspection, for aegirite and jadeite have a different reflection pattern which is subdivided under group B 3. It is clear from Table 18 that both spodumene specimens have practically the same reflection pattern, this may be caused by the fact that their Li and Al content are nearly the same. A chemical analysis will probably bear this out. At any rate one can correlate the powder pattern of spodumene with that of the other groups, although apparently there are great differences so that one may safely conclude that all the investigated clinopyroxenes have a similar structure.

Discussion of the Results

On examining the pyroxenes röntgenographically one can distinguish five groups on the basis of the reflection pattern of the powder diagrams. The orthopyroxenes form one group, easily differentiated from the other groups which are built up of monoclinic pyroxenes. Between these latter four groups

no sharp lines can be drawn because transitions between them are possible. The classification of the pyroxenes according to the chemical composition (page 224) agrees in the main with the grouping on the basis of the röntgenographic investigation.

The chemical composition of the clinopyroxenes in the clinoenstatite — diopside — hedenbergite — ferrosilite field may be determined by a combined optical and röntgenographic investigation. This combination is necessary because the substitution of Fe for Mg has practically no influence on the dimensions of the unit cell, but it does have on the refractive indices, while on the other hand the substitution of Ca for Mg strongly influences the unit cell dimensions.

The remaining pyroxenes (alkali pyroxenes) can be distinguished by röntgenographic inspection. Therefore the röntgenographic method has proven to be of great value for the examination and determination of the pyroxenes.

It may be noted that the X-ray investigation on clinopyroxenes is not yet completed, because much can still be done, for instance in the jadeite-diopside-aegirite field.

SUMMARY

The X-ray powder method for determining minerals has been applied to the important rock-forming mineral group of the pyroxenes in this thesis.

The purpose of the investigation was to seek the relationship between the variations of the intensities and positions of the reflections in the powder diagram and the variations in optical properties and chemical composition. For that purpose a number of pyroxenes from different localities were investigated optically, chemically and röntgenographically.

The orthopyroxenes. — The optical examination of the orthopyroxenes indicates, that the variation of the optical properties is related to the chemical composition (see Table 1).

A difference between plutonic and volcanic orthopyroxenes lies in the size of the optic axial angle 2 V; this appears to be smaller with volcanic orthopyroxenes between En_{80} and En_{15} than with plutonic orthopyroxenes (see fig. 5).

Further a lamellar structure can be observed in the plutonic orthopyroxenes (see figs. 2 and 3) while the volcanics do not have these lamellae but often show zoning (see fig. 1).

It is seen from chemical investigation of the orthopyroxenes that both the plutonic and volcanic orthopyroxenes show about the same variation in Al- and Ca-atomic proportions (see Table 3). It is quite possible that a part of the Ca content of the plutonic orthopyroxenes is present in exsolved diopside lamellae according to the hypothesis of HESS and PHILIPS (1938).

The orthopyroxenes can be distinguished from the clinopyroxenes by X-ray powder diagrams on the ground of their characteristic reflection pattern. These powder diagrams are made by means of a camera with a diameter of 9 centimeters and $FeK\alpha_1$ radiation ($\lambda = 1.93597$ Å). All powder diagrams of the orthopyroxenes are classed as one group (Group A, see fig. 6). The variation in the relative distance between the reflections 10 3 1 and 0 6 0 appears to be connected with the chemical composition. These distances are measured very accurately in millimeters by means of a CAMBRIDGE Universal Measuring Machine and plotted against the chemical composition in fig. 8. Through the influence of Al and Ca, the Mg content cannot be determined unequivocally from this diagram. Therefore also X-ray powder photographs are made of a mixture of 70 % orthopyroxene and 30 % quartz (see fig. 9). The relative distance between quartz reflection $2\,1\,\bar{3}\,1$ and pyroxene reflection 0 6 0 in millimeters and the distance between quartz reflection $(2\,0\,\bar{2}\,3)$ $(3\,0\,\bar{3}\,1)$ and pyroxene reflection 11 3 1 in millimeters depend on the chemical composition which can be seen in figs. 10 and 11, respectively. In fig. 10 two curves are shown, one for orthopyroxenes with an atomic proportion of Al of about 0.010 and one for those with an atomic proportion of Al of about 0.050 in B^{VI} position. In fig. 11 two curves can be seen

which are related to orthopyroxenes with an atomic proportion of Ca of about 0.020 and those with an atomic proportion of Ca of about 0.060. One may determine the chemical composition of an orthopyroxene from these three diagrams (figs. 8. 10 and 11).

For that purpose one should measure three relative distances. In each diagram one can find two values for the Mg content. From these, a total of six values, three will lie close to each other; the average of these three values indicates the Mg content. With this Mg content one can determine the Al and Ca contents in the diagrams.

This röntgenographic method meets with difficulties when there do not occur certain proportions of Al and Ca in the orthopyroxene. Then there may be present two groups of three Mg's which lie close together (see Table 9). In such cases of doubt one must use the optical method to determine the Mg content. By substitution of Fe for Mg, N_z changes strongly, the unit cell dimensions do not, however, and neither do the relative distances. The Al and Ca contents then may be determined by the röntgenographic method. By substitution of Al and Ca for Mg, the unit cell dimensions change strongly and with them the relative distances between the reflections, which are very sensitive.

The variation in the relative distance between the reflections mentioned has been explained by means of a crystal model of enstatite (see figs. 12 and 13). This variation results from the substitution of Fe, Al and Ca for Mg and of Al for Si. The substitution of Fe for Mg increases the unit cell dimensions only slightly so that the shape of the unit cell also changes little. The substitution of Ca for Mg has a great influence on the a- and the c dimension, which both become much greater. The substitution of Al for Mg and of Al for Si strongly decreases the b dimension. These changes in the unit cell occur because all substituting ions have a different ionic radius from Mg and moreover because in the structure of enstatite two kinds of Mg ions occur with altogether different positions and which are linked with the tetrahedra in very different ways.

Since the relative distance in millimeters between certain reflections depends on the camera and radiation used, in Tables 7a, 7b and 7c these distances are stated for a few types of camera and radiation. In addition the differences between the lattice spacings of these reflections are given in Ångström units.

The clinopyroxenes. — In this thesis the optical investigation on clinopyroxenes consists of a description of the specimens, both macroscopically and microscopically and a determination of 2 V and $Z \wedge c$. For a few clinopyroxenes the values of N_z and N_x have also been determined. The described clinopyroxenes are subdivided in a number of groups; this classification is based upon the chemical composition (see p. 224). It turned out that the optical properties of the röntgenographically investigated clinopyroxenes do not differ much from the data mentioned in the literature about this group of minerals (see fig. 20 and Table 10).

The chemical investigation is restricted to the analysis of a few clinopyroxenes; the results are stated in Table 11.

On the basis of difference in position and intensity of certain reflections in the X-ray powder diagrams a classification in four groups has been established for the clinopyroxenes.

Group B 1 (figs. 21 and 23)
The group includes, hedenbergite, diopside, augite and diallage.

Group B 2 (figs. 21 and 23)
Pigeonite belongs to this group.

Group B 3 (figs. 21 and 22)
This group includes, aegirite and jadeite.

Group B 4 (figs. 21 and 22)
Spodumene belongs to this group.

No sharp limits can be drawn between these groups and transitions may exist between some of these groups, as between groups B 1 and B 2 and also between groups B 1 and B 3. Through lack of clinoenstatite and ferrosilite samples we could not check whether any more groups may be distinguished.

Of each of these groups the principal features are discussed on p. 245. Each group has its own characteristic reflection pattern; the similarity between these patterns, however, is great enough to conclude that all the investigated clinopyroxenes have a similar structure. The grouping of the X-ray powder diagrams agrees in the main with the classification of the pyroxenes according to the chemical composition.

The chemical composition of the different clinopyroxenes of the groups B 1 and B 2 may be determined by a combined optical and röntgenographic investigation. This combination is necessary because the substitution of Fe for Mg has practically no influence on the dimensions of the unit cell, but it does have on the refractive indices. On the other hand the substitution of Ca for Mg strongly influences the shape of the unit cell.

For the different clinopyroxenes of groups B 1 and B 2 the variation of the relative distance in millimeters between the reflections 2 2 0 and 2 2 1, the reflections 2 2 1 and 3 1 0 and the reflections 1 3 1 and 2 2 $\bar{1}$ is plotted against the chemical composition in figs. 25 and 26. From these diagrams one may determine the chemical composition by measuring the relative distances mentioned, on the X-ray powder diagrams. In figs. 27, 28 and 29 the relation between the chemical composition and the difference between the lattice spacings of the reflections in question in Å can be seen . Further Tables 16a, 16b and 16c indicate the distances between these reflections for a few types of camera and radiation.

The X-ray powder diagrams of the alkali pyroxenes can be distinguished from those of the other pyroxenes, while they also show great mutual differences. It may be noted, however, that transitions between these pyroxenes always are possible.

The powder diagram of spodumene has its own character, so that this pyroxene can be distinguished very simply from the other pyroxenes by the röntgenographic method.

The X-ray investigation on clinopyroxenes is not yet completed, because much can still be done, for instance in the jadeite-diopside-aegirite field.

SAMENVATTING

De röntgen-poeder-methode ter determinatie van mineralen werd in dit geschrift toegepast op de belangrijke gesteenten-vormende mineraalgroep der pyroxenen.

Doel van dit onderzoek was, de variaties der intensiteiten en de posities van reflecties in het poeder-diagram in verband te brengen met de variaties in optische eigenschappen en chemische samenstelling. Daartoe werden een aantal pyroxenen afkomstig van verschillende vindplaatsen, optisch, chemisch en röntgenografisch onderzocht.

De orthopyroxenen. — Het optisch onderzoek der orthopyroxenen heeft aangewezen, dat de variatie der optische eigenschappen in verband staat met de chemische samenstelling (zie Tabel 1).

Een verschil tussen plutonische en vulkanische orthopyroxenen ligt in de grootte van de assenhoek 2 V: deze blijkt voor vulkanische orthopyroxenen tussen En_{80} en En_{15} kleiner te zijn dan voor plutonische orthopyroxenen (zie fig. 5).

Voorts is in de plutonische orthopyroxenen een lamellenstructuur waargenomen (zie fig. 2 en 3), terwijl de vulkanische vertegenwoordigers deze lamellen niet vertonen, doch meestal een zonaire bouw blijken te bezitten (zie fig. 1).

Uit het chemisch onderzoek der orthopyroxenen is gebleken, dat zowel de plutonische als de vulkanische orthopyroxenen over het algemeen een tamelijk variërend Ca-gehalte en Al-gehalte bezitten. Er is geen enkele aanwijzing, dat deze hoeveelheden voor vulkanische orthopyroxenen hoger liggen dan bij plutonische orthopyroxenen (zie Tabel 3).

De orthopyroxenen kunnen aan de hand van hun karakteristiek reflectiepatroon met behulp van röntgen-poeder-diagrammen worden onderscheiden van de clinopyroxenen. De poeder-diagrammen werden vervaardigd met behulp van een camera met een diameter van 9 cm en FeKα_1-straling ($\lambda = 1.93597$ Å). Alle poeder-diagrammen der orthopyroxenen werden ondergebracht in een groep (Groep A, zie fig. 6).

De variatie in de relatieve afstand tussen de reflecties 10 3 1 en 0 6 0 bleek in verband te staan met de chemische samenstelling. Deze afstanden werden nauwkeurig in millimeters opgemeten met behulp van een CAMBRIDGE Universal Measuring Machine; de resultaten van de metingen werden uitgezet tegen de chemische samenstelling in fig. 8. Door de invloed van Al en Ca is het gehalte aan Mg niet ondubbelzinnig uit deze figuur af te lezen, daarom werden tevens röntgen-poeder-opnamen gemaakt van mengsels van 70 % orthopyroxeen en 30 % kwarts (zie fig. 9). De relatieve afstand tussen kwarts reflectie $2\,1\,\bar{3}\,1$ en pyroxene reflectie 0 6 0 in mm en de afstand tussen kwarts reflectie $(2\,0\,\bar{2}\,3)$ $(3\,0\,\bar{3}\,1)$ en pyroxene reflectie 11 3 1 in mm zijn afhankelijk van de chemische samenstelling, hetgeen respectievelijk in de figuren

10 en 11 te zien is. In fig. 10 komen twee curven voor: één voor orthopyroxenen met een atoomproportie van Al ongeveer gelijk aan 0.010 en één voor orthopyroxenen met een atoomproportie van Al ongeveer gelijk aan 0.050 op de B^{VI} plaats. In fig. 11 zijn twee curven te zien, welke betrekking hebben op respectievelijk orthopyroxenen met een atoomproportie van Ca ongeveer gelijk aan 0.020 en orthopyroxenen met een atoomproportie van Ca ongeveer gelijk aan 0.060. Men kan nu uit de genoemde figuren 8, 10 en 11 de chemische samenstelling van een orthopyroxeen bepalen op de volgende wijze:

Men meet drie relatieve afstanden; in elke figuur kan men twee waarden voor het Mg-gehalte vinden; van deze in totaal zes waarden zullen er drie zeer dicht bij elkaar liggen; het gemiddelde van deze drie waarden geeft het Mg-gehalte; aan de hand van het Mg-gehalte kan men dan in de figuren de gehalten aan Al en Ca bepalen.

Deze röntgenografische methode stuit op moeilijkheden, wanneer er geen bepaalde hoeveelheden Al en Ca in de orthopyroxenen voorkomen. Er kunnen dan twee groepen voorkomen van drie Mg's, welke dicht bij elkaar liggen (zie Tabel 9). In zulke twijfelgevallen moet men om het gehalte aan Mg te bepalen gebruik maken van de optische methode van onderzoek.

Bij vervanging van Mg door Fe verandert N_z zeer sterk, de roosterconstanten — en daarmede de relatieve afstanden — blijven vrijwel onveranderd. Het Al- en Ca-gehalte kan dan bepaald worden met behulp van de röntgenografische methode.

Bij substitutie van Al en Ca voor Mg treedt namelijk sterke verandering op in de roosterconstanten en daarmede ook in de relatieve afstanden tussen de reflecties, die daar gevoelig voor zijn.

De variatie in de relatieve afstand tussen genoemde reflecties kan verklaard worden door middel van een kristalmodel van enstatiet (zie fig. 12 en 13). Deze variatie is een gevolg van de substitutie van Fe, Al en Ca voor Mg en van Al voor Si.

De vervanging van Mg door Fe doet alle roosterconstanten in geringe mate toenemen, zodat de vorm van de eenheidscel weinig verandert. De substitutie van Ca voor Mg heeft grote invloed op de a- en de c-ribbe: ze worden beide veel groter. De substitutie van Al voor Mg en van Al voor Si doet de b-ribbe sterk in grootte afnemen.

Deze veranderingen in de eenheidscel zijn gevolg van het feit, dat alle vervangende ionen een andere ionenstraal hebben dan Mg en dat in de structuur van enstatiet twee soorten Mg-ionen voorkomen, die onderling totaal verschillende posities innemen en bovendien op totaal verschillende wijze met de tetraeders verbonden zijn.

Aangezien de relatieve afstand in mm tussen bepaalde reflecties afhankelijk is van de gebruikte camera en straling, zijn in de Tabellen 7a, 7b en 7c de genoemde afstanden vermeld voor verschillende camera's en stralingen. Bovendien zijn de verschillen tussen de netvlaksafstanden dezer reflecties in Å aangegeven.

De clinopyroxenen. — Als resultaat van het optisch onderzoek der clinopyroxenen volgt hier een beschrijving der monsters, zowel macroscopisch als optisch en een bepaling van 2 V en $Z \wedge c$. Voor sommige clinopyroxenen zijn ook de waarden van N_z en N_x bepaald.

De beschreven clinopyroxenen werden ingedeeld in een aantal groepen, op basis van hun chemische samenstelling (zie pag. 224).

Het is gebleken, dat de optische eigenschappen der röntgenografisch onderzochte clinopyroxenen niet veel afwijken van de in de literatuur vermelde gegevens over deze mineraalgroep (zie fig. 20 en Tabel 10).

Het chemisch onderzoek is beperkt gebleven tot analyse van enkele clinopyroxenen; de resultaten van deze analyses zijn vermeld in Tabel 11.

De monokliene pyroxenen werden op grond van een verschil in positie en intensiteit van bepaalde reflecties in het röntgen-poeder-diagram ingedeeld in de volgende vier groepen.

Groep B 1 (zie fig. 21 en 23).
Tot deze groep behoren bijvoorbeeld hedenbergiet, diopsied, augiet en diallaag.

Groep B 2 (zie fig. 21 en 23).
Tot deze groep behoort pigeoniet.

Groep B 3 (zie fig. 21 en 22).
Tot deze groep behoren aegirien en jadeiet.

Groep B 4 (zie fig. 21 en 22).
Tot deze groep behoort spodumeen.

Tussen bovengenoemde groepen zijn geen scherpe grenzen te trekken. Er kunnen overgangen bestaan, bijvoorbeeld tussen Groep B 1 en Groep B 2 of tussen Groep B 1 en Groep B 3, terwijl door het ontbreken van clinoenstatiet- en ferrosiliet-monsters niet uitgemaakt kon worden of er eventueel nog andere dan de vier genoemde groepen te onderscheiden zijn.

Van elk der groepen zijn de voornaamste eigenschappen besproken op pag. 245. Iedere groep heeft een eigen karakteristiek reflectiepatroon; de overeenkomst tussen deze patronen is echter groot genoeg om te kunnen concluderen dat alle clinopyroxenen welke hier onderzocht zijn, nagenoeg dezelfde structuur bezitten. De groepering der röntgen-poeder-diagrammen komt in grote lijnen overeen met de classificatie der pyroxenen volgens chemische samenstelling.

De chemische samenstelling van de clinopyroxenen der groepen B 1 en B 2 kan bepaald worden met behulp van een gecombineerd optisch en röntgenografisch onderzoek. Deze combinatie is noodzakelijk, omdat de substitutie van Mg door Fe practisch geen invloed heeft op de ribben van de eenheidscel, maar wel op de brekingsindices. Daarentegen heeft de vervanging van Mg door Ca juist een grote invloed op de vorm van de eenheidscel.

Van genoemde clinopyroxenen — die van Groep B 1 en Groep B 2 — is de variatie van de relatieve afstand in mm tussen de reflecties 2 2 0 en 2 2 1, de reflecties 2 2 1 en 3 1 0 en de reflecties 1 3 1 en 2 2 $\bar{1}$, uitgezet tegen de chemische samenstelling in de figuren 25 en 26. Uit deze figuren kan men de samenstelling dezer clinopyroxenen bepalen door genoemde relatieve afstanden aan de röntgen-poeder-diagrammen op te meten. In de figuren 27, 28 en 29 is het verband tussen de chemische samenstelling en het verschil tussen de netvlaksafstanden van genoemde reflecties in Å te zien. Voorts geven de Tabellen 16a, 16b en 16c de afstanden tussen deze reflecties aan voor verschillende camera's en stralingen.

De röntgen-poeder-diagrammen van de alkali-pyroxenen kunnen onderscheiden worden van die der andere pyroxenen, hoewel zij ook onderling grote verschillen vertonen; overgangen tussen deze pyroxenen zijn altijd mogelijk.

Een uitzondering dient echter gemaakt te worden voor spodumeen, waarvan het poeder-diagram een zo geheel eigen karakter draagt, dat deze pyroxeen met behulp van de röntgenografische methode heel eenvoudig van andere pyroxenen kan worden onderscheiden.

Tenslotte dient nog opgemerkt te worden dat het röntgenografisch onderzoek aan clinopyroxenen nog zeer onvolledig is geweest omdat nog veel gedaan zou kunnen worden zoals bijvoorbeeld in het jadeiet-diopsied-aegirien veld.

REFERENCES

Alphabetical and Grouped Numerical Index of X-ray Diffraction Data, including the fifth set of cards. 1954 — American Society for Testing Materials, Philadelphia.

ANDERSON, B. W., 1951 — Gem Testing, Heywood & Company, Ltd., London, W.C. 2.

ATLAS, L., 1952 — The polymorphism of $MgSiO_3$ and solidstate equilibria in the system $MgSiO_3$ — $CaMgSi_2O_6$, Journ. Geology, vol. 60, p. 125—147.

CLAISSE, F., 1950 — A Roentgenographic method for determining Plagioclases, Am. Mineralogist, vol. 35, p. 412—420.

CLARINGBULL, G. F. and HEY, M. H., 1952 — Sinhalite ($MgAlBO_4$), a new mineral, Mineral. Mag., vol. 29, p. 841—849.

CLAVAN, W., MCNABB, W. M. and WATSON, E. H., 1954 — Some Hypersthenes from Southeastern Pennsylvania and Delaware, Am. Mineralogist, vol. 39, p. 566—580.

FORD, W. E., 1949 — Dana's Textbook of Mineralogy, fourth edition, John Wiley & Sons, Inc., New York.

GOODYEAR, J. and DUFFIN, W. J., 1954 — The identification and determination of plagioclase feldspars by the X-ray powder method, Mineral. Mag., vol. 30, p. 306—326.

GOSSNER, B. und MUSZGNUG, F., 1929 — Über Enstatit und sein Verhältnis zur Pyroxen- und Amphibol gruppe, Zeitschr. Krist. 70, p. 234—248.

HANAWALT, H. D., RINN, H. W. and FREVEL, L. K., 1938 — Chemical Analysis by X-ray Diffraction, Ind. and Eng. Chem. Anal. Ed. 10, p. 457—512.

HARCOURT, A., 1942 — Tables for the identification of ore minerals by X-ray powder patterns, Am. Mineralogist, vol. 27, p. 63—113.

HENRY, N. F. M., 1942 — Lamellar structure in Orthopyroxenes, Mineral. Mag., vol. 26, p. 179—188.

HESS, H. H. and PHILIPS, A. H., 1939 — Orthopyroxenes of the Bushveld type, Am. Mineralogist, vol. 23, p. 450—456.

HESS, H. H. and PHILIPS, A. H., 1940 — Optical properties and chemical composition of Magnesian Orthopyroxenes, Am. Mineralogist, vol. 25, p. 271—285.

HESS, H. H., 1941 — Pyroxenes of common mafic magmas, Am. Mineralogist, vol. 26, pp. 515—535 and 573—594.

HESS, H. H., 1949 — Chemical composition and optical properties of common clinopyroxenes. Part I, Am. Mineralogist, vol. 34, p. 621—666.

HESS, H. H., 1952 — Orthopyroxenes of the Bushveld type. Ion substitutions and changes in unit cell dimensions. Am. Journ. Sci., Bowen vol., p. 173—187.

HINTZE, C., 1897 — Handbuch der Mineralogie, Band II, Silicate und Titanate, Leipzig.

ITO, T. I., 1950 — X-ray studies on polymorphism. The rhombic pyroxenes, p. 30—41, Maruzen, Tokyo.

KUNO, H. and SAWATARI, M., 1934 — On the augites from Wadaki, Idu and from Yoneyama, Etigo, Japan, Jap. Journ. Geol. and Geogr., vol. 11, p. 327—343.

KUNO, H., 1938 — Hypersthene from Odawari-mati, Japan, Proc. Imp. Acad. Tokyo, vol. 14, p. 218—220.

KUNO, H. and NAGASHIMA, K., 1952 — Chemical compositions of hypersthene and pigeonite in equilibrium in magma, Am. Mineralogist, vol. 37, p. 1000—1006.

KUNO, H. and HESS, H. H., 1953 — Unit cell dimensions of clinoenstatite and pigeonite in relation to other common clinopyroxenes, Am. Journ. Sci., vol. 251, p. 741—752.

KUNO, H., 1954 — Study of orthopyroxenes from volcanic rocks, Am. Mineralogist, vol. 39, p. 30—46.

KUNO, H., 1955 — Ion substitution in the diopside-ferropigeonite series of clinopyroxenes, Am. Mineralogist, vol. 40, p. 70—93.

MEHMEL, M., 1939 — Datensammlung zum Mineralbestimmen mit Röntgenstrahlen, Fort. Min. Krist. Petr., 23, p. 91—118.

NIGGLI, E., 1953 — Untersuchungen am Varlamoffit, Leidse Geol. Med. 17, p. 207—214.

NIGGLI, E., OVERWEEL, C. J. and VAN DER VLERK, I. M., 1953 — An X-ray crystallographical application of the Fluorine-Dating Method of Fossil Bones, Kon. Ned. Akad. Wetensch., Proc. Series B, 56, No. 5, p. 538—542.

NIGGLI, E. und TOBI, A. C., 1953 — Über ein Cummingtonit-Quarz-Plagioklasgestein als Glazialgeschiebe in Drente (Niederlande), mit einer Bemerkung über die röntgenographische Bestimmung der Amphibole, Kon. Ned. Akad. Wetensch., Proc. Series B, 56, No. 3, p. 280—284.

NIGGLI, P. und NIGGLI, E., 1948 — Gesteine und Minerallagerstätten, B-d I, Allgemeine lehre von den Gesteinen und Minerallagerstätten, Basel.

NIGGLI, P., 1943 — Gesteinschemismus und Mineralchemismus. II Die Pyroxene der magmatischen Erstarrung, Schweiz. Min. Petr. Mitt., Bd. 23, p. 538—607.

NIGGLI, P., 1954 — Rocks and Mineral Deposits, Freeman & Company, San Francisco.

OSTEN, J. F., 1951 — Identificatie van Natuurlijke Alkaliveldspaten met behulp van röntgenpoederdiagrammen. Proefschrift, Leiden, Leidse Geol. Med. 17, p. 1—69.

POLDERVAART, A., 1950 — Correlation of physical properties and chemical composition in the plagioclase, olivine and orthopyroxene series, Am. Mineralogist, vol. 35, p. 1067—1079.

POLDERVAART, A. and HESS, H .H., 1951 — Pyroxenes in the crystallization of basaltic magma, Journ. Geology, vol. 59, p. 472—489.

RAMDOHR, P., 1954 — Klockmann's Lehrbuch der Mineralogie, vierzehnte umgearbeitete Auflage, Ferdinand Enke Verlag, Stuttgart.

TAKANÉ, K., 1932 — Crystal Structure of Bronzite from Chichi-jima in the Bonin Islands, Proc. Imp. Acad., Tokyo, vol. 8, p. 308—311.

TEX, E. DEN, 1949 — Les roches basiques et ultrabasiques des Lacs Robert et le Trias de Chamrousse (Massif de Belledonne). Proefschrift, Leiden, Leidse Geol. Med. 15, p. 1—204.

TRÖGER, W. E., 1952 — Tabellen zur optischen Bestimmung der Gesteinsbildenden Minerale, E. Schweizerbart'sche Verlagsbuchhandlung, Stuttgart.

WALLS, R., 1935 — A critical review of the data for a revision of the enstatite-hypersthene series, Mineral. Mag., vol. 24, p. 165—172.

WARREN, B. and BRAGG, W. L., 1929 — The structure of Diopside $CaMg(SiO_3)_2$, Zeitschr. Krist. 69, p. 168—193.

WARREN, B. E. and MODELL, D. I., 1930 — The structure of Enstatite $MgSiO_3$, Zeitschr. Krist. 75, p. 1—14.

WARREN, B. E. and MODELL, D. I., 1930 — The structure of Anthophyllite $H_2Mg_7(SiO_3)_8$, Zeitschr. Krist. 75, p. 161—178.

WILLIAMS, H., TURNER, F. J. and GILBERT, C. M., 1954 — Petrography, An introduction to the study of Rocks in thin sections, Freeman & Company, San Francisco.

WINCHELL, A. N., 1948 — Elements of Optical Mineralogy, Part II ,third edition, John Wiley & Sons, Inc., New York.

WINCHELL, A. N., 1951 — Elements of Optical Mineralogy, Part II, fourth edition, John Wiley & Sons, Inc., New York.

WYCKOFF, R. W. G., MERWIN, H. E. and WASHINGTON, H. S., 1925 — X-ray diffraction measurements upon the pyroxenes, Am. Journ. Sci., vol. 10, p. 383—397.

YODER Jr., H. S., 1950 — The Jadeite problem, Am. Journ. Sci., vol. 248, pp. 225—248 and 312—334.

ZIRKEL, F., 1903 — Über Urausscheidungen in rhein. Basalten, 28. Bandes der Abhandl. der math.-phys. Klasse der Königl. Sächs. Ges. Wissensch. No. III, Leipzig, pp. 131, 144, 169.